GAS TURBINE BLADE FAILURES—CAUSES, AVOIDANCE, AND TROUBLESHOOTING

by

Cyrus B. Meher-Homji

Engineering Specialist

Bechtel Corporation

Houston, Texas

and

George Gabriles

Consultant

G&B Consultants

Lake Jackson, Texas

Cyrus B. Meher-Homji is an Engineering Specialist with Bechtel Corporation, in Houston, Texas. He is responsible for specification, selection, and implementation of compression and power generation turbomachinery. He has 19 years of industry consulting experience in the areas of turbomachine aerothermodynamics, vibration and performance analysis, compressor rerates, and failure analysis. Mr. Meher-Homji has developed several aerothermal and transient analysis techniques for the condition monitoring of gas turbines and multiobjective optimization approaches for gas turbine maintenance management. He worked as a development engineer on the design, development, and testing of a 365 hp, externally fired steam injected gas turbine.

Mr. Meher-Homji has a B.S. degree (Mechanical Engineering) from Shivaji University, an M.E. degree from Texas A&M University, and an M.B.A. degree from the University of Houston. He is a Fellow of ASME, a registered Professional Engineer in the State of Texas, and has several publications in the area of turbomachinery engineering.

George A. Gabriles is an independent consultant in the field of maintenance and repair of reciprocating and turbomachinery, in Lake Jackson, Texas. His experience background spans more than 45 years of project engineering, maintenance engineering, construction, and management in the petrochemical, marine, and oil and gas industries.

Mr. Gabriles received his B.S. degree (Mechanical Engineering) from the University of Houston (1954), and is a registered Professional Engineer in the State of Texas. He is an instructor of the Dale Carnegie Leadership Courses.

Mr. Gabriles is the recipient of the TSPE (Gulf Coast Chapter) 1989-90 Outstanding Engineer of the Year award, and the Texas Industrial Development Council 1986 Industrial Developer of the Year award. He has authored and coauthored several papers on both turbo and reciprocating machinery. He serves on the Turbomachinery Symposium Advisory Committee.

ABSTRACT

With blading problems accounting for as many as 42 percent of the failures in gas turbines (Allianz, 1978) and with its severe effect on plant availability, there is a pressing need for a unified treatment of the causes, failure modes, and troubleshooting to assist plant engineers in tackling blade failure problems. This paper provides a comprehensive practical treatment of the subject, taking into account the complex nature of blading problems, influence of the operating environment, design factors, and maintenance practices. Blade failure modes such as fatigue, environmental attack, creep, erosion, and embrittlement are addressed along with a synopsis of design tools to review blade reliability. Peripheral issues affecting blade integrity such as fuel and blade quality control are addressed. A blade failure troubleshooting chart is furnished to assist users in diagnosing common failure modes. The object of this paper is to show, in the context of blading problems, the *interrelationship* between design, operation, maintenance, and the operational envelope. Several case studies are presented dealing with a variety of failure modes. The treatment focuses on practical troubleshooting of blading problems augmented, in some cases, by the use of analytical tools. APPENDIX A provides applicable tools, rules of thumb, and formulae that can be used by gas turbine users for design review and troubleshooting.

INTRODUCTION—IMPORTANCE OF THE BLADE FAILURE PROBLEM IN GAS TURBINES

Blade failures have plagued designers and operators since the inception of turbomachinery. Rapid gas turbine development accelerated with the work of Ohain in Germany and Whittle in the United Kingdom shortly before and during World War II. Several of the early turbojets experienced blade failures and much of the work done in blade vibration initiated in this era. The blade failure difficulties experienced by the Junker Jumo 004 (the jet engine for the Messerschmitt ME 262), depicted in Figure 1, are covered in Meher-Homji (1996). Fatigue failures plagued this engine and some novel means of detecting the resonant frequencies were developed, including an approach where the turbine blades were stroked by a violin bow and an experienced musician was employed to detect the tone (resonant frequency) of the blades. In Germany, much of the pioneering work relating to blade vibration and failures was done by the renowned aeromechanical engineer, Dr. Max Bentele, including the solving of a complex turbocharger blade failure fatigue problem shown in Figure 2 (Bentele, 1991). In England, Whittle also struggled with a host of turbine blade and impeller failure problems. Figure 3 depicts an impeller failure on the early Whittle turbojet. Today, *58 years later*, high cycle fatigue still remains a problem.
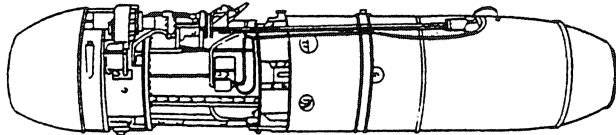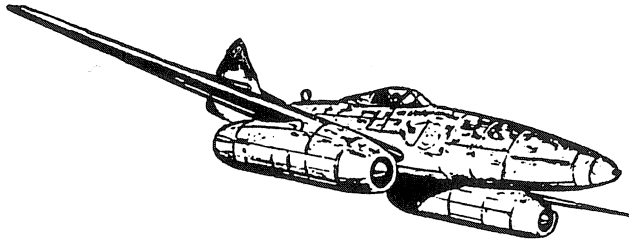
Figure 1. The Messerschmitt ME-262 and the World's First Production Turbojet, the Junkers Jumo 004 B (which suffered with turbine blade fatigue problems). (Meher-Homji, 1996)
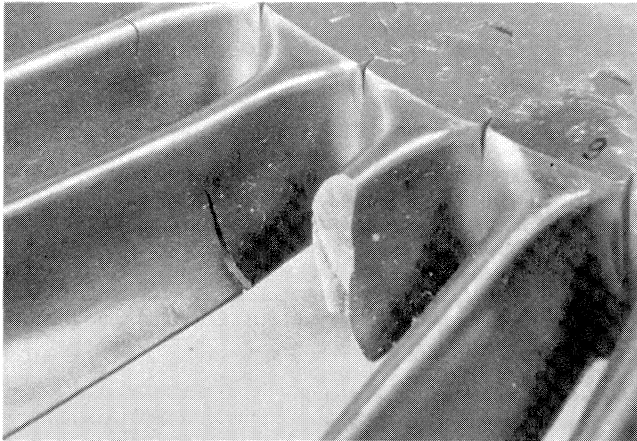

Figure 2. Fatigue Failure on a Turbocharger Used on the Hienkel 111 Aircraft. (Courtesy of Dr. Max Bentele)
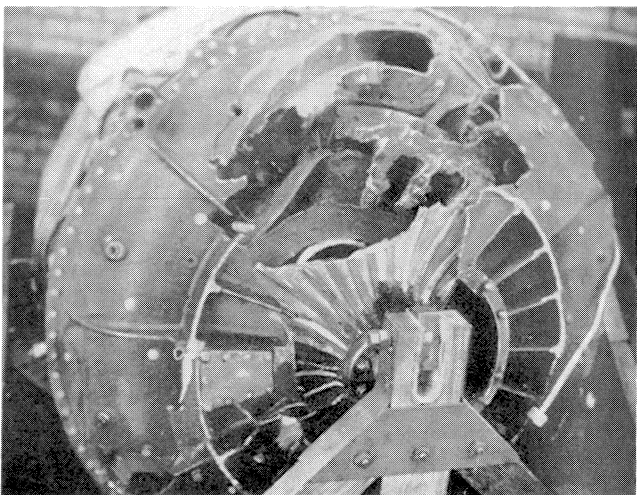

Figure 3. Impeller Failure of One of Whittle's Early Jet Engines. (Meher-Homji, 1997)

In both the industrial and aircraft gas turbine industries, blade problems are of the utmost concern to designers and users. The U.S. Air Force estimates an expenditure of $100 million/year to inspect and fix high cycle fatigue problems (Srinivasan, 1977). With the evolution of gas turbines toward higher turbine entry temperatures and pressure ratios, the problems of blades, especially in the hot section, has been accentuated. Currently, the limiting factor on hot section life is coating durability.

The causes of blade failure are manifold. They include vibration, fatigue, foreign object damage, corrosion, erosion, sulphidation, and creep. In spite of the availability of sophisticated design tools, blade failures are prevalent in both compressors and turbines. There are several reasons for this:

• The presence of unavoidable excitations (of both aerodynamic and mechanical origin) and combined failure modes

• Exceedingly complex vibration characteristics of blades under actual operating conditions that often differ from analytical predictions. These arise because of the intricate blade geometry, which makes advanced finite element modelling difficult. Interaction between the vibration of blades, disks, shrouds, snubbers, and the presence of "assembly modes" further complicates the problem.

• Nonuniformity of supposedly "identical" blades and quality control problems

• Operation of turbine airfoils in a hostile environment, where damage mechanisms of creep, oxidation, hot corrosion, and thermal fatigue often work in conjunction, leading to compound failure modes

• The rapid rate of progression of high frequency fatigue failures

Statistics on industrial gas turbines (Bloch, 1982) indicate that turbine blades and rotor components account for 28 percent of primary causes of gas turbine failures, with turbine nozzles and stationary parts accounting for 18 percent. Dundas (1994) has provided interesting damage cost statistics of gas turbine losses over an eight year timeframe, and found that turbine blade cooling, high cycle fatigue, creep, and surge related failures accounted for 62 percent of the total damage costs for heavy duty gas turbines. Table 1 provides Dundas's findings for both heavy duty and aeroderivative type turbines.

Table 1. Causes of Losses in Gas Turbines (Heavy Duty and Aeroderivative) and Percentages of Damage Cost. (Residuals are from other causes.) (Dundas, 1994)

CAUSE OF LOSS	Damage Cost, % of total- Heavy Duty Gas Turbines	Damage Cost, % of total- Aeroderivative Gas Turbines
Turbine Blade Cooling Air Loss	14	-
HCF of Turbine Blades	12	2
Creep of Rotating Parts	19	-
Compressor Surge	5	24
HCF of Compressor Blades	12	7.5
Turbine Disk Failure	-	7.5
Thermal Cracking	-	11
Internal Overheating	-	12.5
Internal Fire or Explosion	5	-

Publications on blade failures tend to focus exclusively on a particular aspect of the problem, such as metallurgy, vibration dynamics, or design or stress analysis and fail to emphasize the *multidisciplinary* nature of the problem. Some notable exceptions are publications by Dundas (1993a, 1993b), Sohre (1975), Passey (1976), and Armstrong and Stevenson (1960), which provide a practical perspective. It is the object of this paper to extend the work of Meher-Homji (1995) and present a comprehensive, practical, self-contained treatment of gas turbine blade problems.
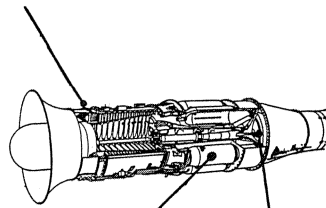
FAILURE MODES IN GAS TURBINE BLADING

Predominant failure mechanisms and commonly affected components, as shown in Figure 4, are:

- Low cycle fatigue—compressor and turbine disks.

- High cycle fatigue—compressor and turbine blades, disks, compressor stator vanes.

- Thermal fatigue—nozzles, combustor components.

- Environmental attack (oxidation, sulphidation, hot corrosion, standby corrosion)—hot section blades and stators, transition pieces, and combustors.

- Creep damage—hot section nozzles and blades.

- Erosion and wear.

- Impact overload damage (due to foreign object damage (FOD), domestic object damage (DOD) or clash/clang of compressor blades due to surge).

- Thermal aging.

- Combined failure mechanisms—creep/fatigue, corrosion/fatigue, oxidation/erosion, etc.

COMPRESSOR

COMPONENT	FAILURE MODE	CAUSE
Rotor Blade and Stators	H.C. Fatigue (resonance) Erosion, FOD, Corrosion Clash, Clang, Fretting	Vibration, flutter, airflow distortion, surge, stall dust in air
Disc	Fatigue - creep, wear, rubbing	Centrifugal loads temperature effects
Compressor tie bolts	Mechanical fatigue, wear, fretting and rubbing	Startup, cycling, vibration

Blade Failures- Aprox. 35%

COMBUSTOR

COMPONENT	FAILURE MODE	CAUSE
Liner	Mechanical fatigue, fretting buckling, wear thermal fatigue, yield slip, thermal distortion and corrosion	Hot spots, temperature gradients, vibration, excessive dynamic pressure pulsations
Casing	Fatigue	Pressure Cycles
Cross fire tubes	Wear, rubbing fretting, corrosion thermal fatigue	Pulsations and vibration
Transition piece	Thermal fatigue, wear, rubbing, fretting	Dynamic pulsations and vibration

TURBINE SECTION

COMPONENT	FAILURE MODE	CAUSE
Turbine Rotor Blades	High cycle fatigue, creep, corrosion, sulphidation, erosion	Centrifugal & temperature stress, vibratory stresses, environment, fuel problems, excessive temperature spreads, cooling problems
Turbine Stator Blades	Creep rupture corrosion, sulphidation, bowing, fatigue thermal fatigue	Cooling problems, Improper temperature profile
Turbine Rotor Disc	Creep-rupture, Low cycle fatigue	Improper wheelspace cooling, Thermal stresses

Figure 4. Pictorial Overview of Failure Modes in Gas Turbines.

Fatigue

Fatigue accounts for a significant number of turbine and compressor blade failures and is promoted by repeated application of fluctuating stresses. Stress levels are typically much lower than the tensile stress of the material. Common causes of vibration in compressor blades include stator passing frequency wakes, rotating stall, surge, choke, inlet distortion, and blade flutter. In the turbine section, airfoils have to function not only in a severe vibratory environment, but also under hostile conditions of high temperature, corrosion, creep, and thermomechanical fatigue. Ewins (1976) provides a detailed treatment of blade vibration.

High Cycle Fatigue

Resonant fatigue is an important failure mechanism that arises when a periodic force acts at a frequency corresponding to a blade natural frequency. If the damping is inadequate for absorption of the periodic input energy, amplitudes and stresses grow until failure occurs by overstress or by propagation of a fatigue crack. High cycle fatigue (HCF) is typically caused by aerodynamic excitations (i.e., nozzle and vane passing frequencies, strut pass frequency) or by self excited vibration and flutter. Whereas the fluctuating stresses may not be very high, the maximum stress at resonance can increase dramatically. High cycle fatigue damage will occur when stress levels are above the fatigue strength. It is important to note that the fatigue strength is severely affected by a corrosive environment, in which the stress versus number of cycles (S-N) curve loses its validity. The growth of vibration at resonance is governed by:

- Magnitude of the exciting force. The stimulus of this force can be a function of the operating condition (e.g., airflow or temperature distortion).

- Damping of blade material (hysteresis damping in the blade and coulomb damping in the fir tree and shroud).

- Resonant response factor, i.e., a measure of the *ability* of the blade (or blade packet) to *accept* energy from the stimulus.

Loss of damping, due to breakage of a lacing wire, can increase the vibratory stresses by a factor of four. This situation can occur when the lashing wire holes in the blade get elongated with wear. A compressor blade that developed a fatigue crack (midspan trailing edge) is shown in Figure 5. The sectioned blade that was cut to display the crack is shown in Figure 6. Some modern engines utilizing integrally bladed disks do not have the friction damping associated with the dovetails and, therefore, dynamic magnification factors can often be two to five times those found in older engines (Griffin, et al., 1998). As these blades do not have platforms, the use of under-platform dampers is not possible. Consequently, blade designs have evolved that utilize insert dampers that are placed within the airfoil. These fit inside the blade cavities and produce frictional damping.
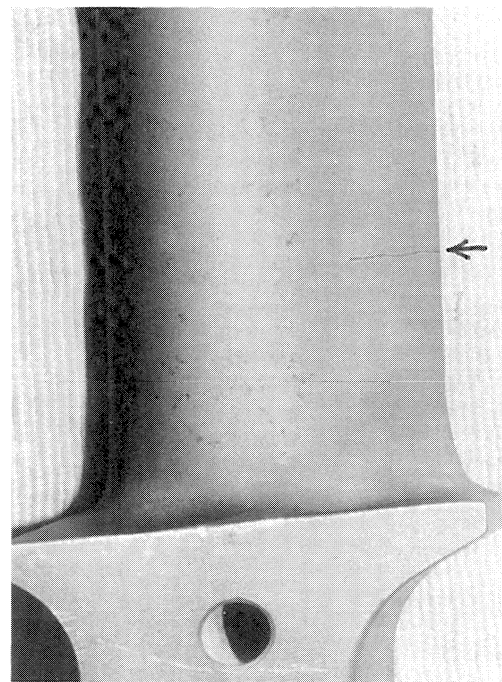

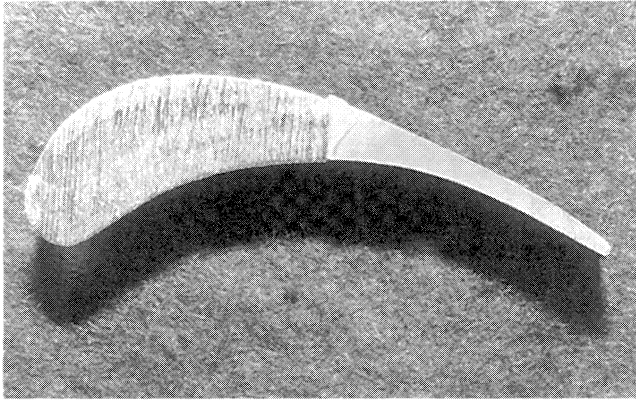*Figure 5. Blade Showing a Mid-Span Fatigue Crack.*

Figure 6. Sectioned View of Blade Shown in Figure 5. (The progression of the fatigue crack can be seen.)

Low Cycle Fatigue

Low cycle fatigue (LCF) occurs as a result of turbine start/stop cycles and is predominant in the bores and bolt hole areas of compressor and turbine disks that operate under centrifugal stresses. It is typically a problem associated with machines that have been in operation for several years. In this situation, minute flaws grow into cracks that, upon attaining critical size, rupture. Cracks also develop in the nozzle sections. To some extent, this is to be expected under normal operation and cycling service.

Thermomechanical Fatigue

Thermomechanical fatigue (TMF) is associated with thermal stresses, e.g., differential expansion of hot section components during startup and shutdown, and is particularly severe during rapid starts and full load emergency trips. The stress levels induced may initiate cracks, if they exceed the material yield stress. Temperature variations as high as 360°F (200°C) per minute are often experienced in hot section blading. This is the reason why full load trips are so detrimental in terms of life reduction, consuming as much as 200 equivalent hours per trip.

Environmental Problems

The environment must be considered when evaluating *any* blade failure. In addition to fouling, which creates adverse conditions for compressor blading, there are other mechanisms that can affect blade integrity. In particular, hot section components are subject to attack from oxidation, corrosion, and sulphidation. Environmental problems do not normally result in catastrophic failures, but work in conjunction with other failure modes. Compressor blades are frequently affected by corrosion and pitting, which can be severe if the ambient air contains salts or other contaminants.

High Temperature Oxidation

High temperature oxidation occurs when nickel based superalloys are exposed to temperatures greater than 1000°F (538°C). Oxygen in the gas stream reacts with the nickel alloy to form a nickel-oxide layer on the airfoil surface. When subjected to vibration and start stop thermal cycles during operation, this nickel oxide layer tends to crack and spall. This phenomenon may also occur on the inner surfaces of blade cooling passages and result in blade failure. Coatings are available to mitigate this effect and can be applied both on the blade surface and internal cooling holes.

Sulphidation

Sulphidation is a reaction that occurs when sulphur (from the fuel) reacts with the protective oxide layer and attacks the base metal. The air ingested by a gas turbine can contain impurities such as SO_2, SO_3, sodium chloride (salt), and chlorine. As these impurities pass over the airfoil, droplets (slag) of liquid sodium sulfate ($Na_2 SO_4$) are formed. Under this slag (and above a threshold temperature that is about 100°C higher for cobalt based superalloys than for nickel based ones), the protective oxide layer is broken down, permitting attack of the parent superalloy and causing very serious damage. Sodium sulfate is highly corrosive causing deep stress riser pits in the airfoil. Sulphidation is of particular concern when it is found in the blade root region, or along the leading or trailing edges, or under the blade shroud. Details on sulphidation are presented in Boyer (1975) and DeCrescente (1980).

Hot Corrosion

Hot section parts are often subject to combined oxidation-sulphidation phenomena, referred to as hot corrosion. Two types of hot corrosion have been identified. Type 1 (high temperature) corrosion occurs at temperatures approximately between 1517°F to 1742°F (825°C to 950°C). A denuded zone of base metal is often found along with intergrannular attack and sulfide spikes. Type 2 (low temperature) hot corrosion occurs at between 1292°F to 1472°F (700°C to 800°C) and displays a layered type of corrosion scale. Typically, no intergrannular attack or denuded zone of the base metal is found. Details on Type 2 hot corrosion may be found in Goward (1985). Coatings are commonly used to mitigate hot corrosion problems. Turbine blades from an aeroderivative gas turbine that experienced hot corrosion are shown in Figure 7.
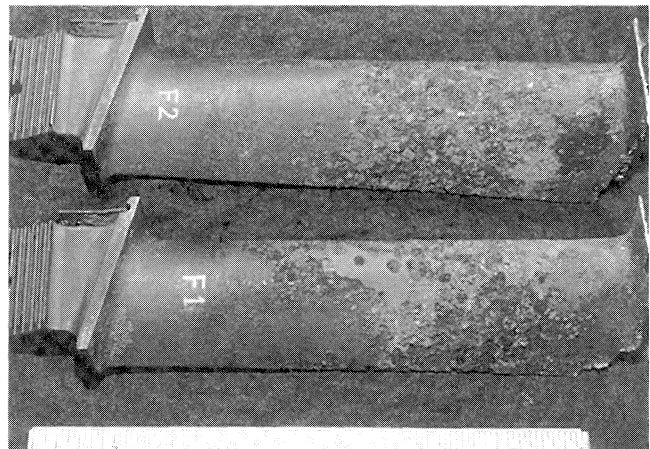

Figure 7. Turbine Blades with Hot Corrosion.

Standby Corrosion

This is a problem that commonly afflicts peaking gas turbines. It occurs during a turbine shutdown and is the result of air moisture and corrosives being present in the machine. Crevice corrosion occurs when corrosion products, which accumulate in the blade attachment areas, act as abrasives and increase clearances. In the presence of corrosives possibly from airborne salt, uncoated airfoils frequently develop corrosion pits, which may then develop into cracks. Blade fatigue strength is significantly reduced by corrosion. Blade failures caused by crevice corrosion will show symptoms typical of stress corrosion fatigue or stress corrosion (Sohre, 1975).

Creep

Creep occurs when components operate over time under high stresses and temperature. Figure 8 shows a typical creep deformation curve. As a rough rule of thumb, a 15°C increase in blade metal temperature cuts creep life by 50 percent. This emphasizes the importance of effective cooling. Creep affects hot section parts and the final stages of high pressure ratio compressors, and is predominant in the midspan region of the airfoil, which

experiences the highest temperature. Creep strain is of interest because it leads to progressive reduction of rotor tip clearances. It can also occur in the disk rim region where high stresses and temperatures can cause time dependent plastic deformation. Creep behavior is commonly modelled by use of the Larson-Miller parameter (APPENDIX A). Figure 9 depicts the sensitivity of life with temperature for a Waspalloy disk in a power turbine. Exposure to creep can be detected by metallurgical tests, common indicators being the coarsening of the gamma prime precipitates and the formation of void cavities at grain boundaries. Details on creep may be found in Greenfield (1972). Often creep failures can be associated with a loss of cooling. This loss can be due to a quality control problem (such as blocked cooling passages) or due to a blockage or malfunction of the cooling airflow.
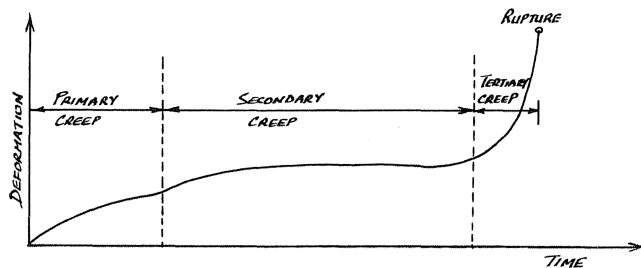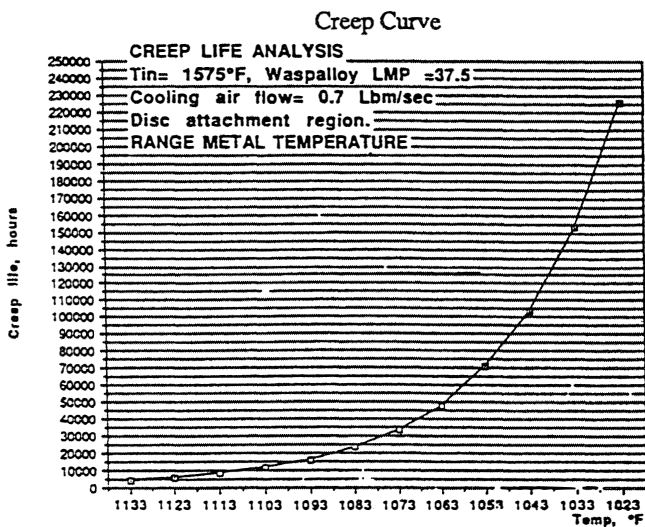

Figure 8. Creep Curve.

Figure 9. Sensitivity of Creep Life with Increasing Temperature for a Waspalloy Turbine Disk. (LMP = 37.5)

Erosion/Wear

These mechanisms rarely cause catastrophic blade failures, but contribute to other failure modes and can be of considerable economic significance, as blade replacement may be necessary. Erosion and wear can occur in both compressor and turbine components. Particles causing erosion in axial flow compressor blades are five to 10 microns or greater in size. In addition to the primary damage caused by erosion, a reduction in the surge margin can occur if the tips get severely eroded. Fretting wear occurs in the blade attachment areas (dovetails) and is often associated with standby corrosion. A review of factors that influence fretting wear is presented by Bill (1982). A considerable amount of dovetail wear (causing bucket rock) occurs during turning gear operation when the blades are not centrifugally loaded. Corrosion in the dovetail region will, of course, accelerate the process, with the corrosives acting as an abrasive.

Hot Gas Erosion

Apart from particulate erosion, there also exists the important phenomenon of hot gas erosion. Modern air cooled gas turbine components operate at metal temperatures, hundreds of degrees lower than the gas path temperatures. The metal surface is protected by means of the natural boundary layer or by a cooling air film. If this cooling layer of air breaks down even for short periods of time, or cooling effectiveness drops, then the surface asperities (roughness) of the blade contacted by the hot gas are subjected to high thermal stress cycles. After several cycles, damage takes place and the increased roughness (erosion) worsens the problem. Typically the most severely affected parts are those in the hottest gas path (e.g., central to the transition piece exit). This problem can occur in the first stage nozzle segments at the platforms and may reflect inappropriate cooling. A problem of this type on a first stage vane inner platform is described by O'Neill (1989).

Embrittlement

Embrittlement is a form of microstructure degradation that results in a loss of impact strength and is a particularly serious problem relating to Udimet 710 and 720 alloys, because it increases the material's susceptibility to foreign object damage (FOD). With embrittlement, brittle intermetallic compounds precipitate in a plate morphology and continuous carbide films form along grain boundaries. According to Stringer and Viswanathan (1990), it is estimated that in the United States, there are blade rows of Udimet 710 worth well over $60 million, suffering from loss of impact toughness. The minimum acceptable impact toughness to avoid serious FOD, as suggested by Crombie, et al. (1977), is 6 ft-lb. (8.1 J) at 1652°F (900°C). This temperature will be reached after 10,000 hours at 1500°F (816°C). Figure 10 (Viswanathan and Dolbec, 1986; Crombie, et al., 1977) depicts the drop in impact toughness for U-710 and IN-738 with increasing exposure in the range of 1450°F to 1650°F (780°C to 900°C). In this figure, time and temperature have been combined in terms of the Larson-Miller parameter. The drop in impact strength for U-710 occurs at 10,000 hours.
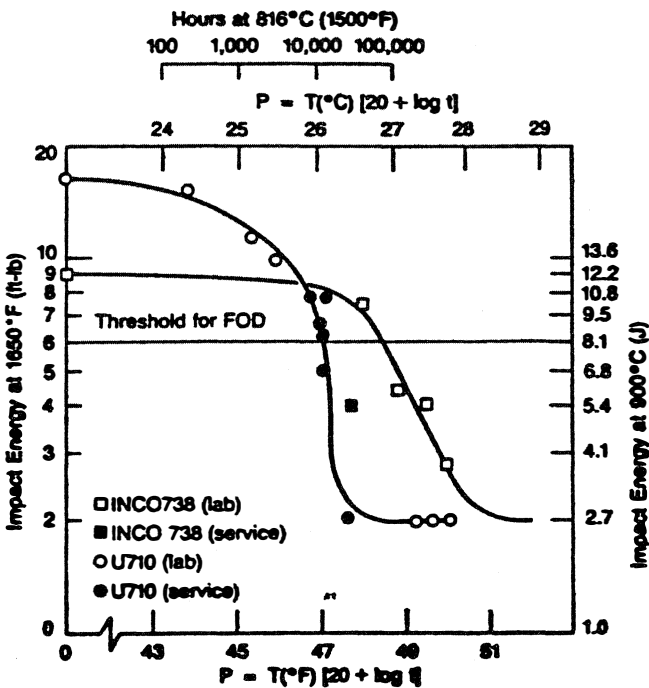

Figure 10. Drop in Impact Toughness for U 710 and IN 738 with Temperature Exposure. (Viswanathan and Dolbec, 1986)

Combination Mechanisms

Blade failures are commonly caused by multiple failure mechanisms. Corrosion, for example, can reduce blade section size and drop the fatigue strength. Fretting wear in the blade attachment regions can reduce damping, causing increased vibration amplitudes and alternating stresses. Foreign object damage can cause nicks and cracks that can then be propagated by low or high cycle fatigue. Consequently, failure analysis must investigate all engineering causes including design issues, environmental factors, cleanliness of the fuel, air quality, material, and gas turbine operating and maintenance history. Problems such as these are quite common and often create significant disputes between the OEMs and the user as to how the damage is to be resolved commercially. A turbine rotor from an aeroderivative gas turbine that experienced a fatigue failure combined with hot corrosion is shown in Figure 11. In this case, severe tip rubs accentuated the problem.
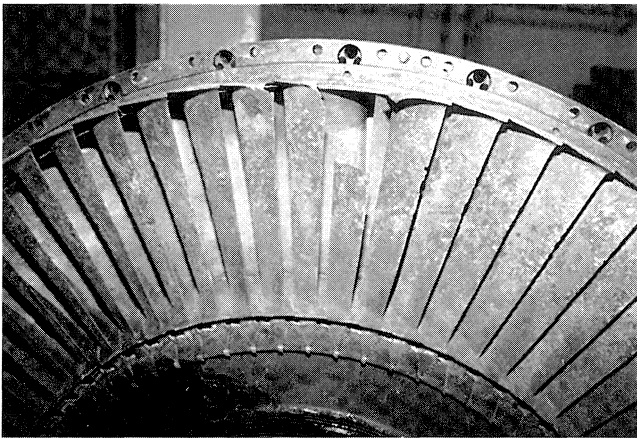

Figure 11. A Typical Combined Failure Mode Showing Both Tip Rub, Hot Corrosion, and a Fatigue Failure.

BLADE VIBRATION, STRESS, AND LIFE ESTIMATION

There are, in general, two kinds of blading vibration—forced vibration and flutter.

Forced Vibration

Forced vibration arises from the movement of the rotor through stationary disturbances such as upstream rotor wakes, support struts, inlet distortion, or by forcing functions such as rotating stall. Analogous to rotor critical speed, forced vibration can lead to high stresses and failure when the excitation frequency coincides with the blade natural frequency. With forced excitation, almost all the sources (except rotating stall) must be harmonics of the rotating speed. It is this feature that permits representation by means of a Campbell diagram. Blade vibration can be caused by nonengine order excitation such as rotating stall at lower speeds, and flutter at higher speeds. Some engine orders are of greater importance than others, with lower engine orders potentially causing high excitation.

Flutter

Although relatively rare, and less predictable than forced vibration, flutter can occur in axial flow compressors. Flutter occurs at frequencies that are not multiples of engine order and at different locations on the compressor operating map. It can occur on either a few blades in a row, or with widely different amplitudes on individual blades. As amplitudes rise, flutter tends to encompass all blades at approximately the same frequency. Flutter typically manifests itself at the blade natural frequency.

Turbine and Compressor Blade Modes

Axial flow blading, centrifugal impeller vanes, and disks have a variety of natural modes (shapes of vibration). These modes occur at characteristic frequencies determined by the distribution of mass and stiffness, resulting from the variable thickness of the blade area. Currently, holographic testing methods are employed for determining and visualizing mode shapes.

Figure 12 (Harmon, 1979) shows mode shapes for axial flow compressor blades and disks. The simplest mode is the first flexural or first flap (1F) mode, where the blade acts as a cantilever bending in its weakest direction. At higher excitation frequencies, the blade may vibrate in the second flap mode (2F), i.e., with one stationary node. The flap modes may cause fretting in the disk rim as the blade root moves within its clearance. Torsional and axial modes occur at even higher frequencies. Turbine modes are similar to those depicted in Figure 12, but no pin-rolling modes occur as the blade attachment is typically a fir tree. A first edgewise (1E) mode of excitation can occur normal to the direction of the first flap (1F) vibration.
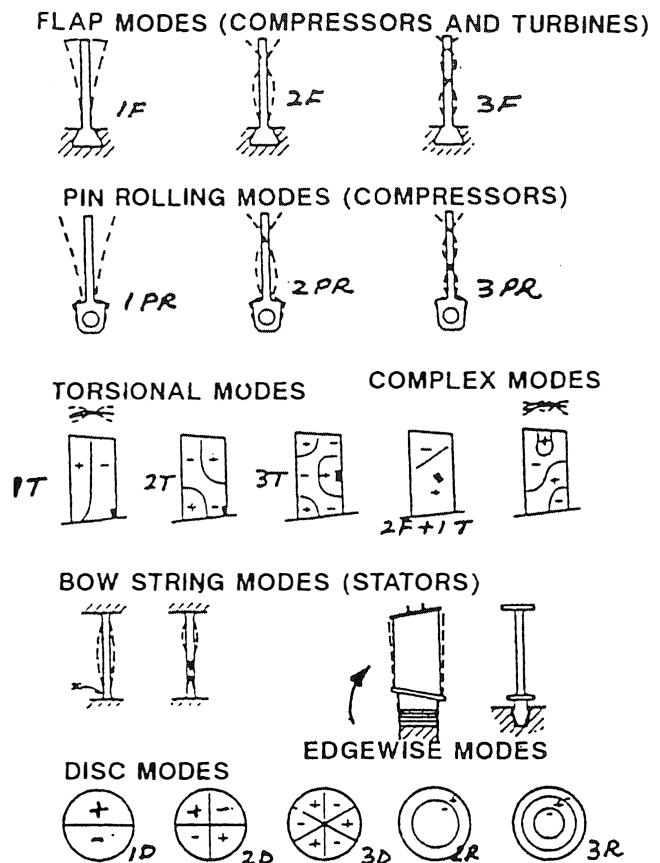

Figure 12. Typical Mode Shapes. (Harmon, 1979)

Blade Disk Vibration

Disks are prone to vibration either on their own or in the form of a rotor disk assembly. Combined blade/disk rim vibration modes also occur. Disk vibration can involve several nodal patterns. As disk vibration can excite blade vibration, attention should be paid to the location of blade failures with respect to the disk. Failures 90 degrees and 180 degrees apart indicate a two nodal diameter mode, and failures 60 degrees apart would indicate a three nodal diameter mode of vibration. This is one reason why, in the course of a failure investigation, the *angular location of the damaged blades with respect to the disk must be carefully documented and sketched, prior to deblading.*

Effect of Speed and Temperature on Natural Frequency

The natural frequency of rotor blade vibration is reduced with increasing temperatures (because of reduction in Young's modulus) and is increased at high speeds because of centrifugal stiffening. The manner in which the natural frequency is affected, depends on the mode under consideration. In a compressor, flap modes tend to rise (centrifugal stiffening effect) with rpm and torsional modes tend to drop with increasing temperature (reduction in modulus of elasticity). Turbine natural frequencies generally fall with an increase in speed, because there is a significant rise in temperature. Formulae for correcting natural frequencies due to temperature effects are provided in APPENDIX A.

Design Evaluation Tools

Campbell and Goodman diagrams are valuable design evaluation tools for troubleshooting blade failures. The Campbell diagram (also called an interference diagram) provides details on natural frequencies and the forcing functions at different operating speeds. The Goodman diagram provides a visual map of stress levels and the estimated limits. Gas turbine manufacturers consider this information proprietary and do not normally provide users with these data. The Campbell diagram can be developed by testing or by analytical methods. It is important for any user considering the use of a new or prototype turbine to insist on reviewing the blade dynamics with the OEM.

Campbell Diagram

A Campbell diagram depicts compressor or turbine speed on the abscissa and frequency on the ordinate. The natural frequencies for different vibration modes are drawn on the ordinate. Excitation frequencies (engine orders) including running speed and its four harmonics, strut-pass frequencies, stator pass frequency are shown on the diagram. The coincidence of natural frequencies with exciting frequencies creates a resonance condition. A typical Campbell diagram is shown in Figure 13. Intersections of the excitation lines with the blade natural frequency lines do not necessarily imply that dangerous vibrations will occur. A buildup of significant vibration and stress would require adequate strength of the stimulus, and appropriate phase and modal coupling. Additionally, the damping present would have to be insufficient to control the vibration.

The "SAFE" Interference Diagram

For resonance to exist, two conditions must be satisfied:

• A coincidence of the exciting force and the blade's natural frequency

• The profile of the exciting force should have the same shape as the associated mode shape of vibration.

The Singh's advanced frequency evaluation (SAFE) diagram is a visual representation of the frequencies of the exciting harmonics and the shape of the harmonics. This diagram permits the visualization of exciting frequencies and phase information. It has been successfully applied to bladed disk assemblies in steam turbines (Singh and Schiffer, 1982; Singh and Vargo, 1989).

Goodman Diagram

The Goodman diagram, shown in Figure 14, is commonly used to evaluate the mechanical integrity of blading. The abscissa of the diagram represents steady mean stress, while the ordinate represents the vibratory stress levels. The Goodman diagram shows a region of acceptable operation (beneath the curve) in terms of steady state and vibratory stresses. In the Figure, "A" represents a point where the steady stress is zero. Point "B" represents no alternating stress. Point "C" represents a hypothetical operating point. A numerical example is presented in APPENDIX A.
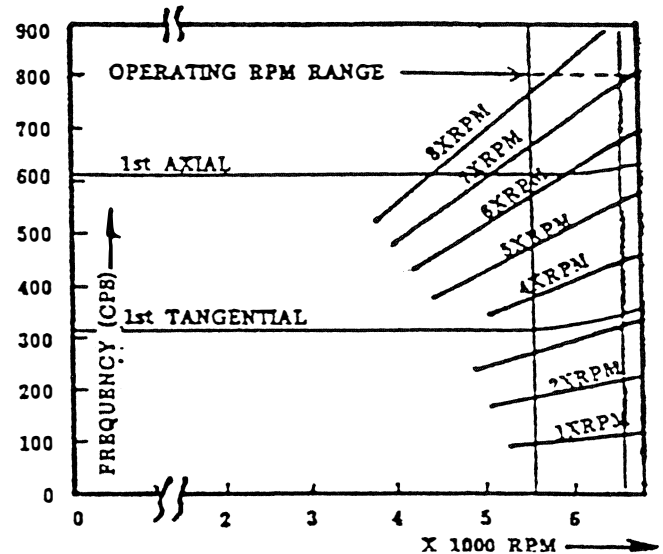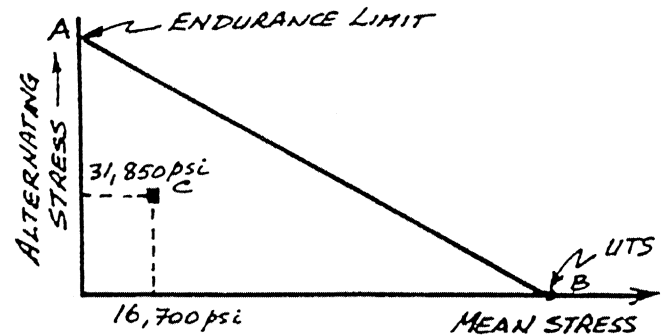

Figure 13. Campbell Diagram for Blading.

Figure 14. Goodman Diagram for Blade Stresses.

Stresses on Blading

The stresses on a blade include:

• Centrifugal stress.

• Gas flow induced steady state stress.

• Gas flow induced alternating stresses.

• Impact stresses caused by FOD.

For a detailed treatment, along with practical formulae of these factors, readers are referred to Sohre (1975), Sorensen (1951), and Dundas (1985).

Centrifugal Stress

Centrifugal force on blading can be exceedingly high, but is rarely the primary cause of failure. It can be a factor in the hot section of gas turbines in conjunction with creep effects. To minimize centrifugal bending stress, the centers of gravity of shroud, foil, root and root lands should ideally be located on a common radial axis. To get a feel for the values involved, the centrifugal force on a 25 inch blade operating at 3600 rpm will be 100 tons (the weight of 60 automobiles). The maximum centrifugal stress occurs at the blade root.

Gas Flow Induced Steady State Stress

Gas flow induced steady state stress is a bending stress superimposed on the centrifugal stress and is proportional to the blade loading (enthalpy drop across stage). The steady state stress

is shown as a horizontal line in Figure 15. In reality, however, there is considerable buffeting as the gas flows through successive nozzles, and this results in an alternating stress shown in the figure.
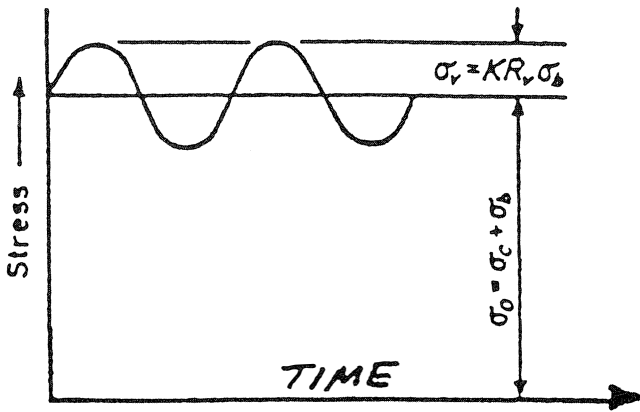

Figure 15. Blade Stresses. (Sorensen, 1951)

Gas Flow Induced Alternating Stress

Alternating stresses can be caused by:

• Stator nozzle wakes (NPF = number of nozzles × rpm).

• Mismatch of nozzle sectors at split line (2× rpm excitation).

• Pitch variations of nozzles or rotor blades.

• Wakes from support struts that can cause failures several stages downstream of the strut.

• Bowed nozzles causing flow distortion.

• Disk-blade vibration interaction.

Alternating stresses are often responsible for blade failures. Studies reported by Walker and Sommerfield (1987) based on strain gauge tests on gas turbine blades, indicated a doubling of alternating stresses with a blocked burner. Gross high pressure turbine nozzle blockage increased alternating stresses by a factor of five.

Foreign and Domestic Object Damage Induced Impact Stresses

Foreign object damage (FOD) is relatively rare in stationary gas turbines, but can occur with poorly designed inlets. In some isolated cases, parts of the combustor lining have loosened and been ingested in the turbine section. Domestic object damage (DOD) also occurs when an initial blade failure causes a destructive "blade salad."

Temperature Stresses

Blades are subjected to severe thermal stresses during transient conditions such as startup and shutdowns. A typical thermal-mechanical cycle for a first stage turbine blade is shown in Figure 16 (Viswanathan and Dolbec, 1986). This figure shows, qualitatively, the metal temperature and the leading edge mechanical strain variations. Thermal stresses are particularly severe in arctic environments where very cold air can come into contact with hot blade, after an emergency trip. Stress levels can reach 100,000 psi near the blade cooling holes during a shutdown.

In nozzle vanes, thermal stresses are induced due to nonuniform temperature distributions and restriction of the thermal expansion. The nonuniform distribution is typical of transient operation (in particular, full load trips). This is why multiple vane nozzles often develop thermal fatigue cracks.

Blade Failure Due to Overspeed

Overspeed is a relatively rare phenomenon in single shaft gas turbines where the axial compressor power absorption limits the
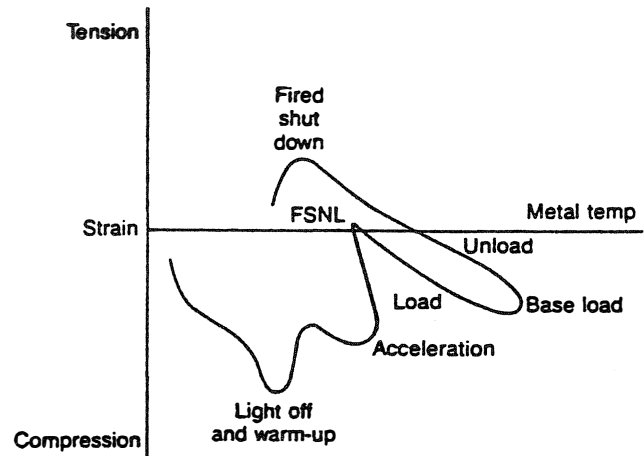

Figure 16. Typical Thermal Strain Cycle for a First Stage Blade. (Viswanathan and Dolbec, 1986)

overspeed excursion. Free power turbines can, however, experience overspeed. Overspeed is often limited by rotor stator contact resulting from the increased thrust loading. At an overspeed of 25 percent, stresses will be approximately 1.56 times their design value.

Blade Life Estimation

Blade life estimation is complicated by factors such as corrosive environment and presence of stress raisers. A comprehensive treatment of blade life estimation is made by Viswanathan (1989) and Rao (1992). This is a complex area where substantial analytical work is underway. On a practical level, there are two philosophies in use. The "equivalent hour" concept, used by some OEMs, expresses hot section life as a function of actual operating hours, number of starts and trips, and other operational profile information (for example, each start would add 20 hours). In this concept, the manufacturer provides an empirical equation that helps in estimating life consumption of hot section parts. This approach assumes that the damage mechanisms interact in a strong way. Other OEMs assume that while the interactions exist, they represent second order effects, and therefore base maintenance intervals on independent counts of number of starts and operating hours (for example, 24,000 operating hours or 1200 starts for a hot gas inspection). These calculations would be modified for varying fuel types and other factors such as water injection, peaking service, and emergency loading conditions. The basic equation for life consumption incorporating the creep and thermal fatigue terms is given by:

$$[T/T_f] + [N/N_p] < D \qquad (1)$$

Where:
T_f = Time to failure due to creep
N_p = Number of cycles to crack
D = Critical damage parameter, which would be 1.0 for superalloys and 0.75 for steels

Blade life estimation is an area far too complex to cover in this paper, especially when additional failure mechanisms are involved. Details of life assessment of turbine blades may be found in Hepworth, et al. (1997). Further details on blade life are available in Bernstein (1990), and Bernstein and Allen (1991).

EFFECTS OF AMBIENT TEMPERATURES AND FUEL SYSTEMS ON BLADING

Ambient Conditions and Blading Problems

Gas turbines operate in extreme temperature ambients ranging from −58°F (−50°C) to 140°F (60°C). This change in ambient

temperature causes a change in air mass flow and differences in aerodynamic blade loading. Clough (1987) describes an interesting case of intermediate pressure (IP) turbine blade failures on aeroderivative engines. Clough's investigations clearly showed the influence of very low ambient temperatures and their effect on blade loading. Ice ingestion is not an uncommon problem in gas turbines and can cause expensive primary and secondary damage to compressor blades. Due to the high intake velocity in the compressor (0.5 to 0.8 mach number), the drop in static pressure and temperature can cause icing conditions at temperatures approaching 40°F (5°C) and relative humidity of 70 percent. The formation of ice in the compressor inlet, or IGVs, causes damage by the following mechanisms:

• Distortion of inlet air flow. This could be due to physical ice buildup or due to uneven temperature at the compressor inlet face when exhaust gas is used for anti-icing.

• Physical FOD when a piece of ice is ingested.

There are a variety of anti-icing solutions including the use of compressor bleed air, direct use of exhaust gas to heat the inlet air, or the use of heat exchangers in the inlet using either glycol, low pressure steam, or exhaust gas. It is important to note that icing can also be caused by leaking evaporative coolers or due to water washing in a freezing environment. Further details on icing are available in Patton (1975) and Binek (1974).

Blading Damage Caused by Fuel and Combustion System Problems

Gas turbine hot section damage can occur due to the presence of liquids in the fuel gas, plugging of fuel nozzles, or due to internal gas turbine fires and explosions. The presence of hydrocarbon liquid can cause overfiring, either in all or a few combustion chambers. The presence of liquid hydrocarbons in natural gas depends on the temperature and pressure of the gas. Despite precautions, it is not uncommon for natural gas to entrain liquids. Liquid carryover from pipeline gas scrubbers can occur due to:

• Foaming.

• Gas flow and pressure that exceeds scrubber capacity.

• Improper operation of a centrifugal separator.

• Surges in liquid due to rapid fluctuations in gas pressure.

Liquids have different volumetric heating values and have different flow characteristics in piping and fuel nozzles. Thus, when liquids are present in natural gas, gas turbine performance is affected depending on the concentration of the liquid to gas. At low concentration levels, the liquid is typically in aerosol form and the turbine control system will react by reducing fuel flow due to the apparent higher heating value of the fuel. The flame will change color from transparent blue to a luminous flame, with a color ranging from yellow to red. This can also occur if iron sulfide or sodium compounds are present. With liquids in the fuel, the combustion may be rough, resulting in gas supply pipe vibration causing wear of transition pieces or manifolds. At moderate liquid concentration levels, the liquid gets segregated due to inertia effects and is unevenly distributed to the fuel distribution system. The control system may then behave in an unstable manner because of exhaust gas temperature variations. Combustion imbalance from one combustion chamber to another can cause high exhaust gas spreads in excess of 80°F (45°C), which have a damaging effect on the blades. If a significant level of liquid is present in the gas (causing the heating value to be greater than 110 percent of the nominal value), then rapid destruction of hot gas components can occur. Exhaust gas temperature spreads can get exceedingly high and, in extreme cases, rotating blades can melt. If the melting is uniform, the vibration levels may not increase. Complete hot gas path destruction can, at times, occur in a period of five to 10 minutes. Damage due to liquids in the natural gas fuel can include:

• Transition piece failures (greater cyclic stresses due to liquids being introduced intermittently, causing pressure pulsations). At times, seals rupture allowing compressor discharge air to enter at the first stage nozzle. This can cause severe temperature distortion that has a deleterious effect on the blades. Unburned liquid droplets can ignite, creating a flame near the stator nozzle.

• Thermal distress of blading (caused due to a distorted temperature profile).

• Compressor surge (due to rapid increase in back pressure).

It is therefore exceedingly important for natural gas fuel to be properly treated *and have a superheat temperature of at least 50°F above the hydrocarbon or moisture dewpoint.* Some rules of thumb pertaining to gaseous fuel treatment have been provided in APPENDIX A.

Low Fuel Nozzle Pressure Ratio and Excessive Pressure Fluctuations

The combustor fuel nozzle tip acts as a metering orifice. The fuel nozzle pressure ratios (FNPR) are defined as:

FNPR = (fuel gas pressure)/(combustor liner pressure)

Excessive pressure fluctuations in the combustor liner would propagate upstream into the fuel nozzle. These pressure pulsations, coupled with low fuel nozzle pressure ratios, cause a high variation in the fuel flow and heat release. Pulsations can damage hot gas components. Liquids in the fuel can contribute to a lower fuel nozzle pressure ratio. The liquids cause an increase in the heating value per unit volume. Consequently, a smaller volumetric flow is required. The reduction in flow results in lower nozzle pressure ratios that further compound the pulsation problems.

Liquids in natural gas fuel can result in a distorted gas temperature profile and hotter metal oxidation temperatures. Liquids following through the gas side of the fuel nozzle do not follow the gas streamlines, and tend to concentrate along the axial centerline of the combustor. The temperatures are also considerably hotter and combustion occurs farther downstream than with dry gas, and the gas does not get cooled with air from the combustion liner cooling holes. As the products of combustion go through the transition piece, the profile distorts and the peak temperature is near the outer radial edge.

Slugs of liquid hydrocarbons in the gas stream can promote compressor surge. This is because the liquid hydrocarbon has a volumetric heating value of 1,500 times the heating value of a comparable volume of fuel gas. The slug of liquid hydrocarbon thus results in a rapid temperature rise (additional caloric input) and an accompanying rise in combustion pressure. This transient back pressure increase moves the operating line toward the compressor surge line.

Problems in the fuel system that can cause blockage of the fuel nozzles will also cause severe vibratory stresses on the blades. Excessive coking on the fuel nozzles (Figure 17) will cause:

• Higher pressure to occur on the other fuel nozzles, which will cause the flame to move downstream in the combustor, as depicted in Figure 18.

• Flow and temperature distortion that can damage the turbine.

Balancing the nozzle flow to less than four percent is recommended and will have a long term benefit to the operation of the turbine.

It is important to note that the blockage of the fuel nozzles may also be due to external factors, such as the debris derived from the fuel filters. It is most important to have a means for detecting such problems by an EGT monitoring system that examines qualitative pattern changes and not just absolute limits.
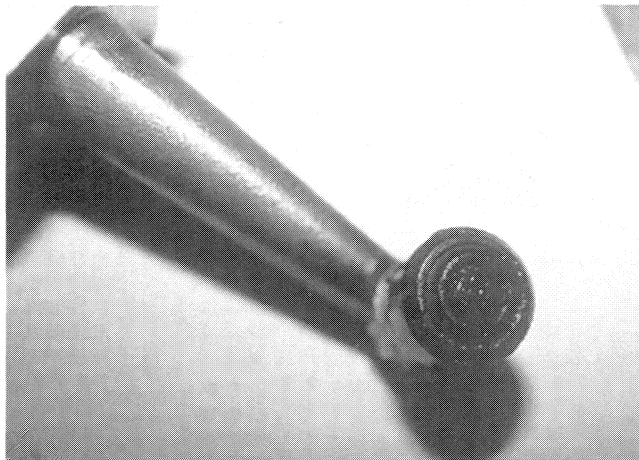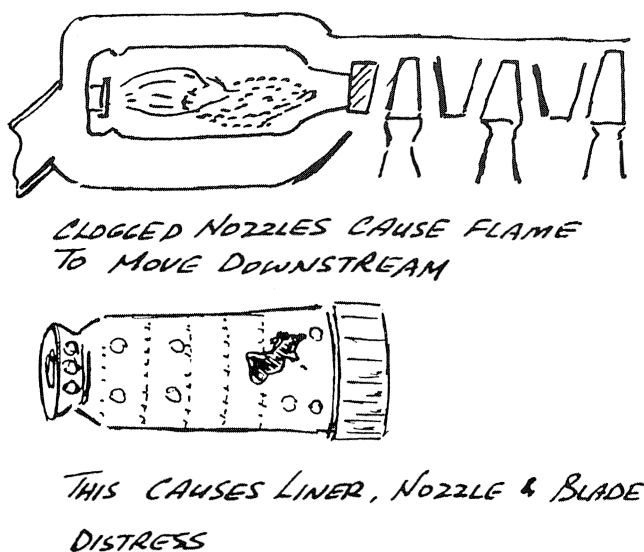
Figure 17. Coking of Fuel Nozzle.

CLOGGED NOZZLES CAUSE FLAME
To MOVE DOWNSTREAM

THIS CAUSES LINER, NOZZLE & BLADE
DISTRESS

Figure 18. Coked Fuel Nozzles Can Cause Flame to Move Downstream Causing Undesirable Temperature Spreads, Overheating, Liner, and Blade Damage.

Internal Fires and Explosions

Explosions occur when fuel is injected into hot engines and uncontrolled ignition occurs causing extensive blade damage. Dundas (1988) lists four potential situations:

• Fuel is injected into a hot engine and does not ignite as intended, but ignites when it comes into contact with hot internal surfaces. Autoignition can occur in the combustor, the turbine section, or the exhaust duct. The autoignition temperature of No. 2 fuel oil is around 500°F (390°C).

• Flameout that occurs when engine is in normal operation. If fuel continues to flow, it may reignite when it touches hot internal surfaces.

• During switchover from liquid to gaseous fuels. Improper purging of the original fuel or improper scheduling of the valving can cause an explosion in the combustion section.

• Fire at the bottom of combustor where liquid fuel collected after shutdown and, for some reason, was not drained. The pool of liquid is ignited by hot gases during a subsequent start. Dundas (1988) points out the importance of shutting off fuel very rapidly and indicates that an *upper* limit of 500 msec is required (ideally <150 ms).

Fires in the turbine enclosure can result in casing distortion causing blade rubs. If fine water sprays are utilized to control the fire, care must be taken to avoid case distortion and consequent tip rubs. Figure 19 shows a photograph of burnt first stage gas generator turbine blades due to a fire caused by fuel.

Figure 19. Burnt Blading Due to Fire in Turbine Section (Fuel Accumulation in Combustors).

Case Study—Fuel System Related Turbine Blade Failure

This case involved a heavy duty gas turbine in 50 Hz power generation service burning heavy fuel. The failure occurred in the third stage turbine. The blades were equipped with an integral shroud at the outer tip diameter. Each shroud was interlocked with the adjacent blades to resist the natural tendency of the blade to untwist with centrifugal force and the effects of airflow. The machine normally ran on a blend of bunker fuel and high speed diesel. When a trip occurred, the fuel left in the piping tended to solidify unless removed while still warm. After a normal shutdown, the procedure followed was to allow the turbine to coast down to a normal stop and then accelerate it on the starter to crank speed, while the fuel line was purged with high speed diesel. The fuel was expected to drain from the machine during the purge cycle.

On the day of the failure, the machine tripped and a purge cycle was initiated. An exhaust gas temperature (EGT) scan made indicated a maximum temperature of 1346°F (730°C), which was much higher than the expected 932°F (500°C). An EGT spread of 500°F (277°C) was also noted. The exhaust gas temperature profile that occurred is shown in Figure 20. Blade metallurgical analysis confirmed that catastrophically high temperatures had been reached. A gamma prime phase modification was found in the microstructure of the blade material.

This high temperature occurred as the engine took fire (autoignition) in an uncontrolled manner, with a fire occurring in the third stage blade area of the machine. The tip shrouds of the
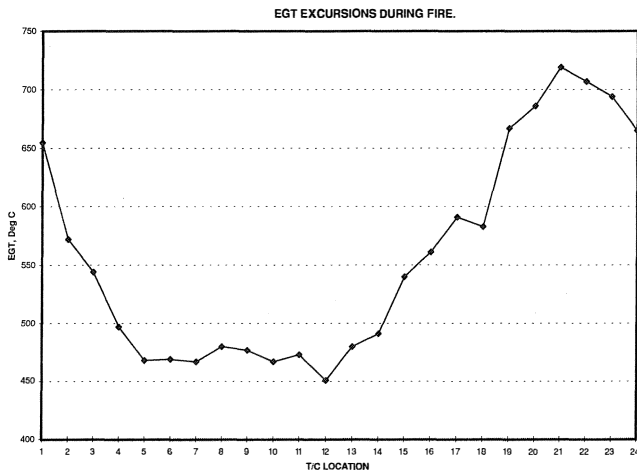
Figure 20. Exhaust Gas Temperature Profile Distortion During Fire (Showing Temperatures as High as 730°C).

blades tipped forward (as depicted in Figure 21) due to the rapid temperature change. The strength of the blading was severely reduced, due to the elevated temperature. Because the tip shrouds were displaced, the natural frequency of the blades were modified to a much lower value. This change in natural frequencies caused a blade fatigue failure. The solution of this problem addressed the modification of fuel purging procedures to ensure that no fuel accumulation could occur.
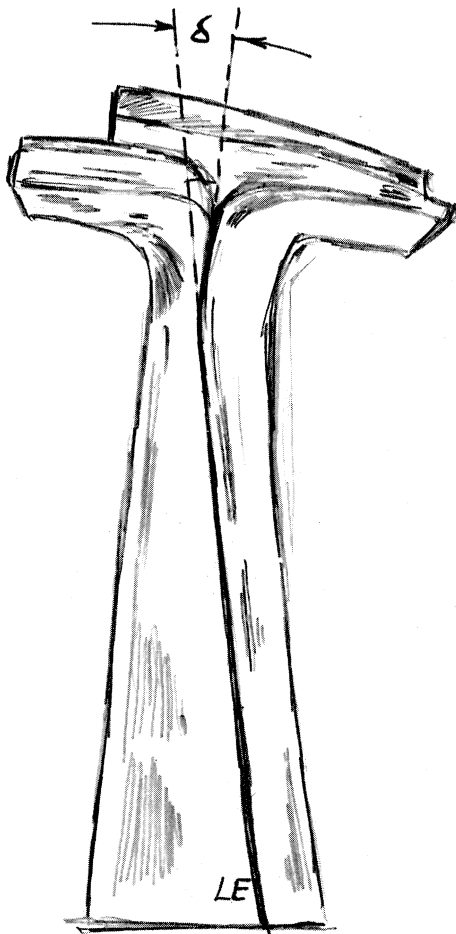

Figure 21. Tipping Forward of Blade Shrouds Due to Fire in Turbine Section.

MANUFACTURE AND QUALITY ASSURANCE

Several gas turbine users utilize the services of non OEM vendors for the manufacture of blades. Whereas several reputable vendors can match the design and quality of the OEM, one has to be exceedingly careful of quality control aspects, especially when it comes to blade redesign. Particular attention should be paid to:

• Writing of tight specifications. The user should institute rigorous checks and monitor the repair quality.

• Even if blades are "replicated," care should be taken that uprates (increased blade loading, speeds, etc.) have not occurred over the years. Very often the OEM has incorporated experiences from failures into upgrades that third party suppliers may not know about.

• If blades are refurbished, it is exceedingly important to clearly specify the procedures and acceptance criteria that one expects, including the procedures for part preparation, coating stripping, heat treatments, and flow checks that are to be done for air cooled components.

Case Showing Importance of Manufacturing Techniques

This case describes a failure of the inlet guide vanes (IGVs) of an axial flow with blades made from 403 stainless steel. Two adjacent inlet guide vanes had failed in fatigue, causing secondary damage to the compressor. All parties agreed that the failure mode was fatigue. Two adjacent inlet guide vanes were damaged. One of the broken airfoils was ingested in the compressor, while the other dropped into the inlet duct.

The OEM conducted experimental tests to determine stress levels and natural frequencies, and concluded that there was no design problem and that the failure occurred due to "poor operation" (specifically, extended operation of the compressor in the surge regime).

A metallurgical investigation of the failed parts, however, indicated that fabrication procedures for the IGV (SS 403 material) did not include preheating or stress relieving, thereby resulting in very brittle metal at the joint (which the OEM claimed was to avoid blade warpage). Brinell hardness numbers were found that were approximately double the number called for by the OEMs specifications. Examination of the welds revealed significant martensite formation in the heat affected zone adjacent to the weld deposits. Cracks were found perpendicular to the weld deposits. The martensite zones had minimum ductility and toughness, and were subject to fatigue failures. There was also significant residual stress present, due to welding being done without preheat and postheat treatment. There was also evidence of pitting corrosion occurring at the edge of the heat affected zone.

There were two other factors that exacerbated the problem. First, the IGV attachment system could come loose, causing the blade fixation to change. Second, there was some evidence that the IGV angles were not uniformly set, which resulted in considerable wake excitation. This case is, therefore, characteristic of several blade failure situations. No single "cause" could be found and a *combination* of factors caused the failure.

AXIAL COMPRESSOR BLADING PROBLEMS

Problems related to vibration and failures in compressor airfoils include:

• Dynamic excitation (high cycle fatigue).

• Axial compressor surge.

• Rotating stall and flutter.

• Blade rubs.

• Foreign and domestic object damage (FOD/DOD).

• Migration of blades.

• Root attachment problems.

• Erosion.

Ideally, compressor blades should possess low density/high stiffness, a high strength/weight ratio, and adequate resistance to corrosion, impact, foreign object damage, fretting, moisture, erosion, and thermal fatigue. Compressor blades have to withstand conditions of surge, rotating stall, and unsteady flow created by inlet distortions. Even with adequate factors of safety, operating conditions may exceed the envelope foreseen by the designer. While temperatures are not severe in an axial compressor, the rear compressor stages of high pressure ratio gas turbines experience high temperatures, and creep resistance becomes an important attribute. It is interesting to note that modern compressor discharge temperatures are approaching the early Whittle jet engine turbine inlet temperatures. Several aeroderivative engines and heavy duty reheat engines have pressure ratios of 30:1. Haskell (1989) provides a detailed overview of the interplay between the compressor operating environment and material evaluation.

Common Causes of Axial Compressor Blading Vibration

Common causes of vibration causing high cycle fatigue of axial flow compressor blades are:

• Stator passing frequency wakes.

• Inlet guide vane created wakes.

• Rotating stall.

• Surge.

• Choke.

• Wakes caused by inlet or diffuser supporting vanes struts.

• Inlet flow distortion (low order, i.e., second, third, and fourth order harmonics).

• Blade flutter.

• Variation in blade tip clearance.

• Rotor vibration (mechanical origin).

• Wakes created by front bearing support struts.

• Beat frequencies caused by the difference in stators upstream and downstream of a blade row.

In a discussion of compressor airfoil reliability, Passey (1976) states that safe alternating stress levels for compressor airfoils are relatively low—10,000 peak-to-peak lb/in^2 for aluminum alloys and about 25,000 peak-to-peak lb/in^2 for titanium alloys and steel. Reasons for these low levels include:

• Presence of surface imperfections. These can be created during manufacture or be the result of foreign object damage. Compressor coatings can help here.

• Notch sensitivity effects.

• Temperature effects on fatigue strength. For example, a typical 12 percent chrome steel will show a 10 percent reduction in fatigue and tensile strength at a temperature of 752°F (400°C). This effect is important in high pressure ratio compressors.

Practical details on compressor vibration are provided in Armstrong and Stevenson (1960).

Axial Compressor Surge

Compressor surge has been the root cause of several compressor blade failures often mistakenly attributed to FOD. If prolonged surge occurs, the blades can be severely damaged because of the excitation caused by flow reversals. Further, rapid speed changes (cycling) can occur as the unit is loaded and unloaded, and several stages pass through resonance conditions experiencing severe vibratory stresses.

A typical axial compressor map is shown in Figure 22. The abscissa is a flow parameter (corrected airflow), while the ordinate is the pressure ratio. Line "AB" depicts the compressor flow

characteristic at a given corrected speed. Point "B" represents a choke point. As the system resistance increases, the operating point moves up the curve toward the surge line. This is exactly what happens as the turbine is loaded from full speed no load (FSNL) conditions, with the increased fuel flow and heat release resulting in a higher back pressure. The rotating stall region is also shown on the compressor map and occurs at low flows and speeds. Surge can be caused by:

• Movement of the operating line to the left (i.e., into the surge region). This can be caused by overtemperature, turbine nozzle blockage, excessive back pressure, or malfunction of the blowoff valves during startup. Excessive steam injection can reduce the surge margin.

• Movement of the surge line *itself* toward the operating line. This could be caused by excessive compressor fouling deterioration, plugged air filters, or erosion. The erosion of compressor blades can affect boundary layer development and increase the tendency toward flow separation on the blade surfaces. Stall can therefore occur at lower incidence angles than with smooth compressor blades. Heavy erosion causes a reduction in blade tip chords, thereby reducing blade tip solidity, which adversely affects stage stability.

• Movement of *both* the surge line and the operating line.

Surge control on most single shaft gas turbines is accomplished by the use of interstage bleed valves that open at part speed; typically less than 95 percent of operating turbine speed. The control system keeps the compressor operating line sufficiently away from the surge line during full speed operation.
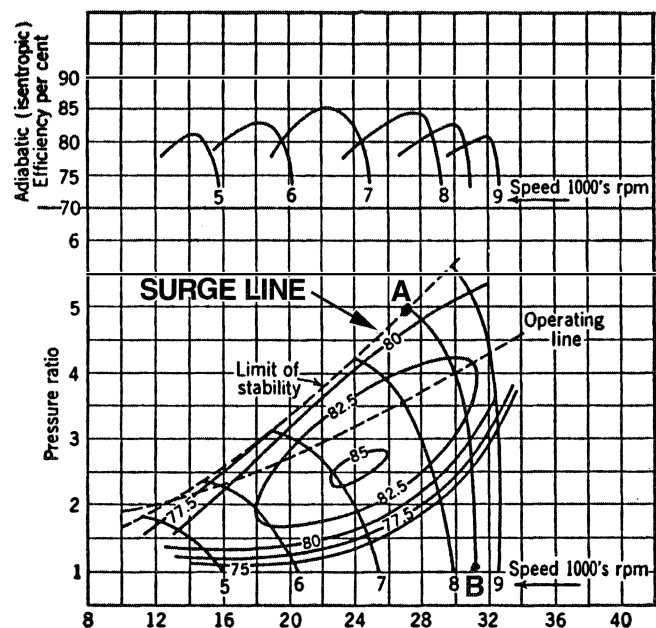
Figure 22. Axial Compressor Surge Map. (Compressor surge is often the underlying cause of blade failures mistaken and dismissed as foreign object damage.)

Surge problems can be accentuated in combined cycle/cogeneration gas turbines and in steam injection applications (Dundas, 1988). In combined cycle operation, HRSG superheat conditions to the steam turbine are maintained at part load by IGV control. The IGVs are modulated to restrict airflow in order to maintain the EGT and this reduces the surge margin. In the case of steam injected gas turbines, the increased back pressure moves the operating line to the left toward the surge line.

Blade Clash and Clang

Blade "clash" and "clang" are descriptive terms applied to damage in the compressor that typically results from surge. Clashing is the term given to stator-rotor contact due to the high blade deflections caused by the surge event. Blades clash with the trailing edges of the prior stator vanes. This often results in a characteristic triangular impact mark on the vane as shown in Figure 23. Blade clang occurs when groups of rotating blades deflect, causing the tip trailing edges to strike the leading edges of the adjacent blades on the pressure sides (Dundas, 1993b; Walker, 1987). Damage caused due to a clash failure is shown in Figure 24. A photograph of a stator blade that failed in fatigue is shown in Figure 25.
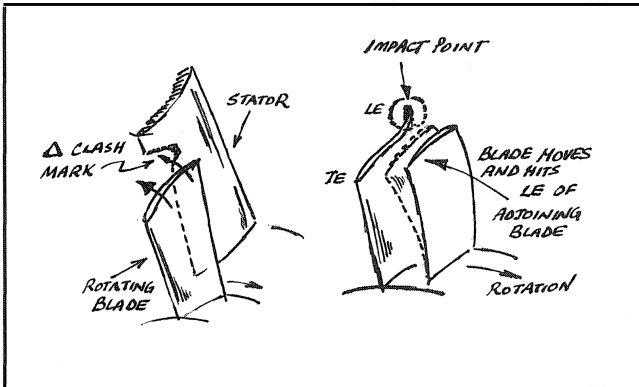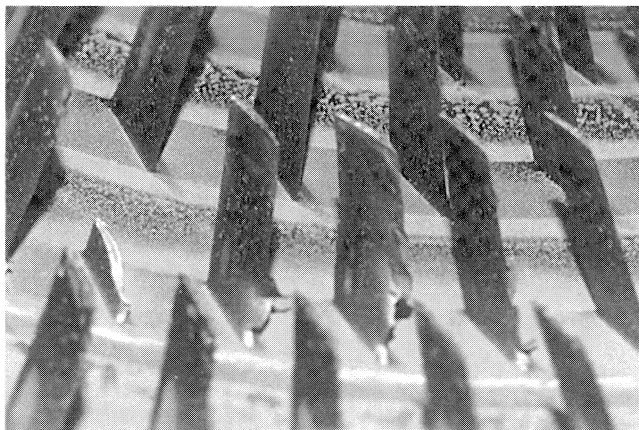

Figure 23. Blade Clash and Clang.

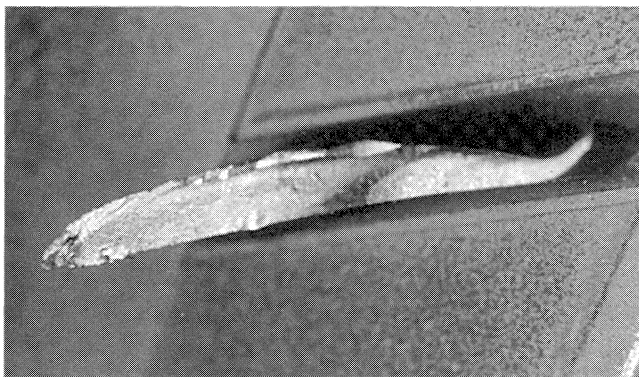Figure 24. Damage Caused Due to Clash Failure. (Stator fatigue failure can also be seen.)

Figure 25. Fatigue Failure of Airfoil.

Inlet Distortion and Its Effects on Axial Compressor Blading

There have been several cases where excessive inlet airflow distortion has triggered a surge event resulting in compressor blade damage. Uneven inlet circumferential distortion can be created by icing of IGVs or inlet structures or by uneven filter clogging. Improperly designed inlets, excessively fouled IGVs or struts, or unequal IGV angle settings can induce severe axial flow compressor airflow distortion and promote rotating stall that could lead to a "deep surge."

Studies reported by Schweiger (1983) have resulted in criteria to ensure distortion free air distribution to help avoid surge problems and excessive excitation of the first row of compressor blades or variable IGVs. Schweiger provides guidelines for intake geometry design, showing acceptable distances for the intake boundary walls from engine flare and centerline. If walls are brought too close to the engine inlet, strong vortices can be generated that can result in blade vibration.

In an inlet duct for a gas turbine, there is a natural variation of inlet static pressure due to the physical shape of the duct. The axial velocity in the upper sector of the axial flow compressor will be higher, because there is less resistance to flow compared with the lower sector (Figure 26). This sort of distortion can induce harmonics of the first through fourth order (Dundas, 1988). Compressor blades should be designed so that there are no critical resonances in the operating range or with any strong harmonic of the circumferential distortion.
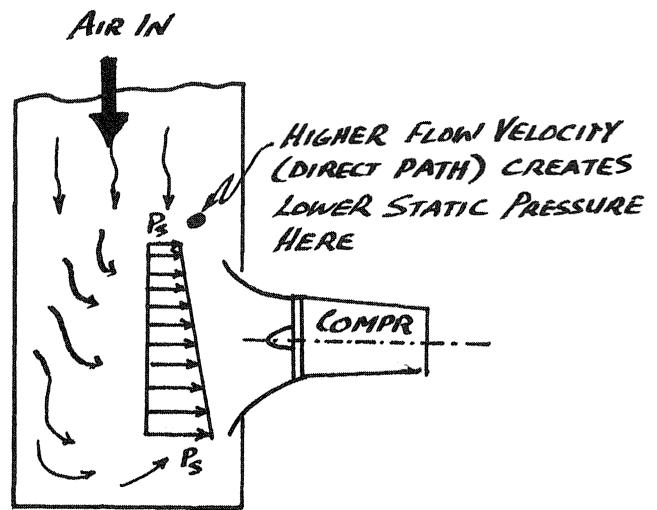

Figure 26. Static Pressure Distortion Due to Inlet Duct Configuration.

Rotating Stall, Individual Blade Stall, and Stall Flutter

There are three distinct stall phenomena—rotating stall, individual blade stall, and stall flutter. Rotating stall and individual blade stall are aerodynamic phenomena. Stall flutter is an aeroelastic phenomenon. A detailed treatment of compressor surge and stall is made by Pampreen (1993).

Rotating Stall

The basic mechanism of rotating stall is shown in Figure 27. Rotating stall (propagating stall) occurs when large stall zones cover several blade passages and propagate in the direction of rotation. The number of stall zones and the propagation rates vary considerably. Occurring typically at a frequency of 30 percent to 70 percent (45 percent to 55 percent is typical) of running speed, rotating stall can lead to increased vibratory stresses and cause blade resonance, if the exciting frequency or an integral multiple coincides with the natural frequency of the

blade. The blade that is closest tuned to the stall propagation speed will go into resonance. In general, the lower the order of the harmonics, the higher the stress levels. According to Allianz (1978), ratios of natural blade frequency to a maximum rotational frequency of 4.5:1 or higher will not normally cause blade failure. Rotating stall can occur in *both* axial and centrifugal flow compressors.
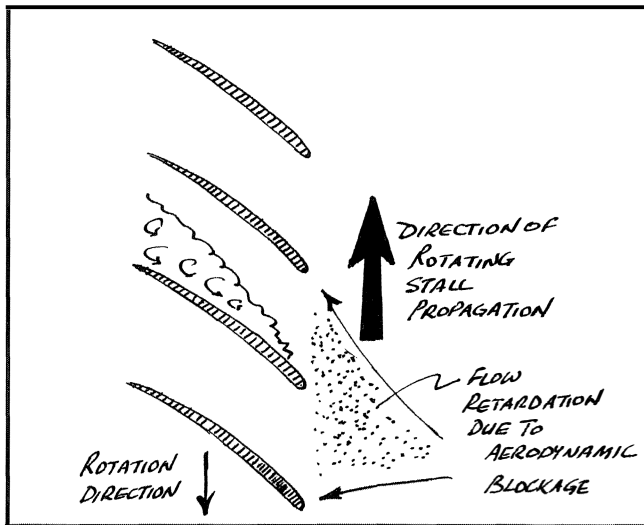

Figure 27. Mechanism of Rotating Stall.

The accurate prediction of rotating stall frequency is very difficult; hence, it is not possible to tune blades to accommodate a range of stall frequencies that may be encountered. One of the best ways of preventing rotating stall is by careful operation at low speeds. Often, part speed operation results in lower densities in the rear stages (due to the lower pressure ratio), which causes velocity in the rear compressor stages to go up, causing choke. This limits the flow in the inlet stages, increasing the angle of attack on the early stages, causing a stall condition. A detailed treatment of rotating stall as it afflicts axial compressors is made by Day and Freeman (1993) that shows that even at high speeds, surge is precipitated by rotating stall.

Individual Blade Stall

Individual blade stall occurs when all the blades around the compressor annulus stall simultaneously, without the occurrence of a stall propagation mechanism. It appears that the stalling of a row of blades generally manifests itself in some type of propagating stall and that individual blade stall is an exception.

Stall Flutter

This phenomenon is caused by aeroelastic self-excitation of the blade, and differs from classic flutter (classic flutter is a coupled torsional-flexural vibration that occurs when the free stream velocity over the airfoil section reaches a certain critical velocity). Stall flutter is a phenomenon that occurs when stalling of flow around a blade creates Karman vortices in the airfoil wake. When the frequency of these vortices coincides with the natural frequency of the airfoil, flutter occurs.

At stall conditions, a sudden decrease in lift occurs, upon which the aerodynamic damping reduces (or becomes negative). The blade movement then accentuates the instability, which creates a self-excited oscillation. While stall flutter problems are relatively rare in industrial gas turbine compressors, some studies have indicated that it can cause blade excitation.

From an operation standpoint, it is important to avoid operation of the gas turbine with high blade incidence angles. Figure 28

shows a flutter map. The ordinate is known as the critical reduced velocity parameter given by:

$$P_{cr} = V/(bf_n) \qquad (2)$$

Where:
b = Blade chord length
V = Air velocity
f_n = Blade natural frequency

The abscissa is the incidence angle. Two flutter boundaries can be seen—the choke and stall flutter boundaries. Operation should be between these two boundaries. Improper adjustment or misscheduling of inlet guide vanes can cause transgression into either of the flutter regimes. Alternatively, a reduction in flow will cause a change in relative velocity.
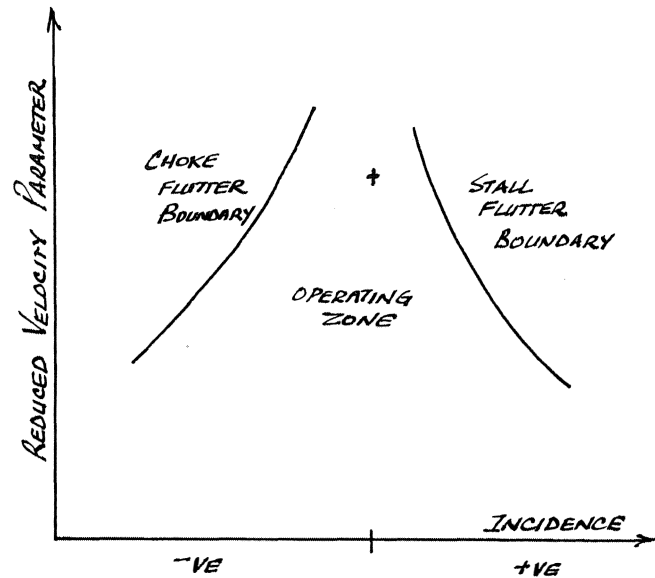

Figure 28. Flutter Map.

Compressor Fouling and Its Effects on Blading Integrity

Gas turbine engines ingest large quantities of air. In a day, a 160 MW gas turbine will ingest 82 million lb of air. Consequently, if foulants are even in the ppm range, a substantial quantity of foreign material will be deposited on the compressor aerodynamic surfaces (typically on the inlet guide vanes and early stages). The problem is worsened by internal oil leaks from the compressor end bearing or by the ingestion of exhaust. Compressor fouling causes changes in blade roughness and blade profile, and a mismatch between the compressor and the turbine. Consequently, the mass flowrate and efficiency of the compressor will drop, resulting in diminished turbine output and thermal efficiency. A treatment of fouling effects, detection, and control is provided in Meher-Homji (1990). Interesting theoretical and experimental findings on compressor fouling have been published by Saravanamuttoo and Lakshminarasimha (1985), Lakshminarasimha and Saravanamuttoo (1986), Dundas (1986), and Zaba (1980). Fouling can contribute to blade failures by the following mechanisms:

● By promoting surge or rotating stall, which might have a dangerous effect on blades.

● In some cases, blading natural frequencies can be affected by the increase in mass due to dirt build up on the airfoil ($f_n = \sqrt{(K/M)}$). A well known case of this occurrence was on a very early Avon turbine where extensive fouling (1/8 inch deposits) pulled the fourth stage's blade first natural frequency down into the running range (*Turbomachinery International*, 1985).

• Excessive dirt on the blades can cause unbalance and an increase in running speed vibration. In some cases, dirt can get between the bearing surfaces of the blade root, causing the blades to operate in a deflected position, which adds to the stresses. If the root constraint is changed due to buildup in the fir tree region, a change in natural frequency could result as the boundary condition changes.

• Foulant buildup on compressor blades can lead to serious corrosion and pitting problems in a salty environment, especially when humidity is high, because of galvanic action. Blade pitting can lead to local stresses that reduce blade fatigue life. Some estimates state that 25 percent to 50 percent of all fatigue failures are initiated by a pit or nick due to FOD. This problem will occur if salt water or salt particles are ingested in the compressor. The dry salt or brine will absorb moisture during high humidity operation or during water washing.

• Small foulants in the two to five micron range can cause blockage in the turbine section cooling holes.

Compressor Foreign and Domestic Object Damage

While FOD is not as serious a problem in industrial gas turbines as it is in aircraft engines, there have been instances where ingestion has occurred. Metallic items such as nuts, washers, etc., can cause both primary and secondary domestic object damage to compressor stages. It is good practice to install a screen prior to the compressor inlet. Some engines require the use of a nylon mesh sock that can be added to the inlet screen. Small ingested items may cause dents or tears, which could then be the initiating point of fatigue cracks. Small marks can be removed by filing and polishing following the OEMs guidelines. Nicks are particularly a problem if they occur below the pitchline. With the ingestion of an external object into an axial flow compressor, the first few stages will bear the brunt of the impact. The level of damage tolerance that is built into an engine involves a trade-off between aerodynamics and mechanical strength. Axial compressors operate at high tip speeds up to 1500 ft/sec (500 m/sec), with early stages often operating transonic. The sharp transonic blade profiles (much thinner than the rugged NACA 65 series blades) are more susceptible to FOD. Brown (1977) describes compressor design features to minimize foreign object damage.

While in most cases FOD will occur via the compressor inlet, there have been cases of entry of components via variable bleed valves used to unload the compressor during start or under emergency trip situations. It is therefore important that this be closed during maintenance shutdowns.

The result of FOD on a gas turbine compressor rotor is depicted in Figure 29. The fracture surfaces of an FOD failure are typical of impact overload and display a "candy rock" appearance as shown in Figure 30. Some relatively minor FOD damage on a turbine stator vane is shown in Figure 31. It is important to note that often the *root cause* of the problem is lost when a pronouncement is made that the damage is due to FOD. Unfortunately, FOD tends to become a "catch all" failure mode when no other clear explanation exists.

The ease with which FOD can be detected is a strong function of the *extent* of the FOD. In some cases, a step change in vibration (typically synchronous, i.e., 1× rpm) may be noticeable. In others, a drop in performance may be noted with FOD, but discriminating between FOD and other kinds of compressor deterioration may not be easy by the use of gas path analysis.

Blade Rubs

Several failures relating to gas turbine blades are caused by radial and axial rubs between rotor and stator components or seals. There can be several reasons for a rub, including stator misalignment, rotor whirl, casing distortion, excessive creep, or operational problems such as surge.
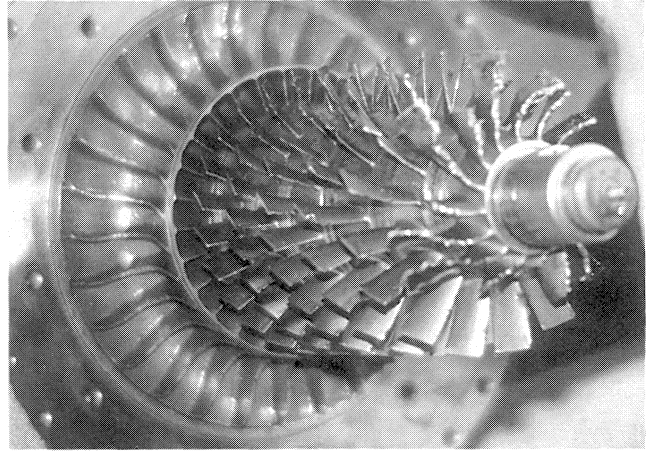

Figure 29. Massive Destruction on a Compressor Rotor Due to FOD.
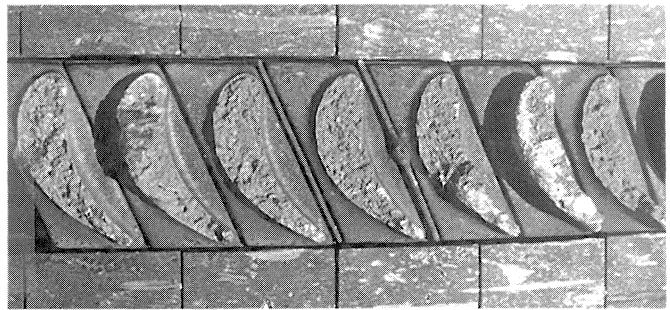

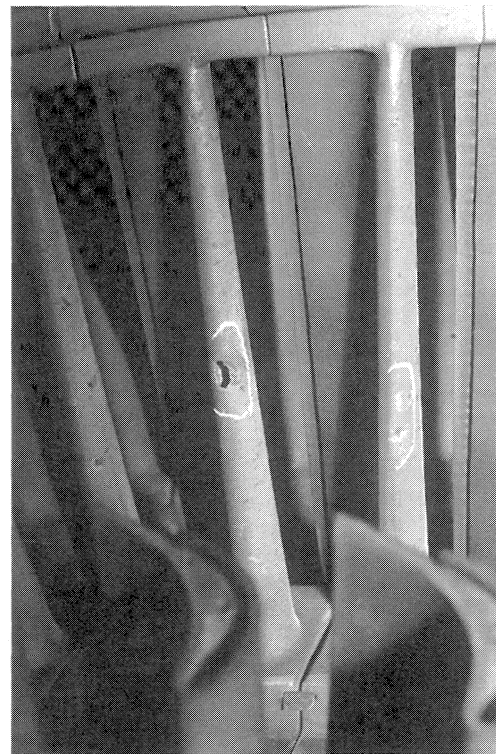*Figure 30. Typical "Candy Rock" Appearance of Damaged Surface with Impact Overload Type FOD Damage.*

Figure 31. Hole in a Stator Vane of a Large Gas Turbine Caused Due to DOD (failure of a single first stage blade).

Axial Blade Rubs

Axial rubs (rotor to stator contact) can occur due to several reasons including:

- Uneven casing or rotor thermal expansion.

- Startup or shutdown temperature transients.

- Failure of blade locking mechanism causing blade "migration" or "walking."

- Blade bending caused by surge (blade clash).

- Excessive creep in the hot section.

Radial Blade Rubs

A common type of blade tip rub is caused by excessive differential expansion of the rotor and casing components during a transient event (shutdown, emergency trip, startup, etc.). Restarts from an emergency shutdown can cause blade casing rubs or even blade failure. It is therefore important to follow OEM guidelines regarding putting the unit on crank, time within which a hot start is permitted, etc. In the case of some aeroderivitive gas turbines, one may have to wait several hours prior to an engine restart. Rubs can also result from blade elongation due to high temperature creep.

A rub on the tip of an axial flow compressor is shown in Figure 32. A severe radial blade tip rub is shown in Figure 33. The blade tip shroud has been severely rubbed in this case.
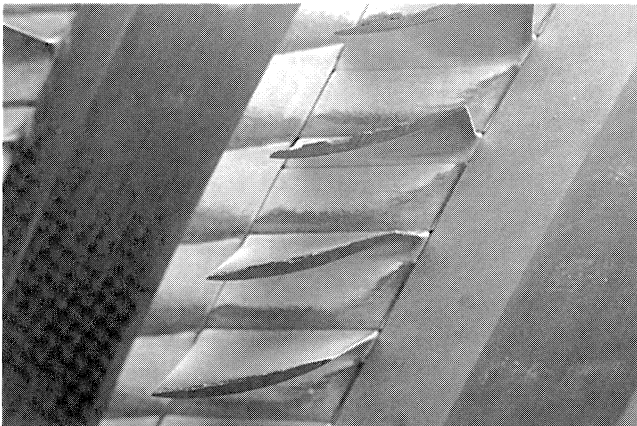

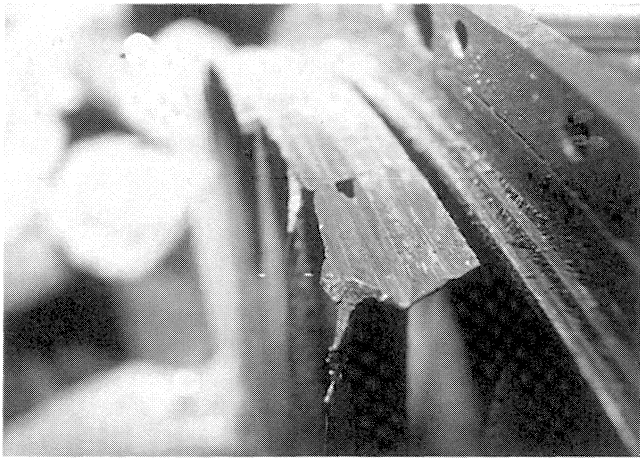*Figure 32. Blade Tip Rub on a Gas Turbine Axial Flow Compressor.*

Figure 33. Severe Shroud Tip Rub in Turbine Section of an Aeroderivative Gas Turbine.

Detection of Rubs

Radial blade rubs can be detected by observing a growth in the vibration spectrum at rotor subharmonic, subsynchronous vibration at the rotor natural frequency, and highly time dependent behavior at running speed and its harmonics. New diagnostic tools are under development for measurement of blade tip clearance.

Migration or "Walking" of Compressor Blades

Blade migration ("walking") is a phenomenon that has occurred in some large gas turbines. Migration refers to a situation in which blades move in their locking slot due to failure of the lock mechanism. As the blade moves, it touches the adjacent stator causing serious damage. A common cause for blade migration is tip rubs that occur because of thermal growth during gas turbine transients. With severe tip rubs, blade anchoring pins may break, permitting the blade to migrate along its slot.

In some situations, users have reported that compressor blades that have corroded in place (when disks are not made from high alloy steel) have not experienced blade migration. The effectiveness of the locking pin cannot, however, be checked without breaking the corrosion. The solution to blade migration problems ranges from design modifications to increasing the tip clearances. Excessive tip clearance reduces efficiency and could promote surge (especially at low compressor air flowrates).

Compressor Corrosion

Experience has shown that deposits on compressor blades often contain sodium and potassium chlorides. These combine with water to form an aggressive acid, causing pitting corrosion of the blades (typically a 12 percent chrome steel such as type 403 or 410). Water often condenses due to the acceleration of the air prior to the IGV, and the salt particles get dissolved and pass through the compressor. The water evaporates as it moves through the compressor and, at times, salt is found deposited on compressor blading as shown in Figure 34. In a salty environment, the fatigue strength of steel can drop 50 percent to 60 percent, and this situation is worsened when notches due to corrosion pitting are present. Even with good air filtration, the right conditions of fog, humidity, or rain can cause migration of the salt through the inlet filter (leeching) and into the compressor. Donle, et al. (1993), have described an inlet air treatment approach that limits ingress of salt.
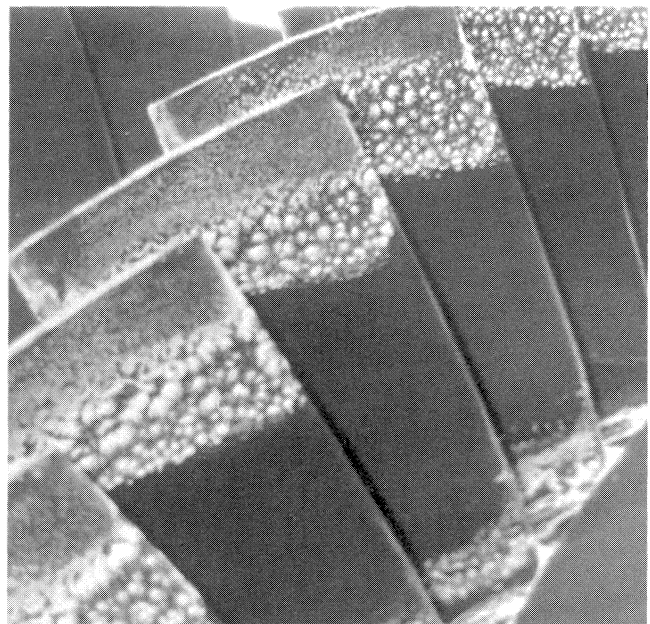

Figure 34. Salt Deposits on Compressor Blading.

Haskell (1989) states that corrosion is rarely observed beyond the eighth compressor stage, as no moisture will survive the temperatures present at this point. A gas turbine compressor rotor that has been severely affected by standby corrosion is shown in Figure 35.
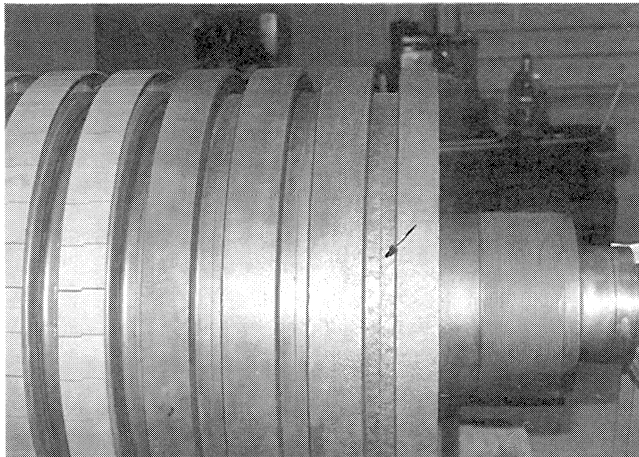

Figure 35. Standby Corrosion on Rotor of a Peaking Gas Turbine.

Bucket Rock Effect of Standby Corrosion

Standby corrosion in the dovetail or fir tree area frequently occurs in peaking gas turbines or machines that operate intermittently. Corrosion byproducts between the disk and the blades form due to condensation when the turbine is out of service and create an increased clearance in the fir tree region. When on turning gear, the corrosion products often abrade the fir tree surfaces, causing a loose fit sometimes called "bucket rock." This condition can, if it progresses, create overstress in the disk fir trees, loss of seating pins, shingling of blade shrouds, or even radial rubs. This problem is particularly severe in peaking gas turbines situated in high humidity geographic regions.

Compressor Blading Erosion

Erosion is the abrasive removal of blade material by hard particles such as sand and flyash, usually greater than five to 10 microns in diameter. Erosion impairs blade aerodynamic performance and mechanical strength. The initial effect of erosion is an increase in surface roughness and a lowering of compressor efficiency. As it progresses, airfoil contour changes occur at the leading and trailing edges, and at the blade tip. Thinning of the trailing edge is detrimental to the fatigue strength and can result in blade failure. Also, a significant loss in tip solidity can promote compressor surge.

Typically, the erosive particles are centrifuged to the outer diameter of the compressor. Rotor blades get eroded at the tip, while the stator blades get eroded at the base, as depicted in Figure 36. As a rule of thumb, blade replacement should be considered when loss of cross sectional area exceeds 10 percent to 15 percent.

Case Study—Fatigue Failure in Compressor Blading

A mechanical drive gas turbine experienced a fifth stage compressor blade failure after 96 hours of operation. Several cracks were noted in the axial direction at the "T" root attachment region of the midcompressor stage rotor blades. The cracked blades were randomly distributed over the circumference, with cracks initiating at both leading and trailing edges, as depicted in Figure 37. The location and progression of the crack indicated problems due to an axial resonance. The fracture was typical of fatigue and no material problems or stress corrosion were noted. The blade natural frequencies of the stages experiencing cracks
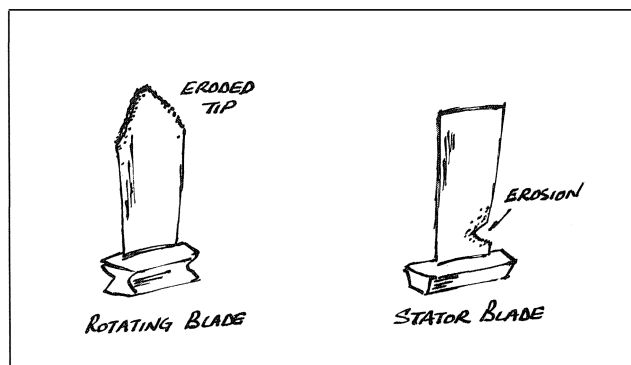

Figure 36. Erosion Patterns.

were between 1,800 Hz to 2,740 Hz. The "time to occurrence" of the failure was approximated by:

Time, hours = $\{10^7/1800$ to 2700 Hz$\}/3600 = 1.5$ to 1 hour

As the turbine had experienced about 20 starts, it was felt that the failures were due to the accumulation of resonances. Another factor was the significant performance deterioration that had been caused by excessive compressor fouling, with considerable buildup on the midstages where the problems were noted. A bleed hole that existed here was also considered to have contributed to the blade excitation because of the wake.
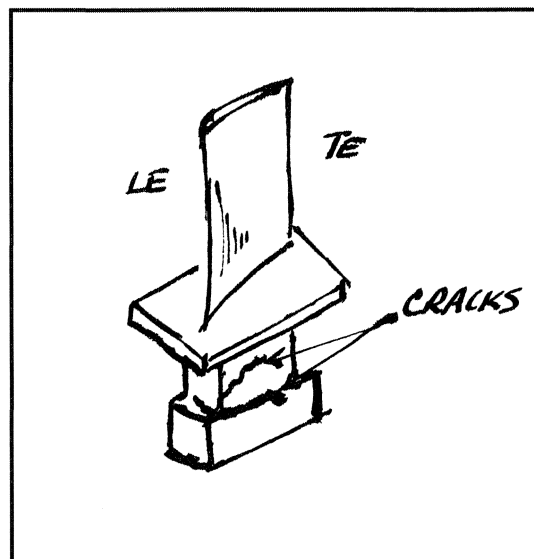
Figure 37. Crack Locations in Turbine Blade.

As the alternating stress level was slightly over the fatigue limit of the material, the blade was strengthened. First, the dimensions of the "T" root of the problem rotor blades were enlarged. The resultant stress reduction was between 30 percent to 40 percent. Secondly, the fatigue strength of the material was improved by a peening treatment. Modifications were also made to the bleed flow openings to improve flow distribution. These changes resulted in successful operation of the machine.

Case Study—Compressor Blade Fatigue Due to Surge

Several compressor blades from an industrial gas turbine rated at 18 MW were found to have developed fatigue cracks. These were discovered during an outage to repair a thrust bearing failure. The blades had operated for approximately 12,500 hours and had cracks in the midcompressor stages. Crack lengths were 0.1 inch to

0.2 inch (2.54 mm to 5.1 mm) and existed in the blade trailing edges above the gas shelf. The blades were roughened by erosion and had concentrations of pits between 0.002 inch to 0.010 inch (.05 mm to 0.25 mm) in depth. In some cases, the cracks intersected the pits.

A metallurgical investigation indicated that cracks were due to high stress, low cycle fatigue with the fractures being clearly transgrannular, i.e., passing through the grain boundaries, typical of fatigue. These observations, coupled with the physical evidence and past engine history, were indicative of high vibratory stresses derived from compressor stall/surge.

Case of Loose IGVs Resulting in Cracks

There have been cases where IGVs of some heavy duty gas turbines have come loose in the bushings and developed cracks due to high cycle fatigue. A typical crack location is shown in the sketch in Figure 38. In other cases, the variable inlet guide vanes have seized in an improper orientation. The wakes cause increase aerodynamic stimulus. Gear backlash of the IGV mechanism must be inspected. It is also important to pay attention to the lubrication of the IGV control ring and actuating arm.
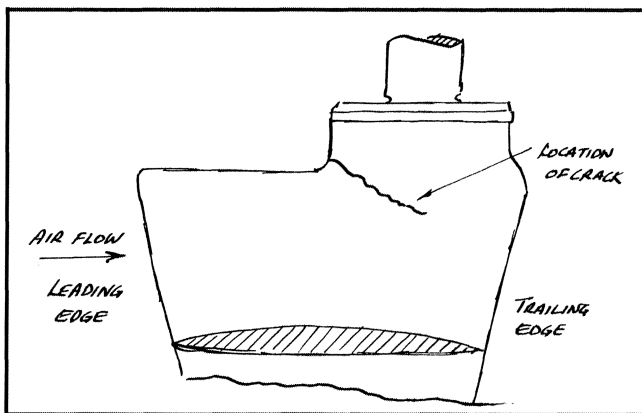

Figure 38. Crack Locations in IGV.

CENTRIFUGAL COMPRESSOR VANE PROBLEMS

Centrifugal compressors are used on small size gas turbine engines. Early British jet engines utilized centrifugal compressors and initially experienced vane fatigue failures. Voysey (1945) published some early work on vibration problems with centrifugal compressors, and also provided an equation for estimating impeller natural frequencies. Haupt, et al. (1982, 1983a, 1983b, 1985a, 1985b, 1989), carried out extensive investigations pertaining to centrifugal compressor vane vibration.

Operational Aspects Pertaining to Vane Vibration

There are several practical and operational factors that can cause failures in centrifugal compressor impellers and disks. These include:

• Distortion of the inlet airflow can cause surge effects sometimes evidenced by an increase in the vane pass frequency. Inlet piping, butterfly valves, and elbows must be carefully designed. Zech (1968) describes a major failure of a syngas centrifugal compressor, due to surge initiated by a handfile left in the inlet inducer. The distortion caused by this blockage surged and eventually destroyed the machine.

• Operation of compressors in choke (stonewall) may, at times, cause failures. Though not as severe a problem as operation under surge or incipient surge conditions, operating a centrifugal compressor at high mach numbers (near choke) at the leading edge of the diffuser vanes can result in excessive shock losses.

Circumferential variations in static pressure can excite the impeller vanes resulting in vibration fatigue.

Rotating stall can occur in both the inducer and diffuser of a centrifugal compressor and can excite subharmonic instabilities. Typical vibration frequencies experienced are 20 percent rpm indicative of diffuser rotating stall and 60 percent to 70 percent rpm indicative of inducer stall.

Case Study—Inlet Distortion
Causing Centrifugal Impeller Excitation

This case pertains to a 10,000 rpm centrifugal turbocharger that had undergone an uprate. Upon startup, as turbocharger speeds exceeded 9,400 rpm, high vibrations at predominantly the vane passing frequency (VPF) appeared. Figure 39 shows a graph made to troubleshoot the problem in the field. Graphs such as these are valuable as they provide the troubleshooter with a quick feel for the situation. The rapid growth of the vane pass frequency at 19× rpm and its extreme sensitivity to speed is evident from the graph. To investigate the vibration behavior, accelerometers were mounted on the turbocharger and data were taped on a AM/FM recorder. A real time analyzer was used to obtain an instant correlation between vibration and noise. Concurrently, dynamic pressure at the compressor discharge was measured and recorded. Three test runs were made including an initial test run, and runs with and without the inlet silencer. The test run data were analyzed on an RTA, and an examination made of the vibration with and without the inlet silencer. These indicated that the silencer was accentuating the problem.
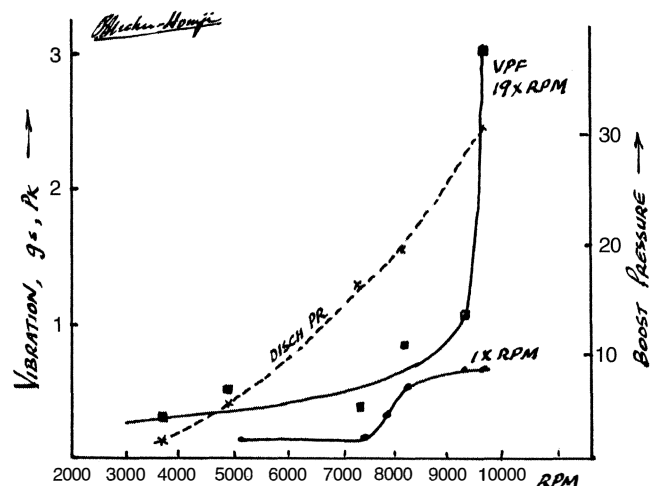

Figure 39. Graph to Show Vibration Response on Centrifugal Impeller (Showing Sensitivity of the Vane Passing Frequency (19×rpm) with Speed).

Physical inspection of the inlet silencer revealed distortion of the intake baffles, which resulted in nonuniform compressor air flow. Even though the distorted silencer existed prior to the rerate, the new flow/pressure characteristics created conditions conducive to stall. Mitchell (1975) has documented a case where approaching surge caused a tenfold increase in vane pass frequency amplitude.

While no failure occurred in this situation, there is little doubt that sustained operation at excessively high vane passing frequency vibration level would have ultimately resulted in a failure. Moreover, this case is typical of a situation in which rapid field analysis is required without any extensive analytical work.

TURBINE BLADE, DISK, AND VANE PROBLEMS

In the gas turbine hot section, problems include:

• High cycle fatigue.

• Low cycle fatigue.

- Thermal fatigue.
- Creep.
- Stress rupture.
- Oxidation/high temperature corrosion.
- Erosion.

Hot section blades are exceedingly expensive, with a stage of intricate aircooled blades for a high output gas turbine costing approximately $1,000,000. The economic impact of blade failure is, consequently, most significant. As pointed out by Stringer and Viswanathan (1990), with large output and high temperature turbines, the metal temperatures experienced by the second and subsequent stages may be equal to, or higher than, the first stage. The reason for this is that high aspect ratios and twist for the low pressure blades may make the inclusion of cooling holes more difficult. Hot section blades and vanes are subjected to damage mechanisms including high cycle fatigue (HCF), low cycle fatigue (LCF), thermal fatigue, creep, stress rupture, hot corrosion/oxidation, and erosion (particulate and hot gas erosion). Other blade damage mechanisms include:

- Repair or disassembly damage.
- Abnormal temperature or speed conditions (overspeed or operation in impermissible speed ranges). These events are often transient in nature and will not be reflected in the operation log sheets.
- FOD/DOD. The objects may be air intake components, combustor hardware, bolts, washers, or failure of upstream blades.
- Environmental conditions. This includes effects of fuel contaminants (e.g., Na, K, etc.) or problems with steam injection quantity or quality.

Turbine Blading Problems—Practical Considerations

Turbine blade design is complicated by a number of hostile environmental factors, which call for the use of very generous factors of safety. The amount of fatigue stress a blade can endure depends upon:

- Mechanical design (section sizes and areas that determine stress levels). Temperature and temperature cycling are also important considerations.
- The amplitudes and frequency of vibratory stress imposed. Excitation can be caused by aerodynamic sources such as nozzle wakes, or by mechanical forces. Uneven blade or nozzle clearances can excite blades at running frequency or lower order multiples. Improperly angled diaphragms can impose uneven forces due to uneven clearances. Flow discontinuities that occur at the horizontal split line can excite blades at a frequency of twice running speed. In general, nozzle throat tolerances should be within ±1 percent. Variable speed machines, such as two-shaft gas turbines, can experience a number of excitation frequencies caused by mechanical and aerothermal forcing functions.

The severe vibratory environment is compounded by high stresses, temperatures, and large temperature gradients. If a vibration fatigue situation is noticed, the following countermeasures may be applied:

- Modify the natural frequency of the wheel or blade to move the troublesome resonance away from the operating zone.
- Strengthen wheel or blade sections to provide lower stress levels. This approach may be constrained by aerodynamic considerations.
- Attenuate or remove the offending forcing function.

An approach used by turbine manufacturers is to provide partial or complete shrouding on high aspect ratio blades, to modify the natural frequencies by providing greater stiffness. The use of shrouding also controls radial flow and provides a smooth continuous sealing surface, thereby minimizing performance loss. The grouping introduces additional degrees of freedom and a corresponding greater number of vibration modes. Group modes are quite complex and may involve tangential, axial, or torsional modes, and reliable design must take these into consideration.

With the existence of shrouding, most of the vibration modes of the complete structure are of an "assembly mode" nature. These are modes that are neither pure blade nor pure disk modes. It has been shown that a relatively small modification to the shrouding, either to its stiffness or its position along the blade, can result in significant changes in the pattern of the assembly natural frequencies. Further complexities are introduced by the fact that there will always be slight variations in the various blade dimensions during manufacture.

In certain cases, adverse internal strains may develop, due to assembly tolerances or rapid changes in turbine inlet temperature. The temperature changes between wheel and shroud could cause a low cycle fatigue effect that may result in failure after a number of operating cycles.

Forcing Functions for Turbine Blading Vibration

Several excitation frequencies can initiate turbine blading vibration problems. These excitation frequencies include:

- Number of combustors × rpm (which can cause blade failures several stages downstream).
- Nozzle and strut passing frequencies.
- Discontinuities in diaphragms or diaphragm holder rings can induce 1× rpm or 2× rpm disturbances.
- Nonuniform spacing of nozzles can set up a wide range of harmonics. In general, the higher the harmonic, the lower the amplitude of blade vibration.
- Low order (1× rpm through 4× rpm).
- Differences between the number of nozzles ahead and behind a row of blades, i.e., "the beat" frequency.
- Number of exhaust struts × rpm.

The number of flame sources (i.e., number of combustors) causes circumferential temperature spreads, inducing variations in the density and velocity that result in cyclic variation of gas forces acting on the blades.

Turbine blades have a variety of natural modes of vibration including coupled modes (i.e., blades combined with disk rim). Common turbine blading modes are the first, second, and third flap mode and the torsional modes. Other modes include the complex modes: (2F + 1T), the first edgewise mode (normal to first flap), disk modes 1D, 2D, 3D, and ring modes. Most vibration mode frequencies decrease with increase in turbine inlet temperature. Engines with single or double combustors located off centerline can induce distortion effects. Campbell diagrams allow a visualization of if and how natural frequencies may be excited during operation at various speeds.

The vibration situation is worsened by high EGT spreads, which can result in high odd-order harmonic content and can produce fatigue failures if any of the rows of turbine blades are in third order resonance. Another source of strong low order harmonic distortion is a vertical collector type exhaust system (Dundas, 1988).

When turbine shrouds are employed (tip or part span), the locking force at the interface at operating speed must be sufficient to avoid slippage across the mating surfaces. Slip and consequent wear of shroud mating surfaces is common and has been the cause for several blade failures.

*Effect of Speed and Temperature
on Turbine Blading Natural Frequency*

Blade natural frequency is dependent on both the operating speed (centrifugal stiffening) and the blade temperature (effect of Young's modulus).

• Natural frequency lines are temperature dependent. For example, if shaker table or rap frequency tests are conducted at temperature T_{test}, and blade operating temperature is T_{op}, then frequency at T_{op} is given by:

$$F_{n,op} = F_{n,test} \times \frac{E_{t_{op}}}{E_{t_{test}}} \qquad (3)$$

For example, in Waspalloy blades, a drop of approximately 10 percent can occur in natural frequency between rap test frequency at 70°F (21°C) and operating blade temperatures of 1200°F (649°C).

• Care should be exercised when blades are operating in a corrosive environment. Fatigue strength is greatly reduced in the presence of a salty atmosphere.

• With hot section blades, creep affects should be considered. Stress-rupture-temperature data are conveniently presented in the Larson-Miller curve, which should be used for any troubleshooting or blade design review work. Maximum blade temperatures experienced by a blade will be the relative temperature given by:

$$T_{rel} = T_{total} - \frac{V^2_{abs} - V^2_{rel}}{2gJC_p} \qquad (4)$$

Turbine Blade Attachment Techniques and Problems

The blade root is a critical region of the blade and has to be manufactured to very strict tolerances, as it is subjected to high stress levels during operation. A root failure causes massive DOD and outage time. Three failure modes that afflict the blade attachment areas are:

• *High cycle fatigue*—Cyclic gas forces can initiate failures that start in areas of high stress concentration. Failures of this nature usually stem from generic design problems and occur relatively early in the operating life of the turbine. It can also be the result of poor assembly.

• *Fretting damage*—Occurs due to relative motion (micromotion) between the surfaces that are in tight contact. The sliding motion produces a high temperature at the rub surfaces, resulting in oxidation and creation of iron oxides that may show up as rust. Fretting damage can promote stress concentration and ultimate damage due to HCF. To some extent, fretting is unavoidable in gas turbines, and coatings are used to alleviate these problems. Figure 40 shows fretting damage on a turbine attachment land.

• *Root corrosion*—This is a problem particularly afflicting peaking gas turbines due to standby corrosion effects. Corrodents can enter crevices and create problems due to erosion, resulting in excessive bucket rock.

Oxidation and Hot Corrosion

Gas turbines have been successfully operated on a wide range of fuels including heavy fuels. Considerable care has to be taken to ensure that the fuel is treated to an acceptable quality prior to being introduced to the gas turbine. Higher firing temperatures have created a host of hot section corrosion problems. Even distillate fuels such as No. 2 diesel oil may, at times, require fuel treatment for removal of salt (Na, K, Ca) and water. Fuel contamination with
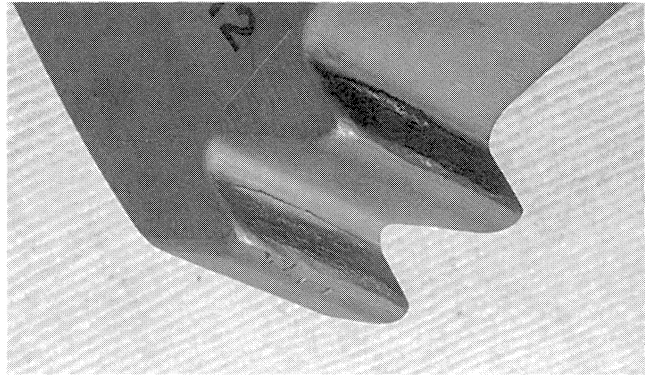

Figure 40. Fretting Damage on Turbine Attachment Lands.

salt water is exceedingly common when fuel is transported by barges. Sedimentation tanks and floating suction devices should always be used. Salt can also enter the machine by means of the air. While this problem is severe in marine and coastal environments, studies have shown that airborne salt can also be a significant problem in inland installations. Airborne salt ingestion, even in the ppb range, can cause hot corrosion.

Hot corrosion is an accelerated damage phenomenon that occurs when high temperature superalloys are operated in an environment containing salt and sulfur. The salt is derived from the air or enters the turbine via the fuel. Sulfur typically enters the turbine via the fuel. The basic reaction that occurs is represented by:

$$4NaCl + 2SO_2 + 2H_2O + O_2 \rightarrow 2Na_2SO_4 + 4HCl \qquad (5)$$
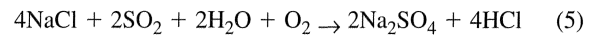
Hot section corrosion can be intensified by the presence of vanadium, which produces V_2O_5, which, in combination with the alkalis, can produce low melting point (approximately 1048°F, 600°C) vanadates, which while molten, can aggressively dissolve metal oxides. Most turbine manufacturers set an upper limit of (Na + K) at 0.5 ppm by weight. The great amount of salts on a turbine nozzle segment is shown in Figure 41. It is not surprising that this turbine exhibited hot corrosion, as can be seen in Figure 42.
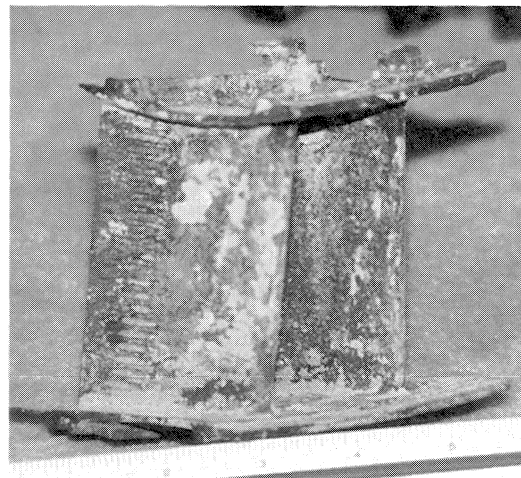
Figure 41. Massive Amount of Salts Found in Turbine Nozzle.

Type I corrosion, known as high temperature hot corrosion, is attributed to Na_2SO_4 deposits on the blade material and occurs in the approximate temperature range of 1517°F to 1742°F (825°C to 950°C). The lower and upper temperature thresholds are associated with the melting point of Na_2SO_4 and its dewpoint, respectively. A uniform, porous surface scale is typically formed, with Ti and Cr sulphide spikes being found in the denuded base metal zone.

Figure 42. Hot Corrosion Damage.

Type II hot corrosion (low temperature hot corrosion) manifests itself in the approximate temperature range of 1292°F to 1472°F (700°C to 800°C). The lower and upper temperature thresholds are associated with the melting point of mixed sulphate salts and the dissociation of the complex to Na_2SO_4 and base metal oxides, respectively. The pitting attack is typically nonuniform here, with layered type corrosion scales being found. No intergrannular attack is found in the base metal and there is very little sulphide formation within the metal. In both types of hot corrosion, there is a breakdown in the protective oxide layer scale (aided by thermal cycling).

It is important to note that the surface roughness caused by sulphidation attack reduces output and stage efficiency and also results in increased heat transfer to the blade, which can reduce blade life. The serious damage to a hot section blade caused by hot corrosion is shown in Figure 43. Note that the leading edge cooling hole has been totally compromised.
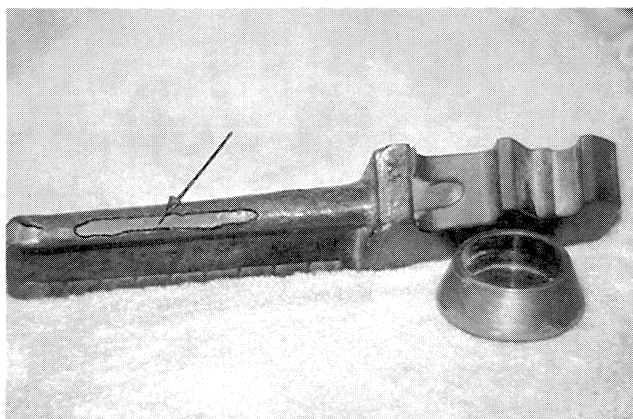

Figure 43. Hot Corrosion Damage Showing Total Defeat of the LE Cooling Hole.

Case Study—Hot Corrosion Damage in an Industrial Gas Turbine

A heavy duty, 65 MW industrial gas turbine that had accumulated 5,000 hours and 110 starts was operating at base load, when it tripped on high vibration. Repeated restarts resulted in vibration trips. Upon disassembly, it was found that 40 percent of the second stage bucket tip shrouds had suffered material loss, due to hot corrosion and weakening of the cross section as shown in Figure 44. The blade material was uncoated IN 738. The material at the blade tip was found to be magnetic. First stage blades also showed signs of hot corrosion.
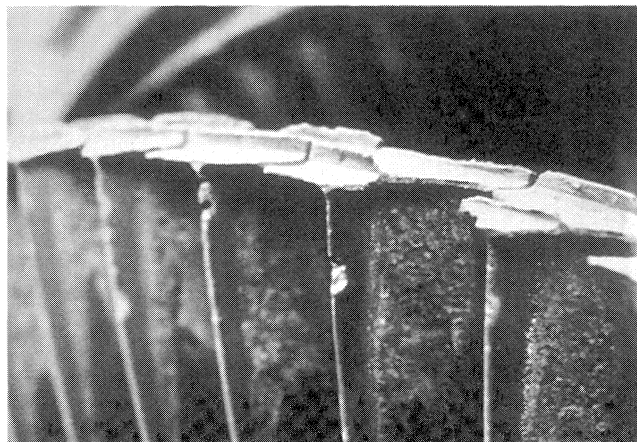

Figure 44. Material Loss at Shrouds Due to Hot Corrosion on Second Stage IN 738 Blades.

A study of the hot gas path deposits indicated that salt, which would have been molten at operating temperature was present. This is typical of Type II (low temperature hot corrosion). Salt concentration levels were 0.1 mg/cm^2, which is enough to cause hot corrosion. By examining the air and fuel side deposit chemistry, it was determined that the salt ingestion was occurring both from the fuel and the air.

Coatings

Hot section coatings are designed to protect superalloys from hot corrosion and oxidation. There are two types of coatings in common use—diffusion and overlay coatings. Blade coatings play an important part in the battle against blade failures, with a wide range of coatings being available for both compressor and hot section blading. With modern day gas turbines, coatings are now the life limiting component of hot section blading. A systems view should be taken when considering coatings. This should include:

• Careful choice of coating process and type. The coating is typically the least durable material in the hot section. For example, an improper heat treatment may degrade the base metal properties.

• Ensuring the coating process itself is done properly. If applied improperly, even the best of coatings are ineffective. Quality control procedures for the coating vendor should be carefully reviewed.

Diffusion Coatings

In a diffusion coating, one of the major coating constituents (nickel) is supplied by the base metal. Diffusion alluminide coatings have Al contents of 20 percent to 30 percent by weight, while diffusion chrome coatings may have chromium content in excess of 35 percent (Wood, et al., 1990). The aluminide layer typically grows inward and is approximately 5 mils (125 microns) thick. Some OEMs go to thicker coatings. Often the alluminide coating is platinum modified for nickel based superalloys.

Overlay Coatings

These are coatings that are generally used for more severe environments, and are typically applied by vacuum plasma spray (VPS) process or physical vapor deposition from an electron beam melted pool. The composition is typically M, Cr, Al, Y, where M = CO, Ni, and/or Fe. Typical thickness of overlay coatings is three to five mils.

Thermal Barrier Coatings

Porous ceramic "barrier" coatings are now available for external surfaces of vanes and blades, which provide an effective barrier to heat transfer. The thermal barrier coating (TBC) acts as an insulator, due to the fact that its thermal conductivity is 10 to 20 times lower than that of the blade metal. Blade temperatures can be reduced by as high as 150°F (83°C). During starts and transients, the thermal stress is considerably reduced. During steady state operation, the lower temperatures improve durability. Thermal barrier coatings are typically over an M Cr Al Y overlay coating. Typical thickness of the ceramic TBC would be five to 15 mils. The principal failure mode with TBCs is spallation, where the TBC flakes off the bond coating due to oxidation of the bond coat and the effect of thermal cycles.

Problems with Coatings

There are two sources of problems relating to coatings:

• *Problems related to the way it is applied*—The proper application of the coating is of utmost importance. This calls for complete removal of the corrosion products and the old coatings, appropriate quality control, and heat treatments required. Residues of sulphur or corrosives can damage the base metal. Chemical or mechanical stripping must be carefully done.

• *Problems related to the coating properties itself*—If a coating has a low resistance to thermal fatigue, coating cracks can develop and progress into the base metal. An important property of the coating is the ductile to brittle transition temperature (DBTT) and is described by Stringer and Viswanathan (1990). Daleo and Boone (1997) have provided a study of coating systems applied to modern high temperature gas turbines including MCrAlY coatings and thermal barrier coatings.

Turbine Blade and Nozzle Erosion

Erosive particles entrained in the air or fuel can cause turbine section erosion. The damage is particularly severe if cooling hole blockage occurs, which can lead to excessively hot blades and ultimate creep rupture. A reduction in the blade section size further compounds the stress problem. Erosive particles in the fuel can result in nozzle wear, resulting in a distorted temperature profile and severe hot spots at the turbine inlet.

Hot Gas Erosion

Apart from particulate erosion, there is also the phenomenon of hot gas erosion, which results from localized overheating and thermal cycling due to intermittent loss of cooling or a breakdown in the coating. After several cycles, damage takes place and the increased roughness (erosion) worsens the problem. This problem can occur in the first stage nozzle segments at the platforms. Typically the most severely affected parts are those in the hottest gas path (e.g., central to the transition piece). A problem of this type on a first stage vane outer platform is shown in Figure 45.

Loss of Cooling Failures

Several hot section failures are caused due to loss of air cooling. This can be caused due to the following reasons:

• Quality control problems within the component (blade or vane) where there is a blockage within the cooling passage
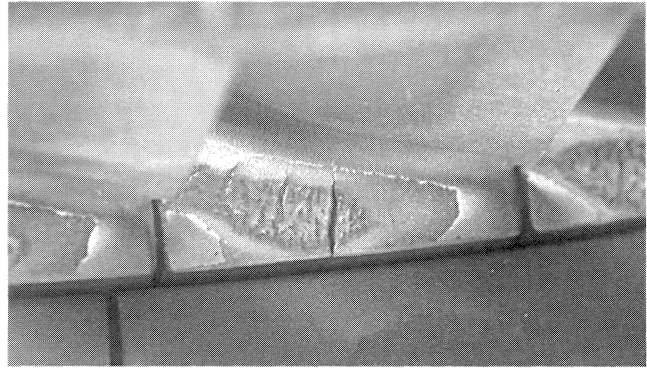

Figure 45. Hot Gas Erosion Phenomenon on Nozzle Outboard Platform. (This can result from localized heating (or poor heat removal).)

• A problem in the delivery system for the cooling air, wherein the delivery system performs below par, thus limiting the flow of cooling air to the hot section component. Some gas turbine designs employ external coolers for the compressor bleed cooling air. Problems in these coolers can cause flow restrictions and subsequent problems (Dundas, 1993b). It is important that these coolers be monitored to ensure that they are operating properly.

A creep failure of a turbine blade is shown in Figure 46. This was due to partial blockage of the cooling hole, which caused the blade to run hot and suffer a creep rupture failure. It is therefore a good idea to insist that all blades be flow checked upon manufacture.

Figure 46. Creep Rupture Failure of a First Stage Blade Caused Due to Blockage of the Cooling Passages.

Creep Failures/Thermal Ratcheting

Creep can affect not only the turbine blades, which are subject to huge centrifugal forces, but also stator parts. There have been cases reported where the nozzle affixment hardware has undergone creep, resulting in downstream movement of the nozzle segment causing rubs with the downstream disk. Often problems such as these are associated with temperature uprates where adequate cooling has not been provided for the nozzle support systems. There have also been cases where thermal ratcheting has played a part in creating uneven blade clearances and rubs due to deflection of the tip seal blade ring (Dundas, 1988).

Turbine Blade Fouling

Turbine fouling occurs when low melting point ashes, metals, fuel additives, and unburned hydrocarbons are deposited in the

form of a scale. Typically, the first stage nozzle will experience fouling and this can cause changes in throat area, causing off-design performance on the turbine. Deposits on the blades can cause a loss of aerodynamic performance. Blockage of blade and disk cooling passages and vents can lead to overheating and shorter component life, or even failure. Fouling in the hot section facilitates hot corrosion and sulphidation. A gas generator turbine with deposits is shown in Figure 47.
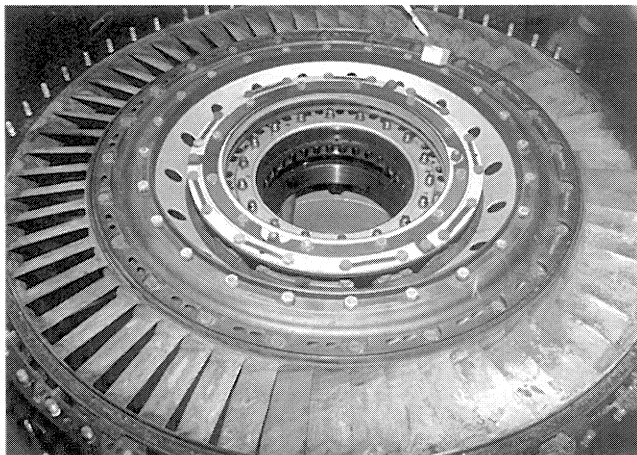

Figure 47. Gas Generator Turbine Section with Foulants.

Turbine Section Domestic Object Damage

The liberation of a blade or ingestion of debris or combustor hardware can cause massive hot section damage. Damage surfaces bear the characteristic impact overload pock marks. Frequently, a parabolic trajectory pattern can be noted on the stator segments, as can be seen in Figure 48.

Figure 48. Typical Parabolic Trajectory Caused by an FOD/DOD Failure.

Damage can also be caused due to improper maintenance actions. The mangled remains of a ladder, shown in Figure 49, that was left inside a silo combustor after an inspection. Upon startup, a tremendous noise emanated from the combustor and the turbine was immediately shut down! While no blade damage occurred in this incident, it shows that maintenance related mistakes do happen.

BLADE MONITORING TECHNIQUES

The avoidance of blade problems requires two conditions to be complied with. First, and most important, the basic *design* has to be sound, with adequate factors of safety being incorporated. Design reviews (Dundas, 1988) help in ensuring a safe design.

Figure 49. Mangled Remains of an Inspection Ladder That Was Left Within a Silo Combustor During Startup.

Second, the operating environment and design envelope must be maintained during gas turbine operation. Monitoring techniques can be of help in detecting and avoiding operating regimes that promote blading distress.

The measurement of blade behavior and underlying operational conditions is valuable from a perspective of both safety and reliability. As delineated ahead, the condition monitoring of blading behavior can be classified into two categories:

• *Direct techniques*—These techniques entail the use of special sensors or approaches to *directly* measure blading vibration or other blade behavior. Included in this group are optical methods, Doppler techniques (both acoustic and laser), strain gauge measurements, tip clearance measurement methods, and the use of optical pyrometers. At this time, direct techniques are employed by OEMs during prototype tests and have not, in most part, been used on routine operational gas turbines. Optical pyrometers are being requested by clients on large advanced gas turbines. Destructive metallurgical examination of hot section blades to determine microstructural changes may also be considered a direct technique.

• *Indirect techniques*—Indirect techniques encompass the use of vibration analysis, dynamic pressure analysis, performance analysis, and exhaust temperature spread analysis techniques to ensure that flow conditions are not conducive to blading distress. These techniques do not provide a *direct* quantitative feel for blade vibration or properties, but furnishe a degree of qualitative insight as to the *underlying operating environment.*

The salient points of key direct and indirect techniques are described below.

Performance Monitoring

Because several blade failures have, as their underlying cause, aerodynamic phenomena such as flow distortion, stalls, surge, etc., a program of performance monitoring and trending of data is of considerable value. Performance analysis can help in uncovering several of the underlying causes of gas turbine blading problems such as fouling, off-schedule IGVs, icing, distortion, nozzle deposits, uneven combustion, and other forms of deterioration. Performance monitoring involves the acquisition of pertinent data (temperature, pressure, and speed) at stations along the gas turbine train, the computation of air mass flowrate, turbine inlet temperature, and compressor and turbine efficiencies. Computational techniques are available for calculation of key cycle parameters such as the turbine inlet temperature and air mass flowrate. The use of performance analysis has been detailed by Cohen, et al. (1987), Dundas (1982), Dundas, et al. (1992), and Meher-Homji and Focke (1985). The application of *transient analysis* of performance and startup data can also be used to

provide insight into operating problems (Meher-Homji and Bhargava, 1992). Performance maps can be generated by obtaining performance data from new and clean machines (Meher-Homji, et al., 1993) and several techniques are available to model performance deterioration (Lakshminarasimha, et al., 1994). With modern day control systems and serial communications capability it is relatively easy to conduct a basic performance analysis calculation, trend data, and map compressor performance. Calculations should be conducted to analyze:

- The compressor map (airflow versus corrected speed).

- Trending of inlet filter conditions.

- Ensuring that no unusual performance pattern has developed.

Several of these calculations can be done by hand or using a spreadsheet, and are invaluable if used.

Trending and Mapping of Performance Data

This is an exceedingly important area and can provide warning of conditions such as reduction of surge margin, compressor and turbine deterioration, or increase in exhaust gas temperature spread, which may promote blade problems. Trending techniques should correct and normalize data and discriminate between changes in parameters due to deterioration, as opposed to "off-design" operation.

The Importance of Monitoring Exhaust Gas Temperature Profile

The clogging of fuel nozzles can cause severe flow distortion that result in vibratory excitation of turbine airfoils. Monitoring the exhaust spread and the average temperature, and relating this to the load and ambient conditions, provides a good measure of combustor status. It is interesting to note that despite this fact, several aeroderivative and older vintage heavy duty machines have thermocouple harness arrangements that do not permit individual access to thermocouples, and just provide an averaged reading used for control purposes. EGT monitoring has been most effective in avoiding turbine section high cycle fatigue failures. Wisch (1993) and Knowles (1994) have addressed approaches of EGT monitoring. Studies conducted by the Royal Navy (Walker and Sommerfield, 1987) have concluded that spread monitoring is among the most effective condition monitoring tools for gas turbines. These studies have shown that vibratory stresses on the blades can increase up to five times, with serious nozzle blockage. A case study showing the criticality of EGT analysis in averting blade failure is presented ahead.

Vibration and Dynamic Pressure
Analysis to Detect Blading Problems

In practical field troubleshooting situations, difficult value judgments regarding machine operability have to be made frequently with incomplete data. In such cases, data from accelerometers or dynamic pressure sensors can prove invaluable. The vibration signatures derived from gas turbines are complex, with the spectrum containing several peaks corresponding to the different number of blades, blade passing frequencies (BPF), and its harmonics, in addition to other forcing functions pertaining to gears, bearings, and other components. By knowing the number of blades present on a certain disk or stage, it is possible to detect problems by observing *relational* changes in the blade passing frequency amplitude levels. Dynamic pressure measurements are also of value in detecting incipient surge conditions and other flow instabilities.

Vibration and dynamic pressure amplitudes are strongly dependent on pressure ratio of the compressor, stator blade angles, and flowrate. Consequently, if meaningful vibration trending is to be accomplished, these factors must be taken into account. It is difficult to pass judgments on the *absolute* amplitudes of vibration

that the blades are experiencing, but *qualitative* judgments can be made. Mitchell (1975) describes work done to determine if changes in the blade passing frequency (BPF) can be used to detect blade problems. In the authors' experience, relational changes in the BPF and its harmonics provide useful information. Blade passing frequencies amplitudes seem to increase at both low flow (near surge) and at high (approaching choke) conditions.

Dynamic pressure is also a valuable condition monitoring tool and several of the newer dry low emission (DLE) technologies have these devices tied into the control system. As a rule of thumb, combustor pulsations should not exceed 0.25 percent of the compressor discharge pressure. For example, on a gas turbine with a pressure ratio of 14.5:1, with a discharge pressure of 228 psig, the dynamic component should not exceed 0.57 psi peak-to-peak. The pulsation levels are a function of water injection levels and are considerably higher for DLE machines. A considerable amount of experimental work still needs to be done to correlate blade problems with signatures, but there is little doubt that useful information does exist in signature analysis. Additional work in the area of the use of vibration analysis for the detection of blade problems is provided by Parge (1990), Parge, et al. (1989), and Simmons (1986, 1987). An examination of casing vibration with respect to the surge map and correlations with dynamic pressure are made by Mathioudakis, et al. (1989). Loukis, et al. (1991a, 1991b), have provided a procedure for fault identification, based on spectral analysis and dynamic pressure, using transducers located on the axial compressor casing.

Acoustic Rub Detection

Dimensional changes occur between the rotor and casing change during transients. These changes may be particularly high during fast starts and emergency trips. Historically, gas turbine operators have detected turbine rubs by the use of stethoscopes during a startup or shutdown of a turbine. A simple device that permits operators to audibly detect rubs that occur during startup and shutdown transients uses a microphone located on a two inch pipe, fixed to the inlet plenum of the gas turbine. An isolation valve is provided that disengages the microphone at a certain speed. Operators can hear the sound during startup or shutdown, or utilize a strip chart recorder.

Use of Doppler Techniques

Laser Doppler Anemometry

Originally developed for the measurement of fluid velocity, the laser Doppler anemometry (LDA) technique has been applied to blade vibration. Because a laser has a coherent wave structure, any motion of a surface normal to the coherent wave front adds a Doppler shift to the frequency of the scattered light, which can then be related to surface velocity. LDA systems are now commercially available. This technique is not being applied as a condition monitoring tool, but it holds promise and may be used in the future. As with several other techniques, judicious selection of an optical window on the machine casing would be required. Details may be found in Kadambi, et al. (1989). A laser based system applied to hot section blading is described by Kawashima, et al. (1992).

Acoustic Doppler Method

The acoustic Doppler method has been under development and refinement for several years, as applied to high aspect ratio LP turbine blades, and is now commercially available (Leon and Trainor, 1990). It was first developed to address the serious problems that occurred with LP blade failures in utility steam turbines. In this method, nonintrusive acoustic sensors are fixed to the casing, downstream of the blade row, to detect sounds radiated by the vibrating blades. Two sensors are required for each monitored blade row. This technique provides a warning when a

resonance condition occurs. As cracks occur in blading, the natural frequency decreases. Thus, a cracked blade may experience resonance conditions even when operating at, say, 3,600 rpm (60 Hz). With the acoustic Doppler technique, these occurrences can be monitored and a historical record maintained.

Strain Gauge Testing of Blades

Strain gauge testing of blades has been used predominantly in test stand situations. The serviceability of strain gauges in the field is a serious problem. Typically, one or several strain gauges are attached to the blade surface. The use of strain gauges on rotating components is problematic in the long run because of the complicated telemetry system that is required. It is, however, a tool utilized by manufacturers in resolving blade problems and to verify blade stresses. Testing techniques are detailed in Strub (1974).

Wear and Rub Detection

Cartwright and Fisher (1991) and Fisher (1988) have described an engine debris monitoring system developed for the Ministry of Defence in the United Kingdom. In this technique, sensors mounted in the gas path monitor the electrostatic charge. Experimental data have shown that the electrostatic charge grows with blade or seal rubs or other faults in the gas path.

Blade Tip Clearance Monitoring

Several blade tip clearance measurement systems are available and are used mainly by gas turbine manufacturers in test applications. Sheard and Killeen (1994) describe a capacitance based probe that is located in the casing and advanced toward the blade tip by a stepper motor.

Use of Infrared Pyrometry for Temperature
Measurement of Hot Section Blading

The use of infrared pyrometry is an increasingly popular tool for condition monitoring and has been applied to a wide range of gas turbines. Some high performance military jet engines have, for several years, used pyrometers for control purposes. In the industrial turbine market (advanced gas turbines), pyrometers are becoming popular as a condition monitoring tool that can provide valuable insight to hot section blading problems (Kirby, et al., 1986). Further details are provided by Barber (1969), Kirby (1986), Beynon (1981), and Schulenberg and Bals (1978). Pyrometry enables the detection and pinpointing of blades that run hotter than others and is a valuable condition monitoring tool. Individual blade temperatures can be identified by use of a key phasor. Figure 50 depicts a pyrometer trace from the first stage of a 160 MW Frame 7F gas turbine. Pyrometers were installed under an EPRI durability study program (Ondryas, et al. 1992). The pyrometer had the capability of measuring approximately 40 points per rotating blade as the blades rotated at 3,600 rpm. Studies and case investigations relating to a Frame 6 gas turbine are also presented by Rooth, et al. (1997). There are two approaches available for pyrometer installation. Dow has patented an approach wherein the insertion is made near the transition piece (Kirby, et al., 1986) and the turbine blade viewed through the stator nozzle. The other approach involves the penetration of the high pressure casing. Figure 51 depicts the two approaches.

Optical Measurement of Blade Vibration

With the new generation of high performance gas turbines, the design tip clearances of the blade tips and interstage seals are minimized to promote high efficiency. The minimum and maximum tip clearances can vary substantially during operational conditions and with deterioration. This can occur during startup and shutdown, as the rotor transgresses its critical speeds, under conditions of rotor thermal bow, and as creep effects manifest themselves. Blade rubs can create loss in efficiency or result in a
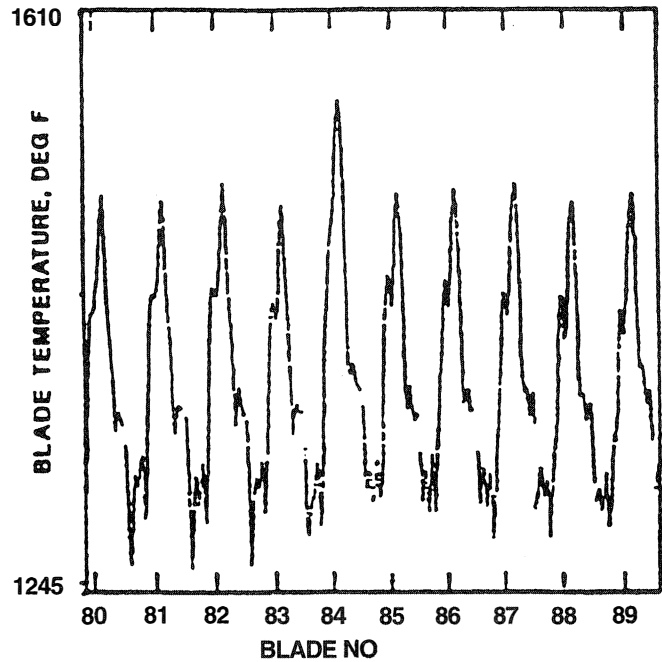

Figure 50. Pyrometer Trace on a 160 MW GE Frame 7F Advanced Gas Turbine. (Meher-Homji, et al. 1993)
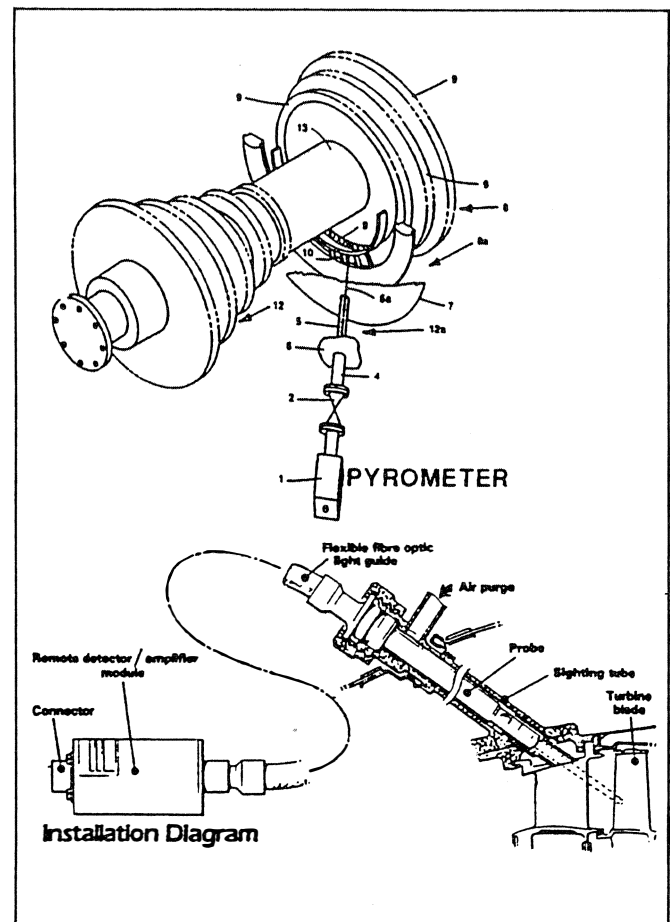

Figure 51. Pyrometer Installation Approaches. (Top arrangement, Kirby, et al. 1986; lower arrangement, Land Instruments.)

catastrophic failure, in severe cases. This approach was originally suggested by Roth (1980). Simmons, et al. (1990), describe an optical blade tip sensor in which laser light is focused on a spot on the turbine blade tip. The spot on the blade is then imaged by the probe on the face of the fiber optic bundle. Because of the angle at which the light strikes the blade, any change in distance between the blade tip and probe will cause the imaged spot on the fiber optic to move across the face of the bundle, the distance being directly related to change in blade to probe separation. This system has been successfully tested in a rig and could be used to monitor gas turbine blading. The system frequency response is adequate to provide real time capability to measure tip clearance and time of arrival measurements for each blade in a blade row.

Metallurgical Testing for Hot Section Blading

Damage to hot section blades can be determined by destructive metallurgical testing. Nickel based superalloys that are commonly used in turbine hot section blades contain a gamma prime phase that is precipitated during blade manufacture. With long term exposure to high temperatures, the morphology of the gamma prime phase changes, resulting in a loss of creep strength. In order to conduct an assessment of blade condition, one or two blades from the turbine should be destructively tested and examined via SEM/TEM techniques. This allows a determination of coating and oxidation degradation to be made. Once an assessment is made, corrective repair workscope procedures can be defined. Details regarding these tests and procedures may be found in Liburdi and Wilson (1983) and Lowden and Liburdi (1987). Barer and Peters (1970) provide an excellent practical treatment of metallurgical failure analysis, and this book is recommended to any engineer involved in failure analysis.

Infrared Photographic Inspection of Blades for Quality Assurance

Techniques have been developed by which infrared photographs can be taken of blades in a test stand, in order to determine quality aspects (Daniels, 1996). Items such as blocked cooling holes or disbonded thermal barrier coatings can be observed. There are two approaches that can be used to heat the air. In the transmission mode, moderately hot air (200°C) can be supplied to the blade, and the temperature pattern observed by means of an infrared photograph, as is shown in Figure 52. Blocked cooling holes can be detected in the blade on the right, while the reference blade image (on the left) shows all the cooling holes operational. Another mode that can be used is the reflection mode where flash lamps are used to deliver a uniform pulse of energy to heat the blade exterior surface. The infrared photograph taken will then show coating condition and will indicate problems with disbonding or delaminations of coatings.

BLADING FAILURE INVESTIGATION GUIDELINES

The guidelines presented here are general in nature and modifications would be required depending on case specifics. Because of the complexities involved in blade failures, the problem is best tackled by a multidisciplinary team. In cases involving potential litigation, several independent teams may work on the blade failure analysis. The authors have been involved in several cases where metallurgical analysis seemed to predominate the investigation. Another common problem has been stated by Dundas (1993a, 1993b) in his exceedingly valuable set of papers:

"One of the greatest barriers to a successful investigation is a tendency to explain a feature of the failure by some very circuitous sequence of events; this is usually accompanied by a challenge to disprove the hypothesis."

Whereas specifics may vary for different investigations, a general investigative procedure that should be followed is provided below.
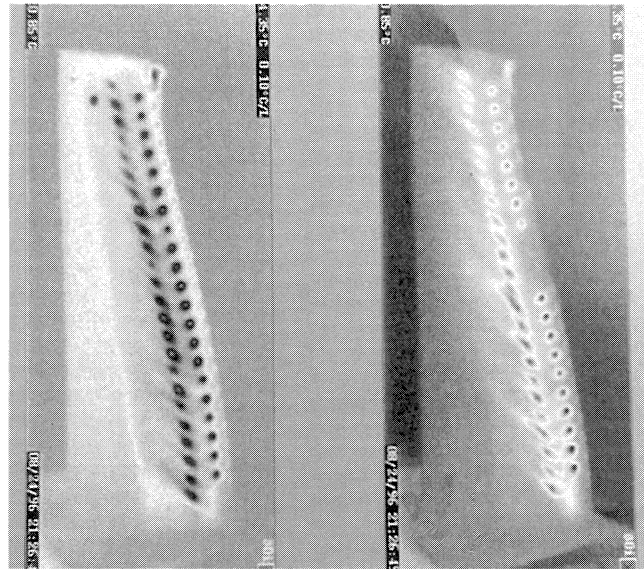

Figure 52. Infrared Photograph of a Turbine Blade Showing Blocked Cooling Holes On Right, Compared to Reference Blade on Left. (Courtesy of Bales Scientific Inc.)

Inspection and Observation of Failed Machine or Blade

This requires a first-hand site survey of the damaged machine as soon as feasible after the failure. It is imperative that all "cleanup" operations be held up unless a major safety hazard exists. If it is not possible for the investigator to reach the site immediately, orders should be issued to suspend all cleanup operations to ensure evidence is not destroyed or modified. The dismantling of the turbine should start after the investigator arrives. Upon arrival at the site, the investigator should carefully inspect the wreckage, take photographs, and take note of *all* details. Sketches should be made to document where pieces came to rest. Important components that warrant further investigation should be identified and tagged. A list of items that the failure investigator should carry is detailed in APPENDIX A. In the case of potential litigation, great care should be taken to tag components and maintain a paper trail.

All fracture surfaces and other components should be carefully examined and photographed. Observations should be made relating to:

- Corrosion.
- Erosion.
- Creep damage (elongation, necking, etc.).
- Blocked cooling holes.
- Blade attachment problems.
- Evidence of rubs, over temperature (examine stators, rotors, and casings).
- Unusual nicks, evidence of foreign and domestic object damage (FOD and DOD).
- Unusual coloration.
- DOD/FOD locations.
- Failure mode, if clearly evident.

It is very important to make a "master diagram" of the machine showing precise locations of struts, obstructions, nozzle or vane segments, etc. Blades should be carefully numbered and shown on this diagram indicating the location of each blade with respect to the disk. The direction of rotation and rub patterns on the rotor and stator should be sketched. Figure 53 (Dundas, 1993b) is a useful diagram that characterizes how blade rub patterns can be used for diagnosis.
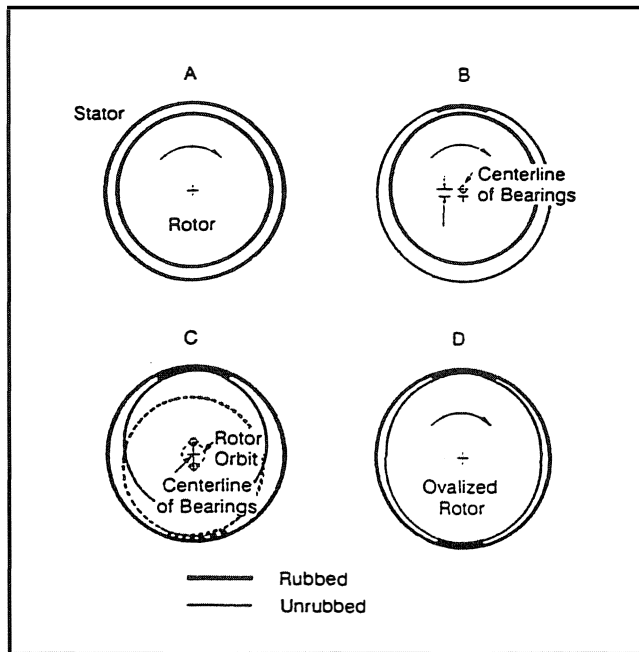
Figure 53. Rub Detection Diagnosis (Dundas, 1993b). (A = 360 degree rub on both rotor and stator (insufficient radial clearance, probably during transient conditions). B = 360 degree rub on stator, local rub on stator (stator misaligned). C = 360 degree rub on stator, local rub on rotor (rotor whirl). D = 360 degree rub on stator, local rub at two diametrically opposed locations on rotor (rotor ovalized by creep).)

All fractured surfaces and components should be carefully wrapped in *clean*, protective wrapping material and put into boxes. Clear lacquer may be sprayed on fracture surfaces to protect the surfaces.

Blade removal (from disk) should be done in a careful and controlled manner. Prior to removal, careful inspection of the tip shrouds should be made looking for deposits, unusual marks, or other telltale signs that the shrouds may have been inactive. Disks can be checked for cracks by NDT methods. All removed blades should be checked for cracks. The results of these checks should be mapped on the "master diagram." This gives valuable indication of any failure patterns that have occurred.

In addition to inspecting the failed hardware and components, an inspection should be made of the *auxiliary* systems that may have been a root cause or indirect contributor to the problem. For example, the fuel system, combustor nozzles, blade air cooling subsystems and heat exchangers, air intake filtration system, should be audited for any indication of problems.

A chart that incorporates several interrelated factors and observations into a single tabulation to assist troubleshooting is presented in APPENDIX B.

Data Gathering

After the inspection is over, a process of data gathering should be initiated. This involves:

● Discussions with operators who witnessed the failure and/or operations surrounding the failure. Discussions should be held with individuals who were there *before and during* the failure. Questions should be asked pertaining to operating history, problems experienced, unusual clues, noises, etc.

● Discussions with plant engineers to obtain engineering details (specifications, design information, performance curves, operating envelope, design and maintenance history, other related problems, etc.) Blueprints and other drawings should be collected at this stage.

● Operational history prior to failure. This is of *critical* importance. Log sheets, strip charts, and other information should be studied. These include:

• Conditions of load pressure, temperature, vibration, EGT conditions (levels and profiles), number of starts, etc., fired hours, trips, types of fuel, etc. Log sheets or printouts from the plant DCS may be used. These data may be entered into a spreadsheet and trends made of key parameters.

• Observations relating to ambient conditions, storms, fog, humidity. This can influence air inlet filtration effectiveness or create blockage, i.e., airflow distortion.

• Thrust position, bearing temperature history.

• Evidence (visual or otherwise) of surge, rotating stall, or any factor possibly causing inlet distortion or blockage.

Analysis of Parts—Metallurgical Studies

Selected parts, including components that have not failed, should be clearly marked, identified, and sent to a metallurgist who has the *relevant background* (i.e., one who has experience with gas turbines and is aware of complex interactions of sulphidation, effects of fatigue, vibration, etc.). The metallurgist should be briefed with the *full background* of the case, i.e., all clues, factors, and engineering information (fuel type, EGT history, etc.) should be provided. A metallurgical investigation typically consists of material checks, visual observations (macro observations), SEM/TEM analysis, and hardness checks.

Hypothesis Development

This phase of failure investigation relates to the examination of evidence and the thought processes of hypothesis formulation and testing. Several scenarios should be considered, keeping the "big picture" in mind. A common error in diagnostic reasoning is error of omission, i.e., certain scenarios/or events are just *not* considered (Meher-Homji, 1985). Brainstorming activities often help during scenario development and evaluation. In several gas turbine failures, there is a complex sequence of events that may lead to the failure. Further, several factors often act in conjunction with one another (vibratory excitation, poor environment, corrosion, material defects, etc.).

In the authors' experience, very rarely does the diagnostic thought process follow the maxim that no causes are to be considered until the evidence is in. Experience and intuition play an important part in rapid selection of hypotheses and then searching for corroborative evidence to support the hypothesis. Few troubleshooters will openly admit this, as we have been brainwashed to think that this is wrong. It is indeed a legitimate approach, given the diffuse manner in which our minds work, as long as one is open minded and ensures that evidence is not "bent" to meet (reconcile with) the hypotheses.

Analytical Investigation/Design Review

If required, an analytical investigation should be performed to include estimation of natural frequencies, mode shapes, and stress analysis. Varying degrees of analytical sophistication can be employed, depending on the particular needs of the failure analysis. In some cases, quick design checks are appropriate to get a feel for the magnitudes of the stresses involved. If more sophisticated analyses are required, then FEM techniques can be used to model the case. Even with these techniques, considerable insight is required in determining *realistic* boundary conditions and in interpreting results. Independent design reviews pertaining to material suitability, manufacturing quality, blade fabrication methods, and stress analysis can be conducted.

CASE STUDIES

When a catastrophic blade failure occurs in a critical gas turbine, there is considerable urgency to get the machine operational

expeditiously. Strategies followed to resolve the problem may involve design changes and, at times, alteration of the turbine's operational envelope. The strategy chosen is dependent on the failure mode and the root cause. In certain situations, *it may be imperative that the machine be kept operational for economic reasons* in spite of obvious mechanical distress. In such circumstances, monitoring of performance and other parameters may be of value, as it allows adjustment of the operational envelope to avoid dangerous regimes until a convenient outage can be taken. Often, short and long term strategies have to be formulated to keep things going in situations where no spare machines are available. Short term strategies could involve changing the operational envelope (speed, power, improving operating conditions, minimizing transients) and close monitoring of operational parameters. Long term solutions may include redesign or strengthening of the blade, reduction of stimuli that excite vibration, or instituting rigid quality control measures to check dimensional accuracy, finishes, and coating quality.

In the case studies presented ahead, dates and other data have been modified in order to keep the user and OEM anonymous. The technical essence of the cases has, however, been maintained.

HOT SECTION BLADING FAILURE
OF A LARGE UTILITY GAS TURBINE

Background

The gas turbine generator that experienced the failure was site rated at 100 MW and operated on distillate fuel. The turbine was inspected three months prior to the failure. During this inspection, corrosion and deposits were found on the hot section, and a decision was made to allow the gas turbine to continue operation to 24,000 equivalent hours before an overhaul outage. The gas turbine was a well proven and reliable design utilizing silo type combustors, operating at a turbine inlet temperature of 1922°F (1050°C), an air mass flowrate of 1056 lb/sec (480 kg/sec), and a pressure ratio of 10:1. It had a 16 stage axial flow compressor and a four stage turbine.

On the day of the failure, the turbine tripped on excessive vibration, while running at a load of 115 MW. The turbine had undergone 473 starts and had 8,900 actual operating hours. Upon dismantling the turbine, 30 first stage turbine blades were found severely damaged. Subsequent DOD had wrecked the other stages. Parts of a fire brick from the top of the right side combustion chamber were found lying in the stationary nozzle vanes located at the six o'clock position. Another piece was found at the center bottom of the inner casing.

The investigation conducted encompassed a detailed review of the failed turbine, metallurgical analyses, and the historical log sheets, which were analyzed for performance data and trends. Special emphasis was placed on evaluation of exhaust gas temperature (EGT) profiles and spreads.

Metallurgical Findings

After examination of the debris, components including the first stage rotor blades, second stage blades, and sections of the first stage nozzle were selected for metallurgical analysis. The conclusions of the metallurgical study were:

• The fracture surface of a particular first stage blade indicated fatigue.

• Blade material was confirmed to be IN 738 with chrome diffusion coatings.

• There was evidence of sulphidation.

• There was no evidence of over temperature.

The observation that the aft portion of the fracture surface on a first stage blade was caused by fatigue, suggested that a fatigue mechanism was present. Observations of the trailing edge (TE)

region of another first stage blade indicated that hot corrosion damage had reduced the pressure side wall of the lowest cooling hole to an extreme thinness. This, in conjunction with the fact that the plane of maximum bending stress coincided with this hole, explained the nucleation and propagation of a fatigue crack. The failure location is shown in Figures 54 and 55.
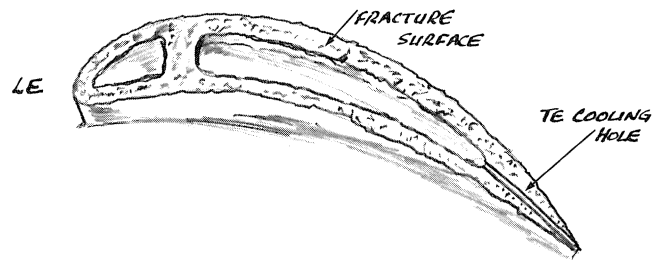

Figure 54. Sketch of Fracture Surface Bisecting Bottom of TE Cooling Hole.

Figure 55. Cooling Hole Crack on Another Blade at 10× Magnification.

Situation Analysis

Some observations pertaining to the failed unit and an identical unit operating at the same site were:

• Analysis of the vibration data of the failed machine (log sheets and strip charts) indicated that there was no progressive growth in overall vibration levels over time. The absolute vibration levels were acceptable.

• Examination of the nozzle section of the operational turbine indicated the presence of salts. This was clear evidence that salt ingestion had taken place. As the fuel treatment system was performing effectively, the salt must have been airborne. Because of the air to fuel ratios involved, 20 ppb of salt in the airflow is equivalent to 1 ppm in the fuel. Moreover, with the large air flowrate of this machine over 900 lb/sec, airborne salt ingestion is a very serious issue. Records of the fuel treatment indicated effective removal of salt.

Figure 56 shows a sketch of the section of the brick that was found lodged in the six o'clock position of the nozzle, accounting for a blockage of about 80 percent of that vane space. This was a significant contributing factor to the failure, as blockage of this nature produced damaging vibratory stresses on the rotating blades by disrupting airflow.
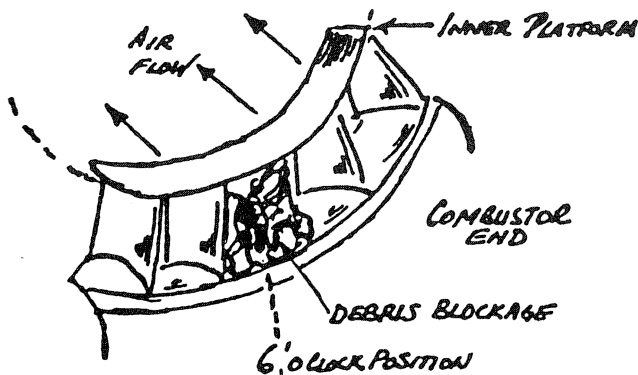

Figure 56. Sketch Showing Brick Trapped in Nozzle Segment.

Data Log Sheet Analysis

Extensive analyses of the "four hour" log sheets were conducted. Calculations and trends were made of the corrected speed, power, pressure ratio, thermal efficiency, compressor efficiency, compressor intake depression, and calculated turbine inlet temperature. From the results, it was evident that there was a degradation in compressor efficiency, which was attributed to axial compressor fouling. This was not, however, a factor contributing to the failure. In addition to basic performance trending, exhaust gas temperature profiles and spreads were examined.

Exhaust Gas Temperature Profiles

A graphical plot was made of the EGT profile, based on the eight exhaust temperature thermocouples, and is presented in Figure 57. In general, the pattern held reasonably well, except for an excursion in the data a few days prior to the failure. Of considerable significance was the fact that for two consecutive hours, thermocouple No. 6 exhibited a significant drop in temperature to 405°C, *when the expected value was 490°C.*
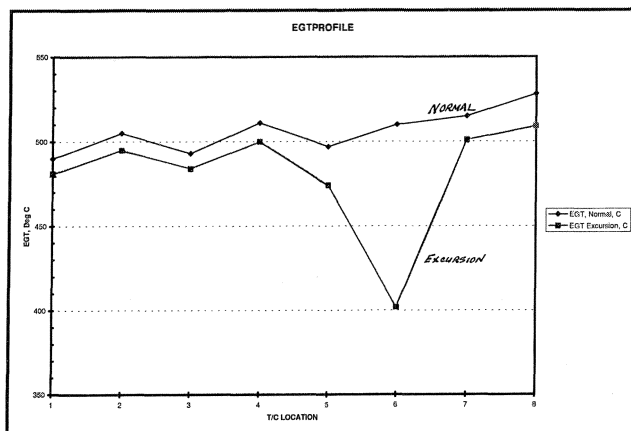

Figure 57. EGT Temperature Profile Excursion Due to Stator Nozzle Blockage.

With respect to the temperature spreads, an X-Y scatter plot was created from log sheet data, by plotting (EGT_{Avg}. − EGT_{min}.) on the abscissa and (EGT_{Avg}. − EGT_{max}.) on the ordinate. This is shown in Figure 58. It is interesting to note that whereas all the

data were within an "acceptable zone" defined by the OEM, there was a significant excursion on the day of the failure. All other data points were highly clustered around coordinates (20, 20).
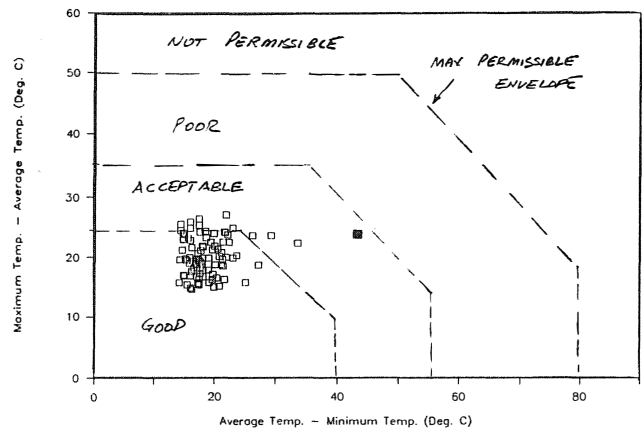

Figure 58. Excursion of Exhaust Temperature Spread. (This clearly shows the importance of monitoring the qualitative shape of the profile to detect changes that may still be within "acceptable" numeric limits.)

This reinforces an important point pertaining to condition monitoring. Visualization step changes that occur in data are of significance even though absolute levels are *quantitatively acceptable.* The importance of trending and evaluating logsheet data is evident in this case.

Sulphidation

Based on visual observations and metallurgical analyses, sulphidation was an important contributing factor to the failure. Figure 59 shows the pressure side of a blade showing hot corrosion damage most severe near the trailing edge. The partial defeat of the walls of some cooling holes can also be seen. Sulphidation can rapidly damage the base material and even a small loss of blade material can shift natural frequencies into dangerous regions, causing resonance and high cycle fatigue. Sulphidation damage to the cooling holes would also result in localized overheating.
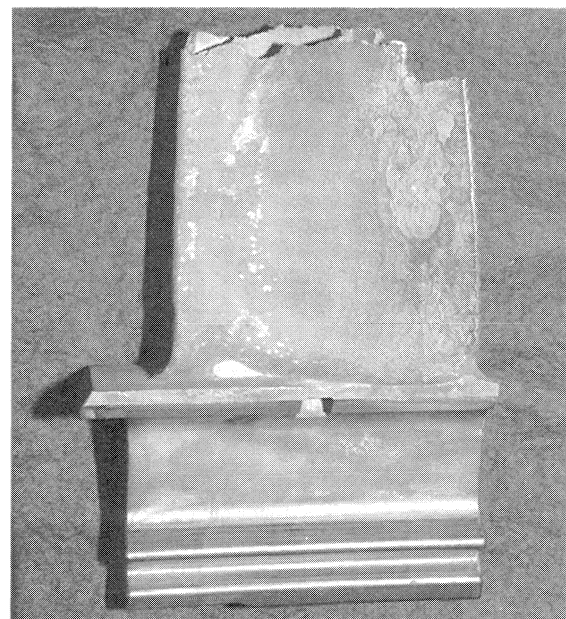

Figure 59. Pressure Side of Blading Showing Hot Corrosion and Partial Defeat of Some Cooling Holes.

Study of Fuel Analysis Reports

Because sulphidation was a factor, possible modes of salt ingress were investigated. The liquid fuel system was first investigated. Data logs of fuel sample analysis were examined to check for the presence of metallic chemical elements harmful to the turbine and showed that contents of sodium, vanadium, and potassium were, on average, less than 0.1 ppm. Lead content was found less than 0.2 ppm. These concentrations were well within acceptable values and the evidence therefore pointed to airborne salt ingestion. Salt deposits on the nozzle segments can be seen in Figure 60.
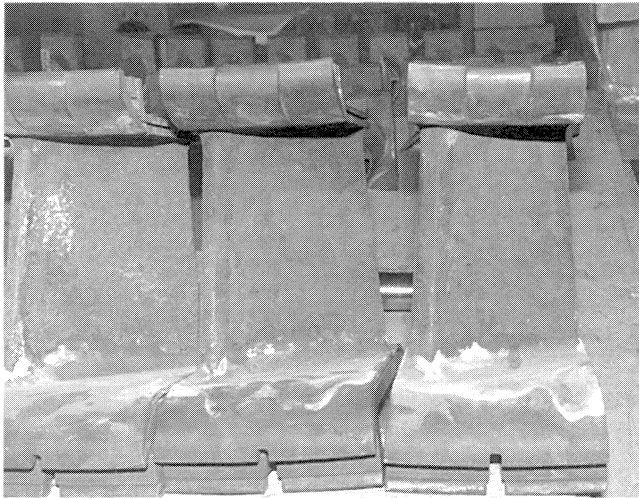

Figure 60. Photo of Nozzles Showing Presence of Salt Deposits.

Blockage of the Nozzle Section
and Its Effects on Blade Vibration

Observations made after the failure indicated that pieces of the combustor firebrick had lodged in the lower nozzle segment, causing a blockage of approximately 80 percent (of that vane space). This occurred in the six o'clock position. It is possible that the blockage may have been far more severe in terms of percentage of nozzle area blocked prior to failure.

The effect of the blockage was to increase vibratory stresses on the blades, resulting in abrupt loading/unloading as the blades traversed this position, as shown in Figure 61. This situation is analogous to partial admission shock loading in a steam turbine. Due to the blockage, the localized mach number and pressure drop affected rotating blade loads. It is difficult to analytically predict the effects of blockage as the severity would depend on the excitation magnitude and the damping associated with the excited mode. However, it is common knowledge that blockage of this nature can promote fatigue failures. Impulse harmonics and weakening of the blade due to sulphidation worked in unison to promote the failure.

Case Summary

The catastrophic damage experienced by the unit was initiated by first stage blade fatigue failure. There were several contributing factors. First, the increased vibratory stresses induced, due to the blockage distortion, caused unusually high alternating stresses. Second, sulphidation weakened the blade. The root cause was breakage of the firebrick from the combustor inner wall. This case illustrates the complicated interaction of operation, design, and environmental factors, and underscores the importance of taking EGT deviations from the norm into account, even when these are within an "acceptable region" in terms of absolute temperature spreads.
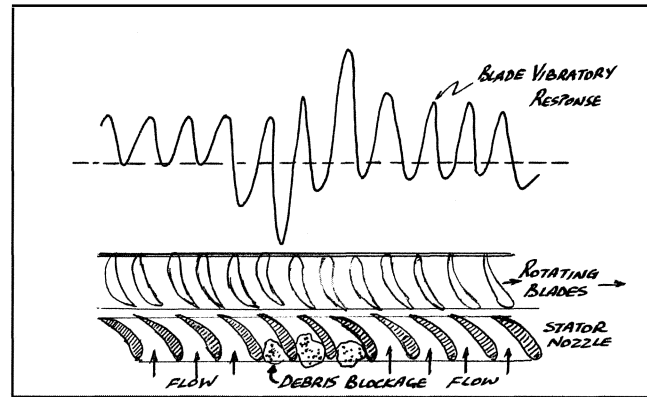

Figure 61. Increase in Blade Vibratory Stresses Due to Blockage.

BLADE FAILURE OF AN AXIAL FLOW EXPANDER

Background

This case involved multiple blading failures on a large single stage axial flow hot gas expander rated at 15 MW and operating at 3600 rpm with an inlet temperature of 1300°F (704°C) and a mass flowrate of 200 lb/sec (91 kg/sec). The expander's availability was of utmost importance to the plant, and financial incentives for keeping the train operational were enormous. Impingement steam was used to cool the expander blades. The expander experienced four blade failures after installation.

First Blade Failure

The first failure occurred after approximately 3,000 hours of operation. Blades were found to be badly affected due to erosion caused by catalyst carryover. The base of the rotor blades had eroded due to steam impingement from the cooling nozzles (the steam flow for impingement cooling was 2,000 lb/hr (910 kg/hr)). The flow pattern on the blades indicated considerable turbulence near the base and at the leading edge at the tip section, which might have excited the blades at operational speeds. It was felt that the rounding of the platform, along with the cutting of the blade in such a uniform manner, could only have occurred from a steady impingement source.

Second Blade Failure

The second failure occurred 10 months later, after 6,200 hours of operation. Blade notching and erosion had occurred at the base due to steam impingement. This was evident by the rounding effect on the blade platform. Catalyst had built up on the shroud. The OEM felt that the failure was due to the *bending* stresses on the blade caused by the catalyst buildup on the shroud. The OEM also felt that the notch at the base was due to catalyst erosion. An alternate opinion was that the notch was caused by the steam injection and that the failure resulted from the high stresses. A study of Larson-Miller parameters and Goodman diagrams was made for the blade material, in order to determine whether a material change from Inconel 750 to Waspalloy should be made.

Third Blade Failure

The third failure occurred eight months after the second failure, after 5,500 hours of operation. The blade material was still Inconel 750 and the disk material Waspalloy. On the run leading to the third failure, steam flow was reduced from 2,000 to 1,000 lb/hr after 1850 hours of operation. Since a decision had been made to replace the blades, a reduction in steam flow was made to minimize the notching problems. When the unit was inspected, cracks were found on the fir tree upper section toward the trailing edge of the blades. The cracks indicated that resonance induced high cycle fatigue was a problem; however, the OEM attributed the cause to

be insufficient cooling. Steam impingement effects were still evident at the leading edge of the blade near the base, but the magnitude was considerably less compared to the second failure. The reduced impingement damage, due to reduced steam cooling flow, confirmed that the problem was not one of catalyst carryover.

Fourth Blade Failure

The fourth failure occurred after an incremental 2,600 hours of operation, approximately five months later. The blade material had been changed from Inconel to Waspalloy and the impingement cooling flow was reduced to 500 lb/hr. This blade failure occurred in the same region as in the third failure (top section of the fir tree); however, the location was on the leading edge of the blade. Electron microscope pictures indicated that a high cycle, low stress fatigue problem existed. Blade resonance conditions were suspected.

Candidate Causes

Based on a study of the four failures, the following candidate causes were considered:

- Resonant frequency of the blade being excited at an "off-design" speed, about 2,450 rpm, at which the unit was run for process reasons.

- Resonant frequency of the blade being excited at design conditions due to process upset conditions or due to increased loading.

- Poor choice of materials. Blade materials were Inconel 750 for the first three failures and Waspalloy for the fourth failure. Both materials have been used extensively in turbomachinery at much higher temperatures. Temperatures in the fir tree section of the rotor were estimated to be between 800°F to 950°F (427°C to 510°C). Consequently, improper materials had a very low probability of being the underlying cause of the failure.

There was a high probability that the third and fourth failures were due to blade resonance and that temperatures may have contributed to the location of the failure position, (i.e., trailing edge for the third failure due to cooling being present at the leading edge, and on the leading edge for the fourth failure due to absence of cooling). The main problem then was to ascertain whether the resonance occurred at the off-design speed range of 2,300 to 2,600 rpm or at the design speed of 3,600 rpm. Blade resonance was recorded by the OEM in a rap test, and spectra indicated that resonances existed in multiples of 520 Hz and 590 Hz. Thus, at speeds of around 2,300 to 2,600 rpm, excitation modes (48E, 12E) could have led to blade resonance and ultimate failure. Blade resonance frequencies were in the 500 Hz to 2,000 Hz range, indicating that failure could occur in one to six hours of operation at these frequencies. In order to investigate the failures, a field test was planned.

Field Test

The objective of this test was to locate the speed and excitation causing the resonance, so as to try to avoid dangerous operational regimes. Air-cooled accelerometers were mounted on the expander mount trunnion and bearings. Signals from the vibration transducers during startup, heating, loading cycles were recorded on an eight channel AM/FM magnetic tape recorder and analyzed using a real time spectrum analyzer.

Campbell Diagram and Modes of Excitation

Natural frequencies for the first flexural, torsional, axial, and second flexural modes were between 540 Hz and 2,133 Hz. Since material stiffness is reduced at operating temperatures, a "hot" and "cold" number were calculated. From the Campbell diagram, it could be seen that excitation was induced by the number of blades (62E), along with the stator (48E), the number of steam injection

nozzles (9E), and the number of struts (8E). During the field test, the data were scanned for resonant peaks, with particular attention being paid to conditions of: change in speed, temperature, load, and injection of cooling steam.

Interpretation of Vibration Spectra

The objective of the vibration spectrum analysis was to detect undesirable excitations, and to examine *relative* changes in amplitude that occurred at specific frequencies with changes in operation.

The vibration response with and without steam injection is shown in Figure 62. This shows how blades resonated as a result of steam injection. Figure 63 depicts the vibration behavior as steam flow increases, indicating an increase in excitation at frequencies of 980 Hz, 1442 Hz, and 1978 Hz (which were close to the blade natural frequencies). The vibration analysis indicated two problems:

- The excitation of blade resonance frequencies at speeds of 2,400 rpm to 2,700 rpm. This implied that these speeds had to be avoided during operation. At other off-design speeds, the blade resonance was negligible.

- Blade resonances were excited as a result of steam injection.

It should be pointed out that detection of blade excitation by the use of high frequency accelerometers is not always possible on turbomachinery. Success in this approach has also been documented by Parge (1990) and Mitchell (1975).
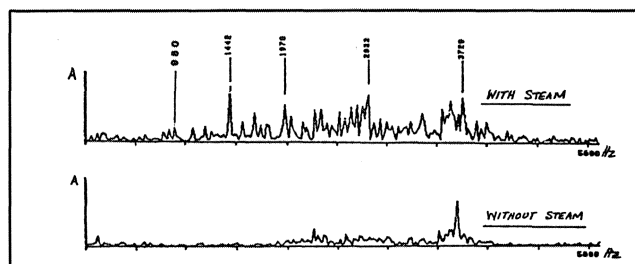

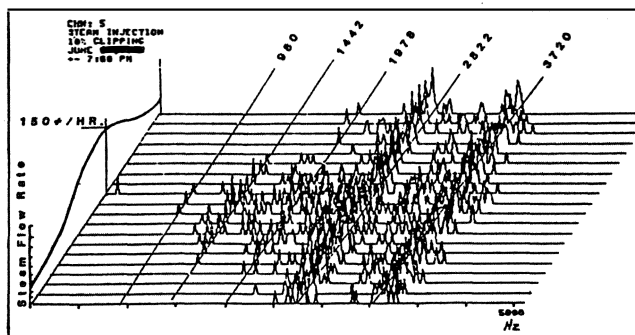Figure 62. Vibration Response With and Without Cooling Steam Injection.

Figure 63. Accelerometer Based Vibration Cascade Showing Response with Steam Injection.

Recommendations and Results

It was recommended that the expander be operated close to its design speed and flow. After a detailed study of blade material capability, a determination was made that steam injection provided minimal cooling benefits and was detrimental in terms of exciting blade resonances. A recommendation was made to discontinue the use of steam for blade cooling and to avoid operation in a particular speed zone. With these recommendations implemented and a careful ongoing vibration monitoring program, an uninterrupted run of over 20,000 hours was achieved.

BLADE FAILURE OF A 15 MW PEAKING GAS TURBINE

Background

This case relates to a 1965 vintage 15 MW natural gas fired peaking gas turbine located in the Gulf Coast region of the U.S. This case demonstrates how practical failure analysis and analytical work can complement each other.

The turbine was a single shaft (60 Hz) unit with a flowrate of 270 lb/sec (123 kg/sec) and a pressure ratio of 7.5:1. The unit had a 19 stage compressor and a seven stage turbine, each being located in individual casings. The unit had run for approximately 29,000 hours with 2,410 starts when the failure occurred. On the day of the failure, operators reported high noise and vibration levels prior to the trip. After coastdown, the rotor locked up. Substantial damage was found in the turbine section.

Description of the Failure

Upon casing removal, the following turbine section damage was found:

● One blade in the fourth stage had migrated and was found cocked axially. This blade was found to have suffered a total failure in the leading edge T-root section (both lands), as shown in Figure 64.

● Severe damage was found in the sixth stage blading with two blades being found broken approximately 1.25 inch from the base. Fracture surfaces were typical of fatigue. One of the fatigued blades is shown in Figure 65.

● Severe blading damage was found in the seventh stage (DOD).

● Vanes in row 6 and 7 were severely damaged (DOD).

● Upon deblading and subsequent NDT inspection, it was found that cracks were present at the T-root sections of the second through fifth stages' blades.

● The blade attachment regions in the drum type rotor indicated wear and corrosion, with the first and seventh stages being in the worst condition.

Figure 66 depicts the damage pictorially and is a sketch made in the field.
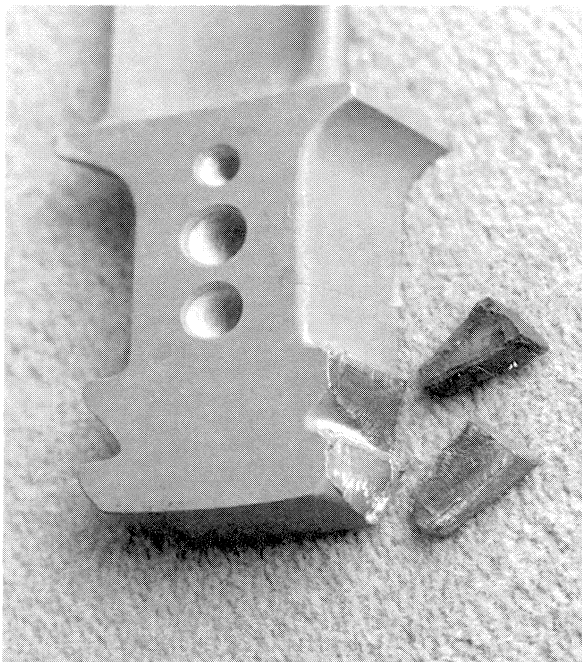

Figure 64. Land Failure on Fourth Stage Turbine Blade.
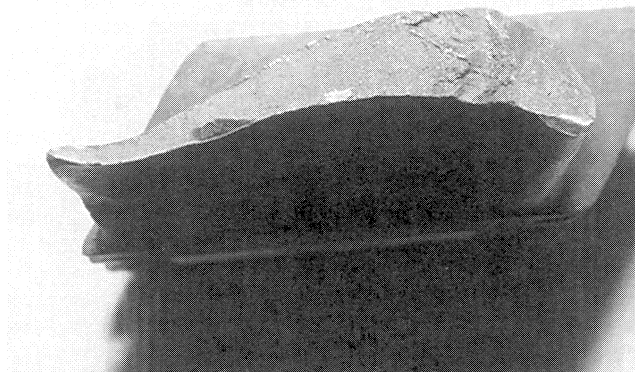

Figure 65. Fracture Surface of Sixth Stage Blade Showing Fatigue.
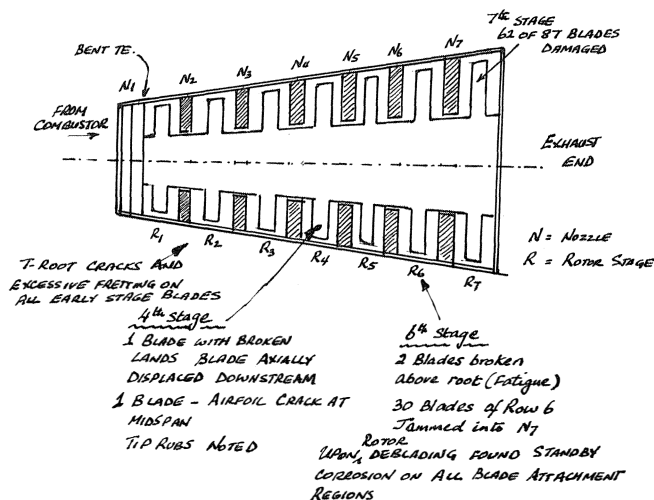

Figure 66. Pictorial Sketch Indicating Extent of Turbine Section Damage.

Metallurgical Analysis

A metallurgical analysis of four blades was carried out. These included two sixth stage blades (fractured through the airfoil) and a fourth and fifth stage blade, which exhibited fluorescent penetrant indications on the blade attachment surfaces. The fourth stage blade had a chordwise crack on the airfoil, emanating from the trailing edge, 1 1/2 inches above the platform.

Visual Observations

The fourth stage blade airfoil tip surface bore evidence of rubbing. This blade did not have a tip shroud or tie wire hole for vibration damping purposes. The airfoil was sectioned to open the chordwise crack, which was 1.5 inches above the platform. The crack was caused by fatigue, with the origin being in or near the trailing edge.

The sixth stage blades examined had ruptured approximately 35 mm and 60 mm above the platform. The fractured surface on one of them was more heavily oxidized than the other, suggesting that one fracture preceded the other. The fracture surface on one blade was so badly oxidized that the typical fatigue crack clamshell markings were not detectable. The oxide coloration on the fracture surface clearly showed that the fracture was caused by fatigue, originating in or near the trailing edge. Fretting damage was seen on the bearing surfaces of both blade attachments. Figure 67 shows the fatigue fracture surface.
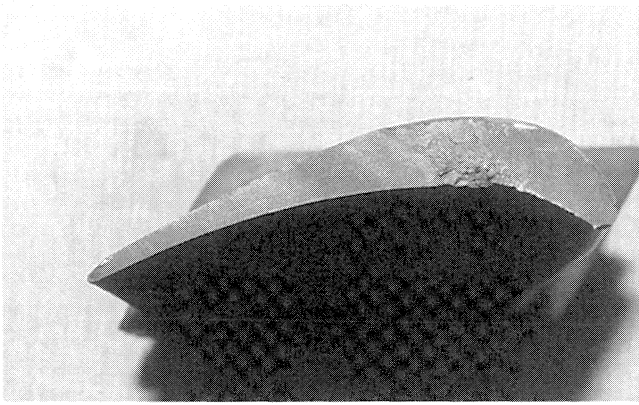
Figure 67. Classic Sixth Stage Fatigue Fracture Surface. (An oxide progressive coloration was observed.)

Metallographic Investigation

Fourth, fifth, and sixth stage blade microstructures were very similar, consisting primarily of austenite grains, similar to type 300 series stainless steels.

Hardness Investigation

Several 5 kg Vickers hardness impressions were made on each of the polished metallographic specimens. The fourth and fifth stage blade materials both averaged equivalent to HRC 16, while the sixth blade material averaged to HRC 24.

Scanning Electron Microscope Investigation

Both of the sixth blade fracture surfaces were examined using a scanning electron microscope (SEM), but this examination did not yield any useful information about the origins of the fractures. The fractures from the fourth blade were also examined in the SEM. Whereas no fracture origin was found, some badly oxidized fatigue striations (i.e., "clamshell" markings) were noted.

In the case of the fourth blade airfoil fatigue crack, there were two considerations. First, the airfoil tip shroud *showed evidence of rubbing*; hence, this strumming may have set up resonant vibration in the airfoil, leading to the nucleation of the fatigue crack. Secondly, the alloy used for the fourth blade had a very low tensile strength. Since fatigue strength is directly linked to the ultimate tensile strength, it follows that fatigue crack initiation is relatively easy with a weak alloy.

Situation Analysis

In order to troubleshoot the failure, the following analytical studies were conducted:

- Review of forces on blade attachments
- Blade stress analysis
- Blade natural frequency analysis
- Review of blading materials (UTS and Ni content)

Migration of the Fourth Stage Blade and Its Effect on Blade Vibration

The displaced fourth stage blade would induce a very high vibratory stress on the downstream blades due to the flow discontinuity effect. This was, in all probability, a major factor leading to fatigue failure in the sixth stage. The resulting flow discontinuity resulted in abrupt loading/unloading of the blades, as they passed this position (analogous to partial admission shock loading). Due to blockage effect, the localized machine mach number and pressure drop changed, which in turn affected the loads imposed on the blading.

Fretting Damage in Blade Roots

Excessive vibration that occurred in the turbine accelerated the process of fretting that caused the cracks found in the roots of almost all stages. The gas turbine hot section uses an internal groove double T-slot arrangement. In this type of design, the assembly is considerably "softer" in the circumferential direction. The circumferential component of the alternating bending forces has historically been a common cause of failure for the internal groove root. This type of root utilizes parallelogram shaped root platforms and is vulnerable to fatigue failures. The highest loading occurs at the top serration near the trailing edge and this is often responsible for inducing fatigue cracks in the adjacent fillet and shank corner. The rotor drum shown in Figure 68 had also experienced severe standby corrosion in the blade attachment regions (Figure 69).
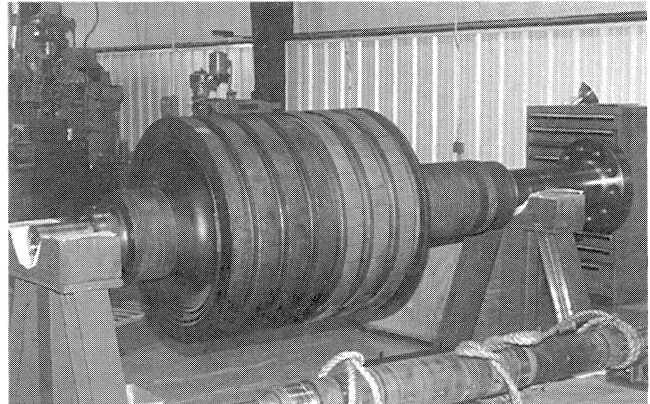

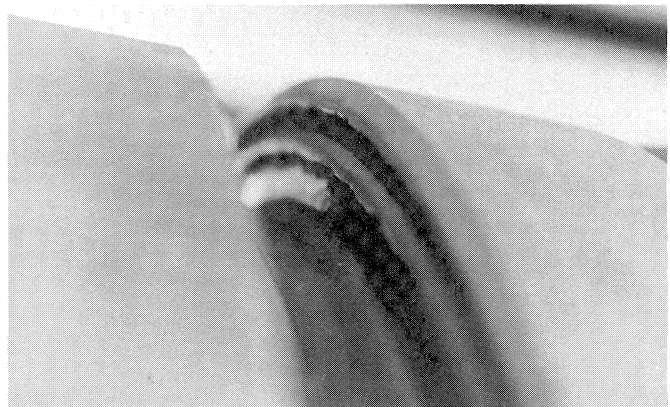*Figure 68. Overview of Drum Type Rotor After Deblading.*

Figure 69. Standby Corrosion Damage to Rotor Drum in the Blade Attachment Region.

Of the blades examined, 63 percent had cracks on the land trailing edge location where, as described above, the stresses are the highest. The blade bending moment is transferred to the rotor, if the shank portion is tight in the rotor drum (a drum type rotor assembly is relatively axially stiff). *If there is any looseness however, the load is transferred to the shank.* This load then added to the existing centrifugal forces that exist and played a role in the fourth stage blade land failure.

Subsequent to the initial failure within the turbine, extended operation at exceedingly high vibration levels caused accelerated wear and fatigue on the blade land regions. Hittori, et al. (1983), examined fretting fatigue in gas turbine disk/blade dovetail region under blade centrifugal and bending loads, and showed that the amount of total slippage is very sensitive to the bending moment (i.e., alternating stress).

Additionally, the blade disk interface provides an important source of damping (stick-slip friction damping) and this is most important for the lower vibration modes of the blade. Goodman and Klump (1956) have found that a highly beneficial reduction in resonant stresses can be achieved by friction damping. Several fatigue failures have typically originated by vibration at the lower modes.

Analytical Model for Root Section Stress

This analysis was conducted to get a feel for the operating stresses and to determine the conservativeness of design of the blading. Dimensions were taken from the blading or scaled from drawings that were available. The approaches followed for the stress calculations were based on methods of Sohre (1975) and Dundas (1985). Several cases were studied to examine the sensitivity of blade stress to bearing area. The analysis pointed out relatively conservative stresses.

Evaluation of Vibratory Stresses

A Goodman diagram created for the third through the seventh stage blading is shown in Figure 70. All of the stage materials have a UTS of approximately 100 ksi. The steady state stress was considered the sum of the gas bending stress and the centrifugal stress. The alternating stress is determined by applying a magnification factor of three to the gas bending stresses (Scalzo, 1991). This has been designated as Case 1. The results have been shown plotted on a Goodman diagram. The results with a higher magnification factor of 4.5 (magnification factor of three, multiplied by a stress concentration factor of 1.5) are also shown in the diagram (Case 2). It is clear that both the sixth and seventh stages are close to design fatigue limit, with factors of safety rapidly eroding as alternating stresses go up. The Goodman factor of safety dips below 1.5 (normally, the minimum acceptable) for the sixth and seventh stages. Thus, any loss of damping would result in a relatively rapid fatigue failure.
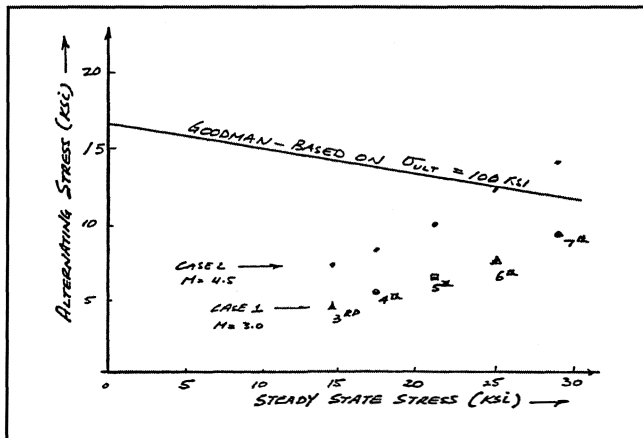

Figure 70. Goodman Diagram Showing Erosion of Safety Factor, Especially for the Sixth and Seventh Stages.

Analytical Model for Evaluation of Blade Natural Frequencies

In order to obtain an estimate of blade natural frequencies, an analytical model along the lines suggested by Marscher (1985) was created to evaluate the bending mode (flap) mode of vibration. The analysis considered a free standing blade as a cantilever. The natural frequency calculated was corrected for centrifugal stiffening effects, blade camber, bow, and taper. Operating temperatures were taken into account by means of reduction in Young's modulus (E). The Young's modulus values for austenitic steel were obtained from Faupel (1964). The effect of blade taper was neglected, because taper ratios were relatively small for all stages and would induce a marginal effect on the natural frequency.

The calculations showed that the first bending to operating speed ratio falls below four for the seventh stage blading. Common design practice requires that a margin of at least four be maintained. The sixth stage blade natural frequency could have easily been excited by the fourth order of the running speed caused by the displaced (cocked) blade, which would cause flow distortion in the upstream stages. It is of critical importance to note that after the first sixth stage fatigue failure, there was a loss of integrity of the damping wire system. The sixth stage blading relied on frictional damping of the lacing wire to absorb vibration energy. With a loss in this damping, vibratory stresses increased by a factor of three to four, causing additional distress.

Blading Materials and Standby Corrosion

Another important factor that contributed to the problems was standby corrosion in the blade root attachment region. This is a problem that commonly afflicts peaking gas turbines. Corrosion products that accumulate in the blade attachment areas act as abrasives and increase clearances. In the presence of corrosives, possibly from airborne salt, uncoated airfoils often develop corrosion pits that could progress into cracks.

Failure Scenario and Root Causes

A combination of fretting wear and standby corrosion in the blade attachment areas caused looseness, and a reduction in the blade bearing area resulted in the total failure of the fourth stage blade land attachment area. The cocking of the fourth stage blade set up wakes, ultimately resulting in the sixth stage blade fatigue failures. This case shows the interaction effects of environment (standby corrosion), design features, and operating conditions. It also shows that considerable insight can be obtained by relatively simple modelling techniques. While there are several cases where finite element models are appropriate, it is the authors' contention that simple hand or spreadsheet type calculations can provide a quick engineering feel for the blade dynamics for use in field troubleshooting situations.

DOD BLADE FAILURE IN A 30 MW GAS TURBINE

Background

The subject gas turbine was a natural gas fired 30 MW single shaft, cold end drive, 3,600 rpm unit that was in power generation service. The gas turbine operated at a turbine entry temperature of 1,565°F (850°C) and with a compressor pressure ratio of 8:1. It had a 15 stage compressor, a single silo combustor, and a five stage turbine. The gas turbine had operated for approximately seven days at a load of 10 MW when it failed. The failure was preceded by a loud noise, after which the turbine tripped on vibration. Vibration trip level was set at 40 microns, peak-to-peak.

Eighteen months prior to the failure, which is the focus of this case study, a similar incident had occurred, after which a new set of blades had been installed. The damage in this previous failure was of a FOD/DOD nature with severe damage occurring throughout the turbine section. The failure mode was impact overload with fracture surfaces being interdendritic in nature. Of particular importance, in this earlier failure, was that some small spherical particles were found adhered to the stator vane surface. At the time of the previous incident, *the root cause for the DOD was not determined and this resulted in the subsequent failure.*

Description of the Failure

The turbine section was totally destroyed and is shown in Figure 71 and Figure 72. A sketch created in the field showing the extent of the damage is depicted in Figure 73. All five turbine stages were severely damaged, with fracture damage being indicative of impact overload. The stator nozzles, the rotor blades, and drum were badly battered. Numerous blades from the first three stages had been cropped, with the third stage rotor blades being totally wiped out.

Several blades in this row had broken at the root near the cooling hole (Figure 74). The compressor section and bearings were not damaged. A few compressor stages indicated tip rubs probably caused by the tremendous unbalance forces that resulted with loss of turbine blading. The rubs occurred at the center of the rotor where deflection would be the greatest.
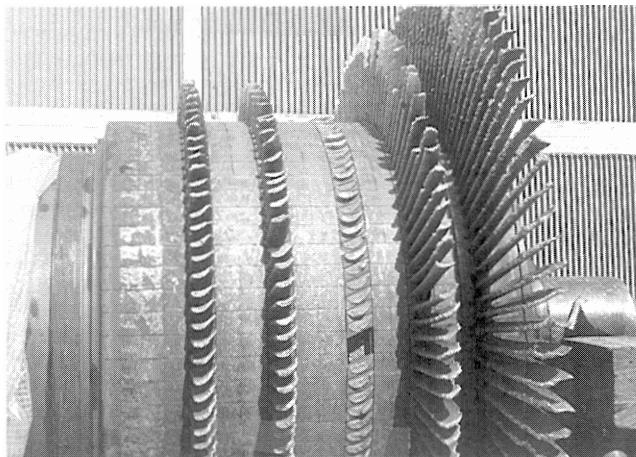

Figure 71. Destruction of Turbine Section.

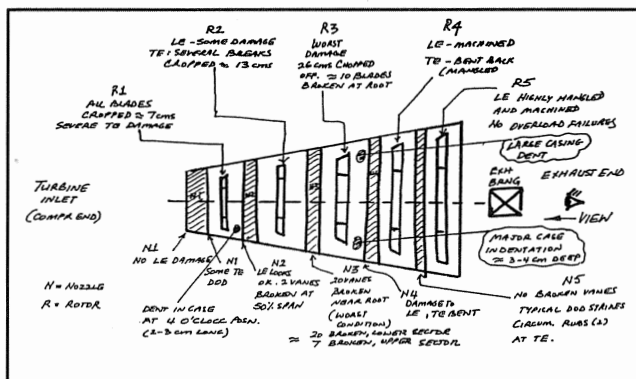

Figure 72. Lower Casing Stator Section Damage.

Figure 73. Field Sketch Detailing Damage. (Sketches, such as these made in the field, are a rapid way of documenting damage.)

Debris in Turbine

Careful examination of the debris in the turbine section revealed what appeared to be a foreign object located in the lower stator case (as shown in Figure 75), before the fourth stage stator vanes.

Figure 74. Blade Breakage at Root through Cooling Hole.

This battered piece shown in Figure 76, was approximately 40 mm long and had a diameter ranging between 15 to 20 mm, and did not look like a turbine section component. Thereafter, the combustor dome was inspected. The dome had six struts to hold the swirl vane support inner ring, which were held by clevis pins approximately 55 mm in length and a diameter of 20 mm. These clevis pins held the strut and were then locked in place by cotter pins. Figure 77 shows details of the construction of the silo combustor and shows the locations of the missing pins. Two of the six struts had missing clevis pins (Figure 78). The ingestion of these clevis pins was the cause of the domestic object damage in the turbine section.

Figure 75. Battered Pin Found in Turbine Debris (Lower Turbine Casing). (This indicates the importance of a careful search of the debris. Missing this evidence on a similar failure in the past, resulted in this "repeat" failure.)

Figure 76. View of Pin Found in Debris. (Length approximately 40 mm, diameter 15 to 20 mm.)
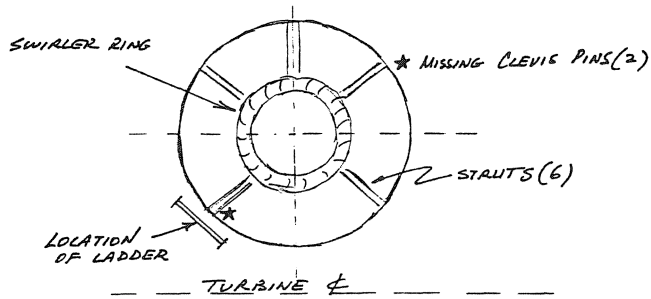
Figure 77. Sketch of Combustor Dome Showing Location of Missing Clevis Pins.

Figure 78. Photograph of Struts with Missing Clevis Pins.

Metallurgical Analysis

Selected hardware items, including blades, stator blades, and other clevis pins from the combustor, were selected for metallurgical examination. The assortment of clevis pins selected for analysis with a section of the battered "foreign object" is shown in Figure 79.
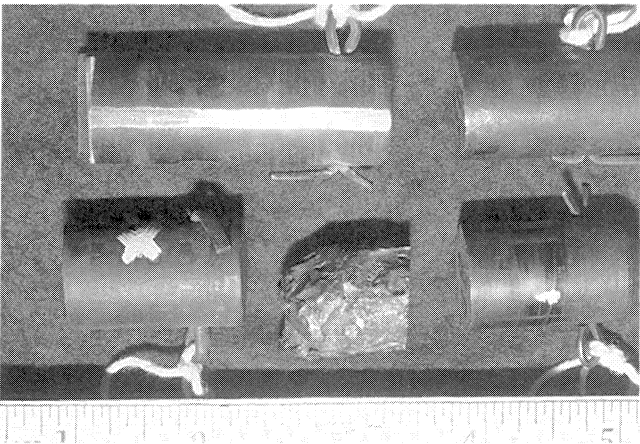

Figure 79. Assortment of Items for Metallurgical Investigation.

Details of the Examination

Clevis Pins—Some of the clevis pins had cotter pins installed that were magnetic and made from relatively large cross-section wire, while one cotter pin was nonmagnetic and was made from a much smaller cross-section wire. Significant fretting corrosion damage was noted where the cotter pins protruded from both ends

of the cross drilled holes—the most serious being on the thin, nonmagnetic cotter pin. *The battered piece found in the turbine debris and the clevis pin samples exhibited substantially the same microstructures.* A 10× photomacrograph of the cotter pin showing the fretting damage and weakening is shown in Figure 80.
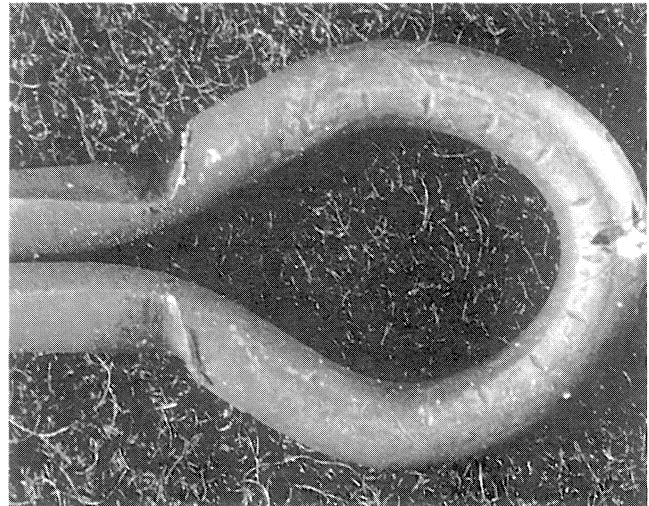

Figure 80. 10× Photomicrograph of Cotter Pin. (Fretting damage and wear can be seen.)

Stators and Blades—All of the fracture surfaces were 100 percent interdendritic in nature. No evidence of creep, stress rupture, or fatigue cracking was observed. All other nonfracture damage (i.e., indentation, smearing, bending, "machining") were considered consistent with overall turbine damage.

Overtemperature Analysis—A standard overtemperature examination was done on one of the first stage stators, comparing the microstructure at the midspan leading edge position on the airfoil with that from a region outside the gas path, as a baseline. No evidence of gamma prime precipitate solutioning (the accepted indicator of service overtemperature of nickel-based superalloys) was observed.

Clevis Pin Transport Model

A simple model was created to examine the transport of the clevis pin in the U-duct and into the turbine. This model evaluated the capability of the air stream to lift the pin vertically into the air stream up the U-duct and into the nozzle section. The transport probably occurred along the duct surface and the pin then was ingested into the turbine in a lengthwise orientation. The model considered the following parameters:

- Pin length 5.5 cm, diameter 1.75 cm
- Material density = 0.283 lb_m/in^3
- Coefficient of drag = 0.7 to 0.8 (cylindrical pin with L/D ≈ 5)
- Gas temperature = 1,565°F (2,025°R)
- Pressure = 116 psia (pressure ratio of 7.85:1 assumed)
- Pin projected area = 1.45 in^2

The governing equation is,

$$Lift = C_d A \rho V^2/2 \qquad (6)$$

Where:
C_d = Coefficient of drag
A = Cylinder projected area
ρ = Air density in slugs
V = Airflow velocity

This equation was used to determine the ability of the airflow to transport the pin to the turbine nozzle vanes. Even at an air velocity of 50 ft/sec, a 1.3 lb pin could be lifted. The new pin was estimated to weigh no more than 0.25 lb.

Case Summary

The massive turbine failure was the result of ingestion of a clevis pin, which had been liberated from the top of the silo combustor. The dislodging was the result of fretting damage, which disintegrated a cotter pin used for retention of the clevis pin. In the light of this finding, it is entirely possible that the earlier failure was also caused by the liberation of a clevis pin from the top end of the silo burner. The low alloy steel globules on the first stage stator airfoil surface, found during the first failure metallurgical study, were definitely low alloy steel, and in all likelihood were derived from an ingested clevis pin. This case stresses the importance of a *thorough search of debris* for telltale clues.

CASE INDICATING IMPORTANCE OF GAS TURBINE FUEL SYSTEM FUEL QUALITY

Background

This case involved a single shaft dual fuel heavy duty gas turbine rated at 18 MW that had operated for 13,000 hours. The failure occurred during a changeover from natural gas to liquid fuel, when the unit output dropped from 18 MW to 8 MW. The operator initiated a change back to No. 2 fuel oil and the turbine tripped on high exhaust gas temperature.

Damage to Gas Turbine and Site Inspection

Due to internal damage to the gas turbine, the rotor had moved over ½ inch in the axial direction, causing damage on the aft end of the first stage turbine wheel. A significant finding was that the fuel gas tip of one of the combustors had come loose and was found lodged in the combustion liner.

The first stage nozzle, directly opposite the combustor can that had the loose gas tip, was burnt away. The nozzle support ring was also severely damaged. The second stage nozzle showed some signs of overtemperature, but the predominant damage was due to domestic object damage. The first stage blades showed signs of overtemperature and burned portions at the base of the blade characteristic of liquid carryover. The damage is sketched in Figure 81.
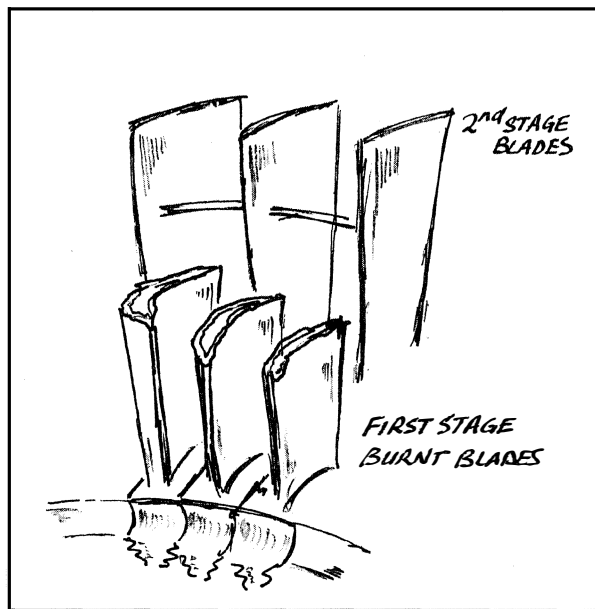

Figure 81. Blade Damage Caused Due to Combustor Fire (Liquid Hydrocarbons in the Fuel).

Situation Analysis

Gas Overfueling without the Presence of Hydrocarbon Liquids

As the nozzle cap unscrewed, there was an increase in the gas flowrate to the combustor. Calculations by the OEM indicated an increase in flow of about two to nine times the normal quantity. (This would have caused a consequent *reduction* in flow to the other combustors). With an increase in fuel flow, the fuel/air (F/A) ratio exceeded the upper limit of flammability, causing the flame to move downstream of the reaction zone. The flame would reestablish itself at a location where there was extra air and some vorticity to slow down part of the flow, for example, at the main dilution holes. At some intermediate stage, it is possible that a long streak of flame could have overheated the liner and transition piece. Corner vortices set up in the transition piece could also act as flameholders. It was also possible that the nozzle vanes themselves acted as flame holders.

Effect of Liquid Hydrocarbon in Gas

If a liquid were present in the gas supply, then, as the nozzle cap became loose, liquid would tend to be transported to the faulty combustor. If a significant quantity of liquid was transported in this manner, through a reaction zone where gas overfueling had caused the flame to move through a reaction zone (downstream), droplets would impinge on the inner partition ring. Influenced by the secondary flow system, the liquid would tend to accumulate against the convex face of the vane and the enhanced flame would attack the partition ring.

Discussion

This case shows how severe blading failure can be caused by design weaknesses (loosening of the burner tip) not directly related to the blades. The fuel nozzle problem was solved by the use of a strap welded to the body and cap, and by the use of lockwire. Furthermore, the case stresses the importance of good fuel quality and effective EGT monitoring.

CLOSURE

Blading failures in gas turbines account for a major proportion of serious outages. The troubleshooting and resolution of complex blade failure problems call for an interdisciplinary engineering effort to ensure that repeat failures do not occur upon startup of the machine. Finding the underlying root cause can be difficult, but is essential. Failures must be examined, not only from a metallurgical perspective, but also from a design, operation, and maintenance standpoint. Investigations have to identify root causes and contributing factors. The ultimate goal is, however, to recommend and institute changes in design, operation, or maintenance procedures to ensure that problems do not recur. This paper has attempted to provide a unified treatment of the causes, failure modes, and troubleshooting to assist plant engineers in tackling blade failure problems and in interacting with the OEM.

APPENDIX A

PRACTICAL FORMULAE AND RULES OF THUMB FOR BLADING PROBLEMS

This appendix provides some basic formulae and rules of thumb to be used for obtaining a rough feel for blading problems, and is not intended to be a review of blading dynamics. The intent is to provide insight in field troubleshooting situations.

1. *Blade Modes*—In general, the most serious (largest amplitude) vibration occurs in one of the blade's normal modes. In almost 90 percent of the failures (in axial flow compressors), these can be attributed to vibration in the first or second flexural mode, the first torsional mode, or the first edgewise mode (Armstrong and Stevenson, 1960). Good rule of thumb is to keep blade natural frequency > 4× maximum operating speed.

2. *Log Damping Decrement*—An important parameter in blading vibration is the log damping decrement d defined as:

$$\delta = \ln\{a_1/a_2\} = \gamma T \qquad (A-1)$$

Where:
a_1 and a_2 = Two consecutive amplitudes
γ = Damping coefficient
T = Period of vibration

The coefficient γ is related to damping factor δ by:

$$\gamma = \beta/(2m) \qquad (A-2)$$

with m being the reduced mass of the blade.

It is the damping decrement that is responsible for the amount of vibration of the blade in or out of resonance. In a resonance condition, the amplification factor (AF), which is the ratio of the amplitude to the static deflection of the blade under the same forces of excitation, is given by:

$$AF = \pi/\delta \qquad (A-3)$$

This factor is also equal to the ratio of the static force to the pulsating force to reach the same deflection. If $\delta = 1.6$ percent, then $AF = 200$. Thus at resonance, a pulsating gas force of 200 times smaller than the static force is sufficient to create the same blade deflection.

Addition of Aerodynamic Excitation

The static bending stress (σ_b) due to aerodynamic excitation is given by:

$$\sigma_b = HS\sigma_g \qquad (A-4)$$

Where:
H = Function of the blade form and of the mode of vibration
S = Stimulus proportional to a fraction of static gas bending stress (σ_g) on the blade, responsible for the excitation

The alternating stress (σ_w) in resonance is given by:

$$\sigma_w = \text{(Amplification factor)} \times \text{(Static Stress)} \qquad (A-5)$$
$$= [\pi/\delta]\, HS\sigma_g$$

As per Strub (1974), for an average value of $\delta = 1.8$ percent for a rotary compressor blade 10 percent off resonance, an amplification factor is about five. For a value of $H = 0.9$ corresponding to the first bending and a stimulus of $S = 0.1$, the alternating stress in the blade is:

$$\sigma_w/\sigma_g = (5) \times 0.9 \times 0.1 \approx 0.45 \qquad (A-6)$$

The stimulus (S) can vary from 0.1 to 0.2, depending on wake intensity, and it is also a function of the distance between the blade rows.

Considering a uniform cantilever vibrating in one of its normal modes of vibration, the maximum stress at the root section (σ_{max}) is given by (Armstrong and Stevenson, 1960):

$$\sigma_{max} = 2\pi \frac{y}{k} \sqrt{(E\rho)af} \qquad (A-7)$$

Where:
$\pm a$ = Leading edge tip amplitude of vibration at f (Hz) (i.e., total amplitude)
k = Radius of gyration
y = Distance of neutral axis to point of maximum stress
E = Young's modulus

ρ = Density
f = Frequency

In examining this equation, it can be seen that neither the length nor chord enters the expression. When the maximum stress is equal to the endurance stress, the factor *af* is *solely* dependent on the section geometry and the material properties. Fatigue tests on blades has shown that *af* for failure does not vary much between different blade designs, but is dependent on the material. Typical values of *af* for 10^7 reversals are:

- Aluminum, 5.5 ft/sec
- Steel, 6.5 ft/sec
- Titanium, 11.0 ft/sec

3. *Blade Stresses*—For practical equations for steam turbine blading, please see Sohre (1975). The appendix of this excellent work provides blade stress evaluation procedures.

Some practical equations from Sorensen (1951) are:

Root section stress due to centrifugal force is given by:

$$\sigma_c = 4.5 l\gamma A \left(\frac{N}{1000}\right)^2 \qquad (A-8)$$

This assumes constant area of blade from root to tip. In practice, blades are tapered to reduce mass at the tip. Including a taper factor, the root force resulting from centrifugal force is:

$$\sigma_c = 4.5 l\, f_t\, \gamma\, A \left(\frac{N}{1000}\right)^2 \qquad (A-9)$$

Where:
σ_c = Average tensile stress, psi
f_t = Taper factor (Figure A-1)
γ = Specific weight of blading material, lb/cu-in
A = Annular flow area of blade ring, sq-in
N = Rotative speed, rpm

Bending stresses are more complicated to evaluate and a method is found in Sorensen (1951).

Typically, the maximum stress at the root section of a compressor blade occurs at the trailing edge, where both the stress due to centrifugal force and gas loading are additive (i.e., tensile). For a turbine blade, the maximum stress will normally occur at the concave side of the leading edge.

4. *Fundamental Mode of Vibration (Natural Frequency)*—For centrifugal impellers, natural frequency can be calculated by the method of Voysey (1945). For an axial blade, the natural frequency may be estimated (Sorensen, 1951) by:

$$f_s = 11.0\, C_f\, \frac{k}{L^2} \sqrt{\frac{E}{\gamma}} \qquad (A-10)$$

Where:
f_s = Natural frequency, Hz
C_f = Frequency correction factor
k = Minimum radius of gyration of base profile, inch
L = Blade length, inch
E = Young's modulus, psi
γ = Specific weight of blade material, lb/cu-in

The effect of taper on blade natural frequency is presented in Figure A-2 (Sorensen, 1951).

5. *Flutter*—Shannon (1945) has proposed a parameter to indicate proneness to flutter. This parameter is given by:

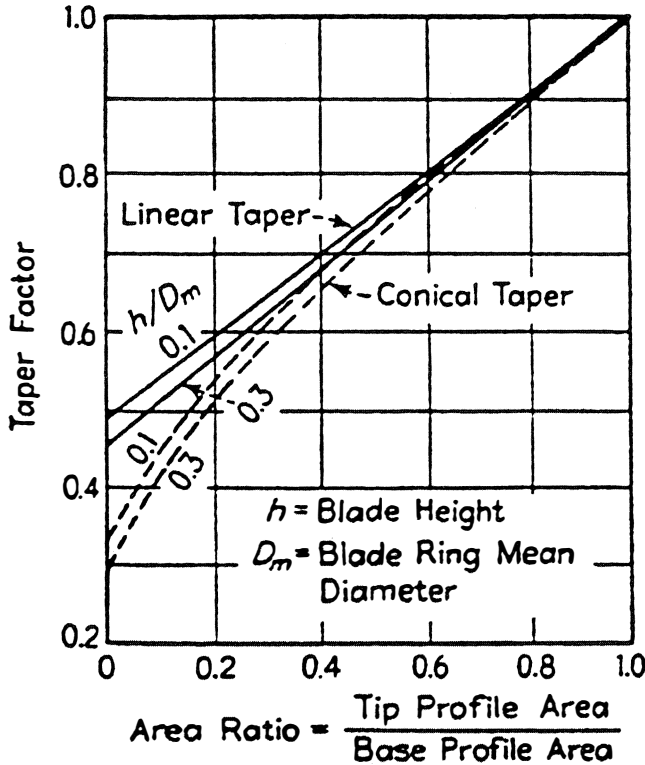$$\lambda = \frac{2\pi\, fc}{v} \qquad (A-11)$$

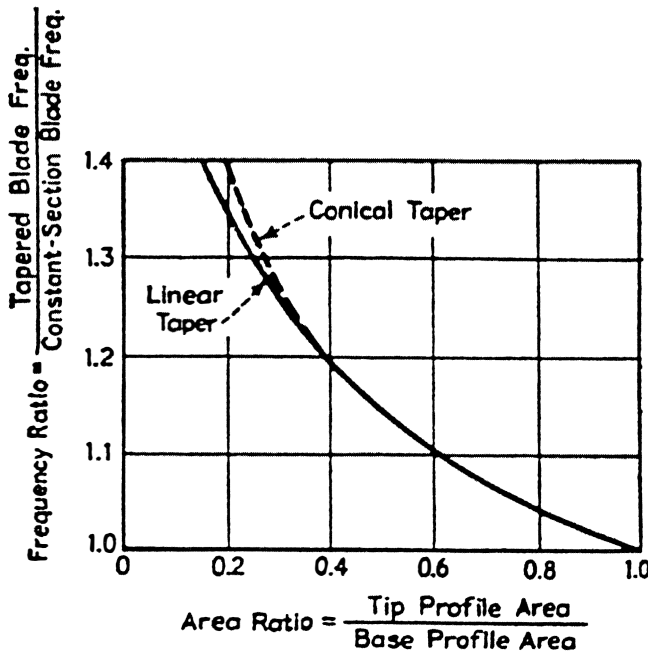*Figure A-1. Variation of Taper Factor with Blade Profile Area Ratio. (Sorensen, 1951)*

Figure A-2. Effect of Taper on Blade Natural Frequency.

Where:

f = Frequency of the blade (in bending or torsion), Hz
c = Blade chord
v = Air intake velocity

Shannon has recommended that this parameter should exceed 1.5 to avoid stall flutter, but considerable disagreement exists as to the application of this parameter. Armstrong (1967) has suggested that two values are required according to the type of vibration:

- Torsional frequency parameter = 1.6
- Flexural frequency parameter = 0.3

Nowadays, a number of 0.33 or 0.35 is normally used as the limit for bending flutter. Using these empirical values, it has been possible to avoid flutter for subsonic inlet flow and, hence, these numbers have remained a widely accepted correlation for this type of instability. Different parameters have to be used for high mach number stages with low hub-casing ratio and high aspect ratio blades.

6. *Asymmetrical Inlet Flow Distortion* (Strub, 1974)—In certain cases, blade resonance can occur at numbers that are not integer multiples of running rpm. This can occur when the disturbance is varying with time, either in amplitude or in position, i.e., moving along the periphery of the inlet channel. If the disturbance is distributed periodically around the periphery of the inlet channel with periodicity K, and if blade angular velocity is w, then the rotating blade would be subject to a disturbance, $c = C \sin (kwt)$. If the amplitude C is also time dependent, $C = c_0 \sin (mwt)$, where m = any integer or fractional number indicating how many times the pulsation occurs in one revolution.

Utilizing the above we have,

$$C = c_0 \, \text{Sin} \, (mwt) \, \text{Sin} \, (kwt) \qquad (A\text{-}12)$$

Thus,

$$C = \frac{c_0}{2} \text{Cos} \, [(k-m) \, wt] - \frac{c_0}{2} \, \text{Cos} \, [(k+m) \, wt] \quad (A\text{-}13)$$

This shows that disturbances of:

$$\frac{1}{2\pi} \, (k-m) \, w \text{ and } \frac{1}{2\pi} \, (k+m) \, w \qquad (A\text{-}14)$$

are present.

7. *Combustor Profile and Pattern Factor*—Since combustor airflow/temperature distortion problems can cause several blade failures, some pertinent design review parameters are presented here (Dundas, 1988):

$$\text{Combustor Profile Factor} = F_p = \frac{(TA-TIT)}{(TIT-TCD)} \quad (A\text{-}15)$$

Where:
TA = Average temperature at given radial station
TIT = Average turbine entry temperature
TCD = Average compressor discharge temperature

Typical peak value of $F_p \approx 0.12$. At outer flow path F_p should be ≤ 0.05.

Note that circumferential averages are used (as opposed to peak temperatures), as these are the temperatures that effect creep life or ratcheting behavior of stationary parts.

$$\text{Combustor Pattern Factor} = F_c = \frac{(TP-TIT)}{(TIT-TCD)} \quad (A\text{-}16)$$

Where:
TP = Peak temperature at any point in the flowpath

This is a measure of the severity of the combustor discharge temperature variation, as experienced by the stationary components of the turbine.

The pattern factor (F_c) defines the highest temperature experienced by the transition and turbine section. Typical value for $F_c \approx 0.2$ to 0.24. As an example, if $TP = 1,180°C$, $TIT = 1,050°C$ and $TCD = 400°C$, then $F_c = 0.2$ (20 percent).

8. *Campbell Diagrams—Static to Dynamic Conditions*—Natural frequencies of blading and packets of blading can be determined by the use of finite element models. Several times, however, in practical troubleshooting cases, it is necessary to know natural

before continuing with photographs of the aft side of the disk. Make a note of this. When the number of photos go into the hundreds, careful documentation along with "extra indicators" are a must. Never rely on memory to differentiate photos as, after several days at failure site, and movement of equipment, mistakes *will* occur without clear documentation. In a failure investigation lasting several days, it is a good idea to submit the photos daily for 1-hour development. This allows a check on photo quality and allows the retake of certain photos if they are of poor quality. Immediately number the photos and link to the negative strip number.

18. *Design of Air Inlet System to Ensure Blade Integrity*—An improperly designed air inlet system to the axial flow compressor can cause performance and blade stresses to be seriously effected. While the responsibility for the design typically rests with the OEM or engine packager, it is useful for users to have a feel for the criticality of the situation. For the inlet system, including ducting, silencers should be designed to provide uniform flow at the compressor inlet section. Excessive pressure distortion can, at times, induce high stresses in blades and vanes, and cause compressor stall. The OEM can provide engine specific criteria and test procedures with respect to inlet distortion limits. Some older heavy duty gas turbines may have been more tolerant of inlet distortion, compared with high performance aeroderivative gas turbines.

Distortion may be quantified by means of Equation (A-23) with measurements being made with several pressure rakes located at centers of equal areas in the inlet.

$$D = \{Ptotal_{max} - Ptotal_{min}\} / Ptotal_{Avg} \qquad (A-23)$$

Where:
D = Steady state distortion measure
$Ptotal_{max}$ = Maximum total pressure of any probe
$Ptotal_{min}$ = Minimum total pressure of any probe
$Ptotal_{Avg}$ = Average total pressure of all probes

Typical (check with OEM) value for *D* may be 0.02 to 0.025. Measurements are typically made at several power levels.

Fast response probes should be used to determine *instantaneous* total pressure distortion using the same equation, and the limits could be, say, 0.1. There are also limits to the amount of swirl permitted (can be as tight as five degrees for some gas turbines) and temperature distortion limits. Turbulence should also be avoided. Things to look out for in inlet system design include:

● Avoid structural members in the inlet plenum that would contact the air and cause distortion.

● Avoid dirt traps that will allow dirt to accumulate.

● Very careful sealing must be done of the inlet system.

● Insist on low point drains in the inlet plenum.

● Check on integrity and quality of wash nozzles installed as a retrofit, and ensure that the distortion limits are not violated with the installation of nozzles.

● All 316L stainless steel construction is *highly* recommended and will help long term reliability. Given the importance of air inlet system integrity and air quality on the availability of the gas turbine, this is an area where the small incremental first cost is well worth it over the turbine's life cycle.

● Beware of modifications made to the inlet system during maintenance and ensure that these do not promote airflow distortion.
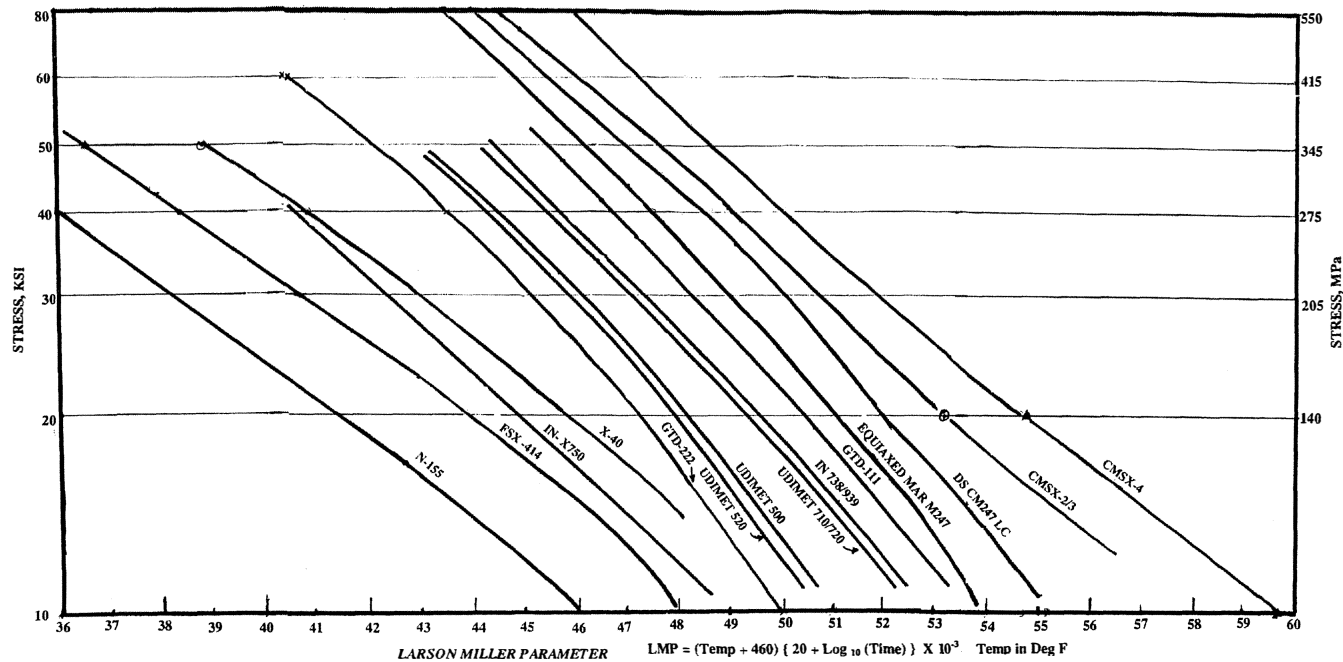

Figure A-4. Larson-Miller Parameter for Several Turbine Materials. (This figure has been constructed from data from several sources including Viswanathan (1989) and Kubarych (1992).)
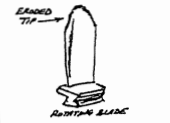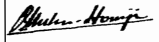
APPENDIX B

BLADE FAILURE TROUBLESHOOTING CHART

A chart that incorporates several interrelated factors and observations into a single tabulation to assist troubleshooting is presented in Table B-1. This chart is intended to provide plant engineers a framework within which to troubleshoot blade failures. It is important to note that combined failure modes do occur and that this chart is by no means exhaustive. The tabulation attempts to address the following in context of blade failure:

- Design aspects
- Manufacturing issues
- Environmental conditions
- Maintenance aspects
- Failure location
- Metallurgical and fracture analysis
- Surrounding evidence
- Failure history
- Operating symptoms

FAILURE MODE	DESIGN ASPECTS	Manufacture	ENVIRONMENTAL CONDITIONS.	MAINTENANCE	FAILURE LOCATION	METALLURGICAL ANALYSIS	SURROUNDING EVIDENCE	FAILURE HISTORY	OPERATING SYMPTOMS
10. HOT CORROSION TYPE I	Coatings are of key importance - have to be suited to environment. Liquid fuel treatment y tem design is most important- use floating suction supply, centrifuging, and inhibition if Vanadium present.	Improper coating application can reduce protection	. Excessive > 0.5 ppm Na+V in fuel or airborne salt ingestion. Lower Threshold (825°C): Melting point of Na_2SO_4. Upper Threshold (950°C): Dew Point of Na_2SO_4. Alkali etals (Na, K) co bine during combustion with Sulpher and O_2 present in fuel to form Na_2SO_4 and K_2SO_4. When these condense on the blade, they destroy the protective oxide cale allowing sulphur to penetrate the base metal. Maintenance: Problems with fuel treatment, open blow in doors in filter, and filtration problems can allow ingress of salt. Leeching of salt through filter) Poor quality of water injection can also be the cause of salt ingress. Improper washing procedures under power with a salt laden compre sor.	Process upsets of Fuel treatment system can allow short term ingestion of Na, S. Poor maintenance of air filtration system can allow airborne Na ingestion. Check Water/Steam injection quality.	Turbine blades and nozzles. First stage blades will suffer more than subsequent stages. Damage typically first occurs on LE of airfoil Roughening of the surface. Look for evidence of low temperature corrosion on cooler part of blade or on vane platform.	Fracture may occur as a result of fatigue or creep in the "thinned down" LE or TE. Can occur as a creep failure especially if cooling system defeated by hot corrosion. Denuded base metal zone often found with intergranular attack and sulfide spikes. Sulfides can be distinguished from internal oxides by their lighter color and non globular appearance. Porous non-protective oxide layer found with metal/oxide layer irregular with intrusions of oxide into the metal and islands of un-oxidized metal within the oxide.	Green coloration of blading (Ni0), blisters, white deposits on turbine nozzles, exhaust system. Sulphidation products are ferromagnetic - check with magnet tied to string. Reduced airfoil sections often get longitudinal cracks on LE & tran verse cracks on T.E. More uniform. porous surface cale.	Large number of starts promotes coating cracking distress which could lead to hot orrosion. Problem an develop rapidly with salt ingestion.	Reduction in performance and efficiency with severe blade degradation.
11. HOT CORROSION TYPE II (LOW TEMPERATURE)	as above	as above	Airborne or fuel born salt similar to Type I.	See Type I	Hot section stators & blades.	Layered type of corrosion scale. No intergranular attack of denuded zone found on base metal. Typically very little sulphide formation within the metal.	Non uniform pitting attack	: Machines operated at part load (lower metal temperatures).	: Loss In performance.
12. BLADE EROSION	Can occur on both compressor or turbine.		erosive particles present in either air, steam or fuel.	Lack of air filtration system integrity, blow in doors open.	Severe attack on LE & TE of concave side.			Air filtration problems, blow in doors open loss of filter housing integrity. Possible surge/stall event if erosion is severe.		Loss of power capabil ity, higher EGT if severe deterioration.

3 of 4

FAILURE MODE	DESIGN ASPECTS	Manufacture	ENVIRONMENTAL CONDITIONS.	MAINTENANCE	FAILURE LOCATION	METALLURGICAL ANALYSIS	SURROUNDING EVIDENCE	FAILURE HISTORY	OPERATING SYMPTOMS
13.: HOT GAS EROSION/ OXIDATION	Vane cooling deficiencies can cause this Can be caused by poor combustor pattern factor	Poor coating quality. Failure of TBC on Nozzle vane or platform,	Excessive number of starts and stops may promote coating break down and additional roughness.		Very often found on 1st stage nozzle vane platforms can be outboard or inboard platform.	Signs of overtemperature.	Damaged coatings, Excessive EGT spreads. Exa ine EGT profiles and spr ads.	Typically noted after several operating hours.	No symptoms. Excessive temperature unevenness may show on EGT analysis/plot. May not be uniform around turbine circumference and is associated with hot r gions from the combustor outlet
14.: STANDBY CORROSION	Coatings are of help here		High humidity coastal locations; salty environment. Industrial pollutants such as chlorine, ammonia, Hydrogen sulphide can promote the problem. Typically on peaking or intermittent use machines.	Improper storage and dehumidification Apply heat for long term storage.	Crevices, rotors, blade attachment areas.	Failure may be in Fatigue initiated by crevice corrosion. Symptoms ay be similar to orrosion fatigue (transgranular)	Wear in dovetail areas, none or excessive bucket rock.	Occurs over several years.	No specific symptoms.
15. RUBS/WEAR	Excessive rotor bow Improper cooling can cause distortions		Assembly clearances faulty		Compressor and Turbine tips	Tip rubs, axial rubs possible.	High Vibration Surge (may be underlying cause) Emergency shutdown or loss of cooling Thermal cracks due to heat generated can cause blade overtemperature failure if rub eroded particles blo k cooling passages.	At startup if inherent design problem. Over several years if creep related.	Loss in Power/Efficiency. In rease in turbine tip clearance will dramatically drop power capability. May see subharmonic activity in vibration spectrum if lucky

REFERENCES

Allianz, 1978, *Handbook of Loss Prevention*, New York, New York: Springer Verlag.

Armstrong, E. K., 1967, "Recent Blade Vibration Techniques," ASME Journal of Engineering for Power, *89*, pp. 437-444.

Armstrong, E. K. and Stevenson, M. A., March 1960, "Some Practical Aspects of Compressor Blade Vibration," Journal of the Royal Aeronautical Society, *64*, (591), pp. 118-130.

Barber, R., April 21-24, 1969, "A Radiation Pyrometer Designed for In Flight Measurement of Turbine Blade Temperatures," Presented at the National Air Transportation Meeting, New York, New York, SAE Paper 690432.

Barer, R. D. and Peters, B. F., 1970, *Why Metals Fail*, New York, New York: Gordon and Breach Science Publishers.

Bentle, M., 1991, *Engine Revolutions—The Autobiography of Max Bentle*, SAE Publications.

Bernstien, H. L., April, 1990, "Life Management System for General Electric Frame 7E Gas Turbine," Proceedings of EPRI/ASM Conference on Life Assessment and Repair Technology for Combustion Turbine Hot Section Components, Phoenix, Arizona.

Bernstein, H. L. and Allen, J. M., June 3-6, 1991 "Analysis of Cracked Turbine Blades," International Gas Turbine and Aeroengine Congress, Orlando, Florida, ASME Paper Number 91-GT-16.

Beynon, T. G. R., March 9-12, 1981, "Turbine Pyrometry—An Equipment Manufacturer's View," ASME Gas Turbine Conference, Houston, Texas, ASME Paper Number: 81-GT-136.

Bill, R. C., 1982, "Review of Factors That Influence Fretting Wear," Materials Evaluation Under Fretting Conditions, ASTM STP 780, ASTM, pp. 165-182.

Binek, J. S., October 21-23, 1974, "Present Practices in Inlet System Design for Stationary Gas Turbines for Cold Weather Operations," Proceedings of the First NRCC Conference on Gas Turbine Operations and Maintenance, Sponsored by National Research Council of Canada, Edmonton, Alberta, Canada.

Bloch, H. P., 1982, *Improving Machinery Reliability in Process Plants, Volume I*, Houston, Texas: Gulf Publishing.

Boyer, H. E., Ed., 1975, "Failure Analysis and Prevention," Metals Handbook, Eighth Edition, *10*, ASM.

Brown, G. J., June 1977, "Engine Design to Minimize Foreign Object Damage," Proceedings of the Second NRCC Symposium on Gas Turbines Operations and Maintenance, National Research Council of Canada, Calgary, Canada.

Cartwright, R. A. and Fisher, C., June 3-6, 1991, "Marine Gas Turbine Condition Monitoring by Gas Path Electrostatic Detection Techniques," International Gas Turbine and Aeroengine Conference, Orlando, Florida.

Clough, H. J., May 31-June 4, 1987, "Blade Excitation Criteria Developed for Aero Derived Engines in Arctic Alaska," ASME Gas Turbine Conference, Anaheim, California, ASME Paper Number: 87-GT-104.

Cohen, H., Rogers, G. F. C., and Saravanamuttoo, H. I. H, 1987, *Gas Turbine Theory*, Essex, United Kingdom: Addison Wesley Longman.

Crombie, E., McCall, W., Beck, C. G., and Moon, D. M., 1977, "Degradation of High Temperature Impact Properties of Nickel Base Gas Turbine Blade Alloys," Proceedings of the Twelfth CIMAC Conference, Tokyo, Japan, *C*.

Daleo, J. A. and Boone, D. H., June 2-5, 1997, "Failure Mechanisms of Coating Systems Applied to Advanced Gas Turbines," Paper Presented at the 1997 ASME Gas Turbine and Aeroengine Congress, Orlando, Florida, ASME Paper Number: 97-GT-486.

Daniels, A., April 10-12, 1996, "Nondestructive Pulsed Infrared Quantitative Evaluation of Metals," Thermosense XVIII, International Society of Optical Engineering, Orlando, Florida, *2766*.

Day, I. J. and Freeman, C., May 24-27, 1993, "The Unstable Behavior of Low and High Speed Compressors," Presented at the 1993 ASME Gas Turbine and Aeroengine Congress, Cincinnati, Ohio, ASME Paper Number: 93-GT-26.

DeCrescente, M. A., 1980, "Sulphidation and Its Inhibition in Turbomachinery," *Proceedings of the Ninth Turbomachinery Symposium*, Turbomachinery Laboratory, Texas A&M University, College Station, Texas, pp. 63-68.

Donle, D. W., Kiefer, R. C., Wright, T. C., Bertolami, U. A., and Hill, D. G., May 24-27, 1993, "Gas Turbine Inlet Air Treatment: A New Technology," International Gas Turbine and Aeroengine Congress, Cincinnati, Ohio, ASME Paper Number: 93-GT-24.

Dundas, R. E., 1982, "The Use of Performance Monitoring to Prevent Compressor and Turbine Failures," ASME Gas Turbine Congress, Paper Number: 882-GT-66.

Dundas, R. E., 1985, "Mechanical Design of the Gas Turbine," *Sawyer's Gas Turbine Engineering Handbook*, *I*, Third Edition, Sawyer, J. W., Ed., Turbomachinery International Publications.

Dundas, R. E., 1986, "A Study of the Effect of Deterioration on Compressor Surge Margin in Constant Speed, Single Shaft Gas Turbines," ASME Gas Turbine Congress, ASME Paper Number: 86-GT-177.

Dundas, R. E., June 6-9, 1988, "Review of Design Parameters in Gas Turbines for the Prospective User," International Gas Turbine and Aeroengine Congress, Amsterdam, The Netherlands.

Dundas, R. E., May 24-27, 1993a, "Investigation of Failures in Gas Turbines, Part 1—Techniques and Principles of Failure Investigation," ASME International Gas Turbine and Aeroengine Congress, Cincinnati, Ohio, ASME Paper Number: 93-GT-83.

Dundas, R. E., May 24-27, 1993b, "Investigation of Failures in Gas Turbines, Part 2—Engineering and Metallographic Aspects of Failure Investigation," ASME International Gas Turbine and Aeroengine Congress, Cincinnati, Ohio, ASME Paper Number: 93-GT-84.

Dundas, R. E., June 13-16, 1994, "A Statistical Study of Gas Turbine Losses and Analysis of Causes and Optimum Methods of Prevention," ASME International Gas Turbine and Aeroengine Congress, The Hague, Netherlands, ASME Paper Number: 94-GT-279.

Dundas, R. E., Sullivan, D. A., and Abegg, F., June 1-4, 1992, "Performance Monitoring of Gas Turbines for Failure Prevention," ASME International Gas Turbine and Aeroengine Congress, Cologne, Germany, ASME Paper Number: 92-GT-267.

Ewins, D. J., 1976, "Studies to Gain Insight into the Complexities of Blade Vibration Phenomenon," Institution of Mechanical Engineers, United Kingdom, Paper Number: C.184/76.

Faupel, J. H., 1964, *Engineering Design*, New York, New York: J. H. Wiley.

Fisher, C. June 1988, "Gas Path Condition Monitoring Using Electrostatic Techniques," AGARD Conference Proceedings, *448*.

Goodman, L. E. and Klump, J. H., September 1956, "Analysis of Slip Damping with Reference to Turbine Blade Vibration," Journal of Applied Mechanics, Transactions of the ASME, *23*, (3).

Goward, G. W., March 18-21, 1985, "Low Temperature Hot Corrosion in Gas Turbines: A Review of Causes and Coatings Therefor," ASME Thirtieth International Gas Turbine Conference, Houston, Texas, ASME Paper Number: 85-GT-60.

Greenfield, P., 1972, "Creep of Metals at High Temperatures," M&B Monograph ME/9, Mills and Boon Ltd., London, England.

Griffin, J. H., Wu, W. T., and El Aini, Y., January 1998, "Friction Damping of Hollow Airfoils Part 1— Theoretical Development, Part 2—Experimental Verification," ASME Journal of Engineering for Gas Turbines and Power, *120*.

Harmon, R. T. C.,1979, *Gas Turbine Engineering*, New York, New York: John Wiley and Sons.

Haskell, R. W., June 4-8, 1989, "Gas Turbine Compressor Operating Environment and Material Evaluation," Paper presented at the Gas Turbine and Aeroengine Congress, ASME Paper Number: 89-GT-42.

Haupt, U. and Rautenberg, M., 1982, "Investigation of Blade Vibration of Radial Impellers by Means of Telemetry and Holographic Interferometery," ASME Paper No. 82-GT-34, ASME International Gas Turbine Congress, London, England. Also in ASME Journal of Engineering for Power, *104*, (4), pp. 838-843.

Haupt, U. and Rautenberg, M., 1983a, "Blade Vibration Measurements of Centrifugal Compressors by Means of Telemetry and Holographic Interferometery," ASME Paper No. 83-GT-131, ASME International Gas Turbine Congress, Phoenix, Arizona. Also in ASME Journal of Engineering for Power, *106*, (1), pp. 70-78.

Haupt, U. and Rautenberg, M., 1983b, "Blade Vibration on Radial Impellers Excited by Rotating Stall Cells and During Surge," Paper No. 83-TOKYO-IGTC-124, International Tokyo Gas Turbine Congress.

Haupt, U., Bammert, K., and Rautenberg, M., 1985a, "Blade Vibration on Centrifugal Compressors— Fundamental Considerations and Initial Measurements," ASME Paper No. 85-GT-92, ASME International Gas Turbine Congress, Houston, Texas.

Haupt, U., Bammert, K., and Rautenberg, M., 1985b, "Blade Vibration on Centrifugal Compressors— Blade Response to Different Excitation Conditions," ASME Paper No. 85-GT-93, ASME International Gas Turbine Congress, Houston, Texas.

Haupt, U., Jin, D. F., and Rautenberg, M., June 4-8, 1989, "On the Mechanism of Dangerous Blade Vibration Due to Blade Flow Interactions on Centrifugal Compressors," ASME Paper No. 89-GT-291, ASME International Gas Turbine Congress, Toronto, Canada.

Hepworth, J. K., Wilson, D., Allen, J. M., Quentin, G. H., and Touchton, G., June 2-5, 1997, "Life Assessment of Gas Turbine Blades and Vanes," Presented at the 1997 ASME Gas Turbine and Aeroengine Congress, Orlando, Florida, ASME Paper Number: 97-GT-446.

Hittori, T., Sakata, S., and Ohnishi, H., October 1983, "Slipping Behavior and Fretting Fatigue in the Disk/Blade Dovetail Region," International Gas Turbine Congress, Tokyo, Japan, Paper Number: 83-TOKYO-IGTC-122.

Kadambi, J. R., Quinn, R. D., and Adams, M. L., October 1989, "Turbomachinery Blade Vibration and Dynamic Stress Measurements Utilizing Non-Intrusive Techniques," Transaction of the ASME, Journal of Engineering and Power, *111*.

Kawashima, T., Iinuma, H., Wakatsuki, T., and Minagawa, N., June 1-4, 1992, "Turbine Blade Vibration System," International Gas Turbine and Aeroengine Congress, Cologne, Germany, ASME Paper Number: 92-GT-159.

Kirby, P. J., May 19-23, 1986, "Some Considerations Relating to Aero Engine Pyrometry," Paper presented at the Sixty-Seventh AGARD Symposium—Propulsion and Energetics. Panel on Advanced Instrumentation for Aeroengine Components, Philadelphia, Pennsylvania, (Conference Proceedings Number: 339).

Kirby, P. J., Zachary, R. E., and Ruiz, F., June 8-12, 1986, "Infrared Thermometry for Control and Monitoring of Industrial Gas Turbines," International Gas Turbine and Aeroengine Congress, Dusseldorf, West Germany, ASME Paper Number: 94-GT-267.

Knowles, M., June 13-16, 1994, "Gas Turbine Temperature Spread Monitoring Detection of Combustion System Deterioration," International Gas Turbine and Aeroengine Congress, The Hague, Netherlands, ASME Paper Number: 94-GT-1891.

Kubarych, K. G., 1992, "High Temperature Metallic Materials," Solar Turbines Publication.

Lakshminarasimha, A. N. and Saravanamuttoo, H. I. H, May 12-14, 1986, "Prediction of Fouled Compressor Performance Using Stage Stacking Techniques," Fourth ASME Fluid Mechanics Conference on Turbomachinery Performance Deterioration.

Lakshminarasimha, A. N., Boyce M. P., and Meher-Homji, C. B., January 1994, "Modeling and Analysis of Gas Turbine Performance Deterioration," Transactions of the ASME Journal of Engineering for Gas Turbines and Power, *116*, pp 46-52.

Leon, R. L. and Trainor, K., February, 1990, "Monitoring Systems for Steam Turbine Blade Faults," Sound and Vibration, pp.12-15.

Loukis, E., Mathioudakis, K., and Papailiou, K., June 3-6, 1991a, "A Procedure for Automated Gas Turbine Blade Fault Identification Based on Spectral Pattern Analysis," International Gas Turbine and Aeroengine Congress, Orlando, Florida, ASME Paper Number: 91-GT-259.

Loukis, E., Wetta, P., Mathioudakis, K., Papathanasiou, A., and Papailiou, K., June 3-6, 1991b, "Combination of Different Unsteady Quantity Measurements for Gas Turbine Blade Fault Diagnosis," International Gas Turbine and Aeroengine Congress, Orlando, Florida, ASME Paper Number: 91-GT-201.

Liburdi, J. and Wilson, J., 1983, "Guidelines for the Extension of Turbine Blade Life," *Proceedings of the Twelfth Turbomachinery Symposium*, Turbomachinery Laboratory, Texas A&M University, College Station, Texas, pp. 21-30.

Lowden, P. and Liburdi, J., May 31- June 4, 1987, "Observations on the Life and Overhaul Requirements of Aero Derivative Engines on Base Load Industrial Applications," ASME Gas Turbine Congress, Anaheim, California, ASME Paper Number: 87-GT-105.

Marscher, W. D., 1985, "Structural Design and Analysis," *Sawyers Gas Turbine Handbook*, *I*, Turbomachinery International.

Marson, E., June 1-4, 1992, "Effect of Manufacturing Deviations on Performance of Axial Flow Compressor Blading," ASME Gas Turbine and Aeroengine Congress, Cologne, Germany, ASME Paper Number: 92-GT-326.

Mathioudakis, K., Loukis, E., and Papailiou, K., June 4-8, 1989, "Casing Vibration and Gas Turbine Operating Conditions," International Gas Turbine and Aeroengine Congress, Toronto, Canada, ASME Paper Number: 89-GT-78.

Meher-Homji, C. B., April 16-18, 1985, "Reasoning Foundations for Machinery Diagnostics—Thought Processes and Expert Systems," Fortieth Meeting of the Mechanical Failure Prevention Group, National Bureau of Standards, Gaithersburg, Maryland, Published by Cambridge University Press.

Meher-Homji, C. B., August 27-29, 1990, "Gas Turbine Axial Compressor Fouling—A Unified Treatment of its Effects, Detection and Control," ASME Cogen Turbo IV, New Orleans, Louisiana. Also in *International Journal of Turbo and Jet Engines*, *9*, (4), 1992, pp. 99-111.

Meher-Homji, C. B., June 5-8, 1995, "Blading Vibration and Failures in Gas Turbines: Part A—Blading Dynamics and the Operating Environment, Part B—Compressor and Turbine Airfoil Distress, Part C—Detection and Troubleshooting, Part D—Case Studies," Fortieth ASME Gas Turbine and Aeroengine Congress, Houston, Texas, ASME Paper Numbers 95-GT-418, 95-GT-419, 95-GT-420, 95-GT-421.

Meher-Homji, C. B., June 1996, "The Development of the Junkers Jumo 004B—The World's First Production Turbojet," ASME Gas Turbine and Aeroengine Congress, Birmingham, United Kingdom, ASME Paper Number: 96-GT-457. Also in ASME Journal of Engineering for Gas Turbine and Power, *119*, (4), October 1997, pp. 783-789, and ASME's Mechanical Engineering Magazine, September 1997.

Meher-Homji, C. B., June 2-5, 1997, "The Development of the Whittle Turbojet," 1997 ASME Gas Turbine and Aeroengine Congress, Orlando, Florida, ASME Paper Number: 97-GT-528. Also in ASME Transactions, Journal of Engineering for Gas Turbine and Power, April 1988, *120*.

Meher-Homji, C. B. and Bhargava, R. B., June 1-4, 1992, "Condition Monitoring and Diagnostic Aspects of Gas Turbine Transient Response," International Gas Turbine and Aeroengine Congress, Cologne, Germany, ASME Paper Number: 92-GT-100. Also in International Journal of Turbo and Jet Engines, *11*, (1), 1994, pp. 99-111.

Meher-Homji, C. B. and Focke, A. B., September 10-13, 1985, "Performance and Vibration Monitoring for the Prevention of Gas Turbine Airfoil Failures," Sixth ASME Biennial Conference on Failure Prevention and Reliability, ASME Bound Volume H-331.

Meher-Homji, C. B., Lakshminarasimha, A. N., Mani, G, Boehler, P. D., Dohner, C. V., Ondryas, I., Lukas, H., and Cincotta, G. A., May 24-27, 1993, "Durability Surveillance of Advanced Gas Turbines— Performance and Mechanical Baseline Development for the GE Frame 7F," International Gas Turbine and Aeroengine Congress, Cincinnati, Ohio, ASME Paper Number: 93-GT-276.

Mitchell, J., October 14-16, 1975, "Examination of Pump Cavitation, Gear Mesh and Blade Performance Using External Vibration Characteristics," *Proceedings of the Fourth Turbomachinery Symposium*, Turbomachinery Laboratory, Texas A&M University, College Station, Texas, pp. 39-45.

O'Neill, S. T., June 4-8, 1989, "Operating Experience with a 42.5 MW Gas Turbine Used in a Cogeneration Plant at a Paper Mill in the US," ASME Gas Turbine and Aeroengine Conference, Toronto, Canada, ASME Paper Number: 89-GT-197.

Ondryas, I. S., Meher-Homji, C. B., Boehler, P., and Dohner, C. 1992, "Durability Surveillance Program on the Advanced Gas Turbine GE Frame 7F," Thirty-Seventh ASME Gas Turbine and Aeroengine Conference, Cologne, Germany, ASME Paper Number: 92-GT-334.

Pampreen, R. C., 1993, *Compressor Surge and Stall*, Concepts ETI Inc.

Parge, P., October 22-25, 1990, "Non-Intrusive Vibration Monitoring for Turbine Blade Reliability," Proceedings of the Second International Machinery Monitoring and Diagnostic Conference, Los Angeles, California, pp. 435-446.

Parge, P., Trevillion, B., and Carle, P., September 11-14, 1989, "Machinery Interactive Display and Analysis System Description and Applications," Proceedings of the First International Machinery Monitoring and Diagnostic Conference, Las Vegas, Nevada, pp. 176-182.

Passey, R. D. C., 1976, "Reliability of Compressor Airfoils," Prog. Aerospace Science, *17*, pp. 67-92.

Patton, R. E., 1975, "Gas Turbine Operation in Extreme Cold Climate," *Proceedings of the Fourth Turbomachinery Symposium*, Turbomachinery Laboratory, Texas A&M University, College Station, Texas, pp. 83-94.

Rao, J. S., 1992, *Turbomachine Blade Vibration*, New York, New York: John Wiley and Sons.

Rooth, A., Agema, K. S., and Hiemstra, W., June 2-5, 1997, "Metallurgical Analysis of Temperature Monitored Gas Turbine Blades," ASME Gas Turbine and Aeroengine Congress, Orlando, Florida, ASME Paper Number: 97-GT-212.

Roth, H., 1980, "Vibration Measurements on Turbomachine Rotor Blades with Optical Probes," ASME Joint Fluids Engineering Conference, Measurement Methods in Rotating Components of Turbomachinery.

Saravanamuttoo, H. I. H. and Lakshminarasimha, A. N., 1985, "A Preliminary Assessment of Compressor Fouling," ASME International Gas Turbine and Aeroengine Congress, ASME Paper Number: 85-GT-153.

Scalzo, A. J., June 3-6, 1991, "High-Cycle Fatigue Design Evolution and Experience of Freestanding Combustion Turbine Blades," International Gas Turbine and Aeroengine Congress, Orlando, Florida, ASME Paper Number: 91-GT-13.

Schulenberg, T. and Bals, H., May 31-June 4, 1987, "Blade Temperature Measurements of Model V84.2 100 MW/60 Hz Gas Turbine," ASME Gas Turbine Conference, Anaheim, California, ASME Paper Number: 87-GT-135.

Schweiger, T., September 1983, "North Sea Operating Experience—Air Intake Design," Proceedings of the Fifth NRCC Proceedings on Gas Turbines Operations and Maintenance, National Research Council of Canada, Calgary, Canada.

Shannon, J. F., March 1945, "Vibration Problems in Gas Turbine Centrifugal and Axial Flow Compressors," ARCR&M 2226.

Sheard, A. G. and Killeen, B., June 13-16, 1994, "A Blade by Blade Tip Clearance Measurement System for Gas Turbine Applications," International Gas Turbine and Aeroengine Congress, The Hague, Netherlands, ASME Paper Number: 94-GT-40.

Simmons, H. R., 1986, "A Non -Intrusive Method for Detecting HP Blade Resonance," ASME Paper Number: 86-JPGC-Pwr-36.

Simmons, H., 1987, "Non -Intrusive Detection of Turbine Blade Resonance," Third EPRI Conference on Incipient Failure Detection in Power Plants, Philadelphia, Pennsylvania.

Simmons, H. R., Michalsky, D., Bruewer, K. E., Smalley, A. J., June 14-19, 1990, "Measuring Rotor and Blade Dynamics Using an Optical Blade Tip Sensor," ASME Gas Turbine and Aeroengine Conference, Brussels, Belgium, ASME Paper Number: 90-GT-91.

Singh, M. P. and Schiffer, D., 1982, "Vibrational Characteristics of Packeted Bladed Disks," ASME Paper Number: 82-DET-137.

Singh, M. P. and Vargo, J. J., October 1989, "Reliability Evaluation of Shrouded Blading Using the SAFE Interference Diagram," ASME Journal of Engineering for Gas Turbines and Power, *111*, pp. 601-609.

Sohre, J. S., 1975, "Steam Turbine Blade Failures, Causes and Corrections," *Proceedings of the Fourth Turbomachinery Symposium*, Turbomachinery Laboratory, Texas A&M University, College Station, Texas, pp. 9-30.

Sorensen, H. A., 1951, *Gas Turbines*, New York, New York: Ronald Press.

Srinivasan, A.V., October 1997, "Flutter and Resonant Vibration Characteristics of Engine Blades," ASME Journal of Engineering for Gas Turbine and Power, *119*, (4), pp.742-775.

Stringer, J. and Viswanathan, R., April 1990, "Keynote Address on Life Assessment Techniques and Coating Evaluations for Combustion Gas Turbines," Life Assessment and Repair Technology for Combustion Turbine Hot Section Components, EPRI-ASM-19.

Strub, R. A., 1974, "Field Measurements of Blade Stresses on Industrial Turbomachines," *Proceedings of the Third Turbomachinery Symposium*, Turbomachinery Laboratory, Texas A&M University, College Station, Texas, pp. 23-34.

Trumpler, W. E. and Owens, H. M., 1953, "Turbine Blade Vibration and Strength," American Society of Mechanical Engineers, ASME Paper 53A-98.

Turbomachinery International, March 1985, "History of the Gas Turbine—The Rolls Royce Avon."

Viswanathan, R., 1989, *Damage Mechanisms and Life Assessment of High Temperature Components*, Metals Park, Ohio: ASM International Press.

Viswanathan, R. and Dolbec, A. C., June 8-12, 1986, "Life Assessment Technology for Combustion Turbine Blades," ASME International Gas Turbine Conference, Dusseldorf, Germany, ASME Paper Number: 86-GT-257.

Voysey, R. G., 1945, "Some Vibrational Problems in Gas Turbine Engines," Lectures on the Development of the Internal Combustion Gas Turbine, Proceedings of the Institution of Mechanical Engineers, United Kingdom, *153*, War Issue No. 12, pp. 483-495.

Walker, J. L., 1988, "US Naval Marine Gas Turbine Maintenance," *I, Sawyers Turbomachinery Maintenance Handbook*, Turbomachinery International Publishers.

Walker, J. and Sommerfield, A., 1987, "Marine Gas Turbines—Engine Health Monitoring—New Approaches," ASME Gas Turbine Conference, ASME Paper Number: 87-GT-245.

Wilkes, C. and Dean, A. J., June 2-5, 1997, "Gas Fuel Conditioning System Design Considerations for Utility Gas Turbines," Paper Presented at the 1997 ASME Gas Turbine and Aeroengine Congress, Orlando, Florida, ASME Paper Number: 97-GT-227.

Wisch, H. W., May 24-27, 1993, "A Review of the Full Capabilities of Blade Path Thermocouples," International Gas Turbine and Aeroengine Congress, Cincinnati, Ohio, ASME Paper Number: 93-GT-222.

Wood, I. H., Foster, A. D., and Schilke, P. W., 1990, "High Temperature Coating for Improved Oxidation/Corrosion Protection," GE Turbine Reference Library Publication GER 3597.

Zaba, T. 1980, "Losses in Gas Turbines Due to Deposits on the Blading," Brown Boveri Review, 12-80, pp. 715-722.

Zech, W. A., February 19-21, 1968, "Discussion of Mechanical Failures of Centrifugal Compressors as Experienced in High Pressure Installations," Presented at the Symposium of Loss Prevention in Process Industries, St. Louis, Missouri.

ACKNOWLEDGEMENTS